Insights into TALK-1 Channel Modulation of Islet Cell Calcium Homeostasis and Hormone Secretion

By

Nicholas C. Vierra

Dissertation

Submitted to the Faculty of the

Graduate School of Vanderbilt University

in partial fulfillment of the requirements

for the degree of

DOCTOR OF PHILOSOPHY

in

Molecular Physiology and Biophysics

August 11, 2017

Nashville, Tennessee

Approved:

Richard M. O'Brien, Ph.D.

Roger J. Colbran, Ph.D.

Eric J.Y. Delpire, Ph.D.

Jerod S. Denton, Ph.D.

ACKNOWLEDGEMENTS

First, I must thank the members of my thesis committee, Drs. Richard O'Brien, Roger Colbran, Eric Delpire, and Jerod Denton, for their invaluable support and contributions to this dissertation. I am truly grateful for the feedback and guidance they provided which encouraged me to think more critically and fostered my development as a scientist. I must also thank Karen Gieg for her tremendous assistance in helping me coordinate committee meetings and navigate the paperwork of graduate school.

The work presented herein would not have been possible without the past and present members of the Jacobson lab, including Prasanna Dadi, Imju Jeong, Matthew Dickerson, Molly Altman, Sarah Milian, and Kelli Jordan, who provided a supportive setting and gave me the resources I needed to succeed. I must also thank the many trainees in the Jacobson lab who contributed to the data presented herein. Moreover, I could not have performed much of this work without the assistance of Prasanna Dadi. His immense help in the lab enabled my scientific pursuits, and his friendship outside of lab provided much-needed support and entertainment. I will truly miss his humor and advice.

I must also express my gratitude to the Powers lab, who provided thoughtful feedback and suggestions regarding the direction of my studies. They took the time to provide meaningful comments on my research projects during joint lab meetings, which greatly improved my communication skills and helped me expand my scientific knowledge. The members of the β-cell Interest Group also provided helpful guidance and greatly enriched my training experience at Vanderbilt. In addition, the expertise and support provided by numerous scientists was critical for this work. I am particularly grateful for the assistance provided by Dr. Marcela Brissova and

Anastasia Coldren in the Islet Procurement and Analysis core; Dr. David Wasserman; Dr. Owen McGuinness; Dr. Paige Vinson, Emily Days, and Dr. Dave Weaver in the High-Throughput Screening facility; Dr. Bob Matthews and Dr. Jenny Schafer in the Cell Imaging Shared Resource; Dr. Dale Edgerton and Susan Hajizadeh in the Hormone Assay core; Dr. David Piston; and Dr. David Powell. I would also like to acknowledge the funding sources which enabled my training and the studies described herein: the Molecular Endocrinology Training Program (5T32DK07563), a Ruth L. Kirschstein National Research Service Award (F31DK10962), and support provided to Dr. David Jacobson through the National Institutes of Health (K01DK081666, R01DK097392), the Vanderbilt Diabetes Research and Training Center (P60DK20593), and the American Diabetes Association (1-17-IBS-024).

I could not have succeeded in graduate school without the endless hours of support and patience given to me by my mentor, Dr. David Jacobson. I was very fortunate to be David's first graduate student trainee, and I will be forever grateful for the invaluable guidance and advice he provided over the last four years. His mentorship taught me to pursue the important questions and to think critically about experimental findings, instilling a greater sense of curiosity which makes me enjoy being a scientist even more. I could not have asked for a better advisor, and I am confident that my gratitude for his mentorship will continue to grow as I move on to the next stages of my career.

Lastly, I would not have made it through graduate school without the support of my family. To my parents, Frank and Sheila, thank you for continuously encouraging my interest in science. To my brothers and sisters, Jaimie, Angela, James, and Aaron, thank you for your help and love along the way. I was fortunate to attend graduate school near my uncle Mark, who provided endless support throughout my education for which I am truly grateful. To George,

Elsa, and McKinley, I sincerely appreciate your constant encouragement and assistance. Finally, to my wife Sierra, thank you for your loving and continuous support. I am so thankful that I have such an incredible person as a spouse and best friend.

TABLE OF CONTENTS

Page

ACKNOWLEDGEMENTS ii

LIST OF TABLES viii

LIST OF FIGURES ix

LIST OF ABBREVIATIONS xii

Chapter

I. INTRODUCTION 1

Preface 1
Glucose metabolism and the pancreatic islets 1
Cytoplasmic Ca^{2+} determines islet hormone secretion 4
K^+ channels control cytoplasmic Ca^{2+} influx 4
Mechanisms of islet cell hormone secretion 8
β-cells 8
K^+ channel regulation of β-cell electrical activity 10
Pulsatile insulin secretion and its underlying mechanisms 11
The role of ER Ca^{2+} in regulating β-cell function 13
α-cells 15
Electrical activity in α-cells 15
δ-cells 17
Electrical activity in δ-cells 18
PP- and ε-cells 19
Diabetes mellitus and islet dysfunction 20
Islet dysfunction as a driver of diabetes mellitus 22
K^+ channels in T2DM 24
Two-pore domain (K2P) channels 26
Physiological roles of K2P channels in excitable cells 29
K2P channels in the islet 30
TWIK-1 channels 30
TASK-1 channels 31
TALK-1 channels 32
Goals of this thesis 34

II. TALK-1 CHANNELS MODULATE β-CELL ELECTRICAL EXCITABILITY, 2ND-PHASE INSULIN SECRETION, AND GLUCOSE HOMEOSTASIS 36

Preface 36
Introduction 37
Results 39
Pancreatic β-cells express functional TALK-1 channels. 39
TALK-1 channel activity and surface expression is sensitive to *Ct* charge 45
TALK-1 regulates β-cell electrical excitability and Ca^{2+} entry 49
TALK-1 channels are critical for maintaining fasting glycemia 54
TALK-1 channels modulate food intake and weight gain 57
Discussion 60
Research Design and Methods 64
Kcnk16$^{-/-}$ mouse preparation 64
Islet and β-cell isolation 65
Plasmids and transient expression 65
Electrophysiological recordings 66
Surface expression analysis 66
Measurement of cytoplasmic calcium 67
Immunofluorescence analysis 67
Insulin secretion measurements 67
Glucose and insulin tolerance testing 68
Statistical analysis 68

III. TALK-1 CHANNELS CONTROL β-CELL ENDOPLASMIC RETICULUM Ca^{2+} HOMEOSTASIS 69

Preface 69
Introduction 70
Results 73
TALK-1 activity promotes Ca^{2+}_{ER} leak 73
TALK-1 and TASK-1 form functional channels across the ER membrane 85
TALK-1 regulation of β-cell Ca^{2+}_{ER} handling modulates islet Ca^{2+} oscillations 87
TALK-1 channel activity exacerbates islet ER stress 92
Discussion 96
Research Design and Methods 100
Mouse models 100
Islet isolation and culture 101
Cell culture and luciferase assays 101
Patch clamp electrophysiology 102
Calcium imaging 103
Site-directed mutagenesis 105
Immunofluorescence 106
Statistical analysis 108

IV. TALK-1 CONTROLS PANCREATIC DELTA-CELL Ca^{2+}-INDUCED Ca^{2+} RELEASE AND SOMATOSTATIN SECRETION 109

Preface 109
Introduction 110
Results 112
TALK-1 channels are expressed in δ-cells 112
TALK-1 KO δ-cells are modestly depolarized 117
CICR is enhanced in TALK-1 KO δ-cells 119
Glucagon secretion is reduced from TALK-1 KO islets 123
Discussion 127
Research Design and Methods 132
Chemicals 132
Biological materials and study approval 132
Immunofluorescence 133
Calcium imaging 134
Patch clamp electrophysiology 135
Hormone secretion 136
Statistical analysis 136

V. SUMMARY AND FUTURE DIRECTIONS 138

Significance 138
How does inhibition of TALK-1 channel activity protect from fasting hyperglycemia and obesity? 139
The relationship between TALK-1 channel activity, Ca^{2+}_c homeostasis, and stimulus-secretion coupling 142
Differences between β- and δ-cells in cellular Ca^{2+} dynamics 150
Closing remarks 155

REFERENCES 156

LIST OF TABLES

Table Page

1.1. Major K^+ channels involved in regulation of islet cell electrical activity....7

2.1. V_m values recorded in WT and TALK-1 KO β-cells 52

2.2. Action potential characteristics in WT and TALK-1 KO β-cells 53

2.3. Islet and pancreatic hormone content of WT and TALK-1 KO mice....56

2.4. Islet donor characteristics for electrophysiology experiments using human islet cells 65

2.5. Human pancreas donor characteristics for immunofluorescence 67

3.1. Human islet donor characteristics....101

3.2. Human pancreas donor characteristics....108

4.1. Action potential characteristics in WT and TALK-1 KO δ-cells 119

4.2. Human pancreas donor characteristics....133

LIST OF FIGURES

Figure Page

1.1. Islet morphology in human and rodent islets. 3

1.2. Glucose-stimulated oscillations in β-cell electrical excitability 6

1.3. Consensus model of glucose-stimulated insulin secretion (GSIS) 9

1.4. Hypothesized destructive feedback loop leading to T2DM 21

1.5. Membrane topology and quaternary structure of K2P channels 28

2.1. TALK-1 is functionally expressed in mouse β-cells 40

2.2. Truncated TALK-1 mRNA in TALK-1 KO mice 41

2.3. Human β-cells contain functional TALK-1 channels 43

2.4. TALK-1 G110E (TALK-1 DN) suppresses TALK-1 WT-mediated whole-cell K^+ currents 44

2.5. TALK-1 A277E exhibits increased open probability and surface expression 46

2.6. TALK-1a P301H does not exhibit changes in channel activity 47

2.7. Unitary single channel currents measured from TALK-1 WT and TALK-1 A277E channels 48

2.8. TALK-1 regulates β-cell electrical activity 50

2.9. Ca^{2+}_c influx, oscillation frequency, and GSIS are increased in TALK-1 deficient islets 51

2.10. TALK-1 channels regulate fasting glycemia. 55

2.11. Representative islets in pancreas sections from TALK-1 WT and TALK-1 KO mice. 56

2.12. Enhanced hepatic insulin sensitivity and GSIS in TALK-1 KO mice fed a HFD for 8 weeks 58

2.13. TALK-1 regulates weight gain and adiposity 59

3.1. TALK-1 channels modulate β-cell ER Ca^{2+} homeostasis. 74

3.2. TALK-1 exhibits ER localization. 75

3.3. Islet cell number and proliferation are not modulated by TALK-1 activity 77

3.4. Intracellular Ca^{2+} stores are increased in TALK-1 KO islet cells 78

3.5. TALK-1 channels modulate human β-cell ER Ca^{2+} homeostasis 79

3.6. The K^+ channel function of TALK-1 contributes to its regulation of ER Ca^{2+} homeostasis. 81

3.7. Pharmacological manipulation of K2P channel activity can alter steady-state Ca^{2+}_{ER} concentrations 82

3.8. TASK-3 and TASK-1 K2P channel activity can alter Ca^{2+}_{ER} concentrations 84

3.9. Functional TALK-1 and TASK-1 channels are present in the ER membrane 86

3.10. ER Ca^{2+} leak is accelerated by TALK-1 channels 88

3.11. TALK-1 reglates ER Ca^{2+} handling during plasma membrane Ca^{2+} influx in β-cells 89

3.12. Reduced K_{slow} currents are associated with altered ER Ca^{2+} dynamics. 91

3.13. TALK-1 channel activity exacerbates ER stress. 94

3.14. Hypothetical model depicting potential molecular mechanisms of TALK-1 channel modulation of β-cell ER Ca^{2+} handling and cytosolic Ca^{2+} oscillations. 95

4.1. TALK-1 channels are expressed in mouse and human δ-cells 113

4.2. TALK-1 limits δ-cell Ca^{2+} influx and somatostatin secretion 115

4.3. Glucose synchronizes WT and TALK-1 KO δ-cell Ca^{2+} with β-cells 116

4.4. Electrical activity and VDCC currents in WT and TALK-1 KO δ-cells 118

4.5. ER Ca^{2+} stores are greater in TALK-1 KO δ-cells 121

4.6. Ca^{2+}-induced Ca^{2+} release is increased in TALK-1 KO δ-cells 122

4.7. Reduced glucagon secretion from TALK-1 KO islets 124

4.8. TALK-1 KO α-cells exhibit altered Ca^{2+} dynamics only in intact islets 126

5.1. Functions of islet K2P channels 140

5.2. TALK-1 is expressed in gastric somatostatin cells 142

5.3. Multiple metabolic parameters are altered in TALK-1 KO mice fed a HFD 144

5.4. TALK-1 KO islets show an altered sensitivity to muscarinic receptor stimulation 146

5.5. δ-cell ER Ca^{2+} handling is different from β-cells 152

LIST OF ABBREVIATIONS

ADP	Adenosine diphosphate
ATP	Adenosine triphosphate
BrdU	Bromodeoxyuridine
Ca^{2+}_{c}	Cytosolic Ca^{2+}
Ca^{2+}_{ER}	ER Ca^{2+}
cAMP	Cyclic adenosine monophosphate
CICR	Ca^{2+}-induced Ca^{2+} release
CPA	Cyclopiazonic acid
Ct	COOH-terminal tail
DRG	Dorsal root ganglion
E_K	K^+ equilibrium potential
ER	Endoplasmic reticulum
G6P	Glucose-6-phosphate
GABA	γ-aminobutyric acid
GI	Gastrointestinal
GIRK	G protein-coupled inwardly-rectifying K^+ channel
GPCR	G protein-coupled receptor
GSIS	Glucose-stimulated insulin secretion
GTT	Glucose tolerance test
HFD	High-fat diet
IP3	Inositol 1,4,5-trisphosphate

IP3R	Inositol trisphosphate receptor
ITT	Insulin tolerance test
KCNK16	Potassium two-pore domain channel subfamily K member 16
K2P	Two-pore domain K^+ channel
K_{ATP}	ATP-sensitive K^+ channel
KO	Knockout
M3R	Muscarinic acetylcholine receptor M3
NDM	Neonatal diabetes mellitus
PC	Prohormone convertase
PLC	Phospholipase C
PP	Pancreatic polypeptide
RyR	Ryanodine receptor
SERCA	Sarco/endoplasmic Ca^{2+} ATPase
SOC	Store-operated current
SOCE	Store-operated Ca^{2+} entry
SST	Somatostatin
SSTR	Somatostatin receptor
T1DM	Type 1 diabetes mellitus
T2DM	Type 2 diabetes mellitus
UPR	Unfolded protein response
VDCC	Voltage-dependent Ca^{2+} channel
V_m	Plasma membrane potential
WT	Wild-type

CHAPTER I

INTRODUCTION

Preface

Glucose metabolism and the pancreatic islets

Glucose is a fundamental metabolic substrate for nearly all eukaryotic cells. Serving as a primary source of energy and precursor for the synthesis of numerous macromolecules, the ability to precisely control systemic glucose levels is essential for proper physiological function. In humans, acute deviations from a narrow range of blood glucose concentrations ("euglycemia," approximately 4.0 – 6.0 mM (*1*)) can be hazardous, and chronically elevated blood glucose levels cause severe and permanent damage to several organs. Therefore, the body has complex regulatory mechanisms which exert tight control over circulating blood glucose levels. Preservation of euglycemia in the context of the daily fluctuations in systemic glucose supply and demand is accomplished by a complex network of signaling molecules released from many tissues, including the brain, digestive tract, liver, adipose tissue, muscle tissue, kidneys, and the endocrine pancreas.

The pancreatic islets (or islets of Langerhans) are the endocrine component of the pancreas. Islets serve a central role in controlling systemic glucose metabolism by producing insulin and glucagon, the body's primary blood glucose-lowering and -raising hormones. Insulin is released in response to elevations in blood glucose, suppressing hepatic glucose production and triggering target tissue glucose uptake. Glucagon is secreted under low glucose conditions to

stimulate glucose release from the liver, thus raising blood glucose levels. Together, insulin and glucagon constitute a bi-hormonal feedback system essential for euglycemia. Impairments in the mechanisms which control the secretion or response to these hormones results in disease.

First described in 1869 by German physiologist Paul Langerhans (*2*), islets are spherical micro-organs approximately 50 μm in diameter, comprising 1-2% of the tissue volume of the pancreas (*3, 4*). Individual islets are clusters of neuroendocrine cells including β-cells, α-cells, δ-cells, PP-cells, and ε-cells. Each of these cell types synthesize and secrete a characteristic hormone, respectively insulin, glucagon, somatostatin, pancreatic polypeptide (PP), and ghrelin. The secretion of islet hormones is tightly controlled by numerous islet-intrinsic and extrinsic factors which ensure that blood glucose levels are maintained within a narrow range. As islets are highly vascularized (receiving 10-20% percent of the pancreatic blood flow), they quickly sense and respond to changes in blood glucose levels.

Species-dependent differences in islet architecture (Figure 1.1) have important implications for understanding the molecular basis of dissimilarities in islet function and glucose handling between rodents and humans (*5*). For example, rodent islets contain proportionately more β-cells than human islets (75% versus 54%). Conversely, human islets possess relatively more α- and δ-cells than rodent islets (34% versus 19% for α-cells, and 10% versus 6% for δ-cells) (*6*). Rodent islets also show a clear cellular organization, with a β-cell core separated from a mantle of α- and δ-cells. Although the distinct organization of islet cell types is not as obvious in adult human islets (*5*), glucose regulation of hormone secretion is perturbed when islet cells are physically dissociated from each other (*7*). Such observations have led to the proposal that the arrangement of cells within the islet is crucial for physiological function (*8*).

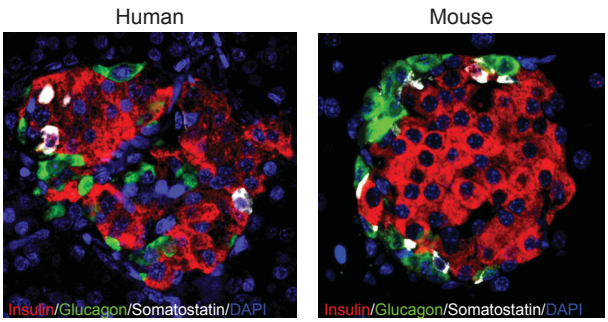

Figure 1.1. Islet morphology in human and rodent islets. Immunofluorscence of a human and mouse pancreas section stained for insulin (red), glucagon (green), somatostatin (white), and DNA (blue).

Cytoplasmic Ca^{2+}determines islet hormone secretion

It was first demonstrated in 1966 that extracellular Ca^{2+} is required for glucose-stimulated insulin secretion (GSIS) (*9*). It has been subsequently determined that all stimuli which elicit islet hormone secretion require Ca^{2+} influx to trigger an elevation in islet cell cytosolic Ca^{2+} (Ca^{2+}_c) (*9-12*). Cytosolic Ca^{2+} entry is mediated primarily by plasma membrane ion channels (voltage-dependent Ca^{2+} channels, VDCCs) whose activity is governed by the plasma membrane potential (V_m). Because the physiological functioning of VDCCs requires V_m depolarization and rapid repolarization (i.e., an action potential), modulation of the islet cell V_m is a key physiological mechanism controlling VDCC activity and hormone secretion. Indeed, elevated glucose levels stimulate the islet cell electrical activity necessary for insulin secretion, as first demonstrated by Dean and Matthews nearly 50 years ago (*13*).

K^+ channels control cytoplasmic Ca^{2+} influx

Virtually all cells maintain a trans-plasma membrane potential. The membrane potential is usually negative on the interior of the cell relative to the exterior, due to impermeant anions within the cell and the activity of the Na^+/K^+ pump. In electrically excitable cells, such as those of the pancreatic islet, the V_m is largely determined by plasma membrane K^+ permeability. Because of the large K^+ concentration gradient between the cytosol and the outside of the cell, plasma membrane K^+ channel opening promotes cellular K^+ efflux which hyperpolarizes the plasma membrane, K^+ channel regulation of the V_m thus serves a fundamental role in enabling the regenerative action potential firing and sustained Ca^{2+} influx required for hormone secretion. Studies as early as 1966 revealed that changing the extracellular K^+ concentration (which alters the V_m) dramatically impacts islet hormone secretion (*9, 14, 15*). Since these early investigations, many of the K^+ channels which regulate islet cell V_m and VDCC activity have been identified.

Although these studies have provided valuable insight into the importance of K^+ channels in islet cell function, when these studies began critical aspects of their roles in islet electrophysiology remained elusive. For example: 1) although it is well-established that islets generate oscillatory electrical activity in response to glucose (Figure. 1.2), the ionic mechanisms which regulate these oscillations are poorly understood; 2) while it is well-known that organelles such as the endoplasmic reticulum (ER) produce Ca^{2+} signals which regulate plasma membrane K^+ channel activity, the molecular mechanisms controlling these signals are largely unidentified; 3) the ER K^+ channels which determine ER Ca^{2+} release in islet cells are essentially unknown; 4) we have a poor mechanistic understanding of the mechanisms regulating electrical excitability in α- and δ-cells. These topics are further detailed in this introduction and achieving progress towards addressing these questions was a central focus of this dissertation.

Modern sequencing technologies immensely increased our ability to identify not only the genes encoding putative K^+ channels, but also the cell types which express them. In addition, genome-wide association studies (GWAS), which involve analyzing the genome of large populations to identify genetic markers associated with human disease, have identified candidate genes which regulate islet cell function and contribute to disease risk. To date, this approach has identified at least four K^+ channel genes associated with type-2 diabetes mellitus (T2DM) susceptibility, including *KCNJ11*, *KCNJ15*, *KCNQ1*, and *KCNK16* (a list of major K^+ channels identified to serve important roles in islet cell function is provided in Table 1.1). Transcriptome analysis of pancreatic islets revealed that the two-pore domain K^+ (K2P) channel TALK-1 encoded by *KCNK16* is the most abundantly expressed K^+ channel of the islet (at least at the mRNA level), and multiple groups have reported the primarily islet-restricted expression of TALK-1 (*16-20*). In 2012, a GWAS performed in individuals of East Asian ancestry identified a

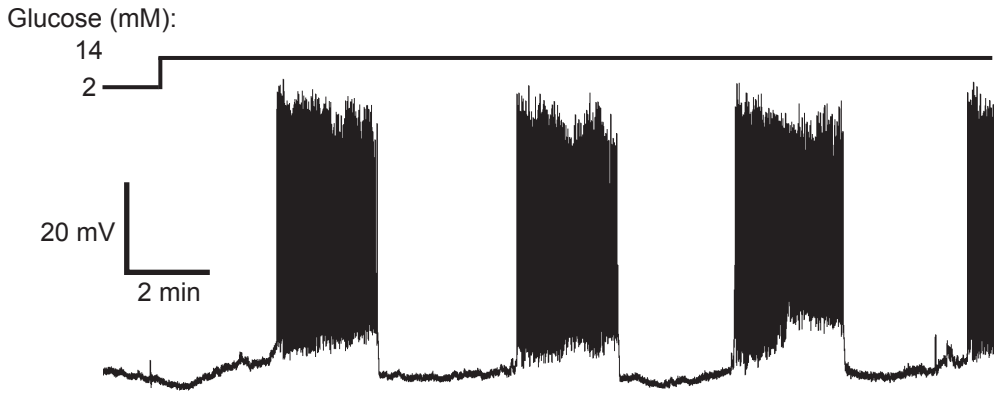

Figure 1.2. Glucose-stimulated oscillations in β-cell electrical excitability. Mouse β-cells were recorded in intact islets using the perforated patch-clamp technique and stimulated with the indicated glucose concentrations. The electrically silent periods between each oscillation are due in-part to activation of a Ca^{2+}-sensitive K^+ current, the "K_{slow}" current.

K^+ channel gene	Encoded protein	Role in islet cell function	Identified association with T2DM?
KCNJ11	Kir6.2	Glucose-dependent control of V_m	Yes (*21-24*)
KCNJ15	Kir4.2	Regulation of resting V_m	Yes (*25*)
KCNQ1	KCNQ1	Unclear; may regulate granule exocytosis	Yes (*22, 26*)
KCNB1	Kv2.1	Regulation of action potential repolarization; insulin exocytosis	No
KCNB2	Kv2.2	Modulation of somatostatin secretion	No
KCNMA1	KCa1.1 (BK)	Action potential repolarization	No
KCNN3	KCa2.3 (SK3)	Action potential repolarization	No
KCNN4	KCa3.1 (IK)	Action potential repolarization; component of K_{slow}	No
KCNK1	TWIK-1	Unclear	No
KCNK3	TASK-1	Regulation of plateau potential	No
KCNK16	TALK-1	(subject of this dissertation)	Yes (*27-30*)

Table 1.1. Major K^+ channels involved in regulation of islet cell electrical activity

non-synonymous polymorphism in *KCNK16* associated with susceptibility to T2DM. Similarly, rs1535500 was also found to be associated with T2DM in Pima American Indians (*28*). Interestingly, rs1535500 has not been directly associated with T2DM risk in individuals of European ancestry, although a trans-ethnic meta-analysis demonstrated that carriers of the rs1535500 allele have an increased risk for T2DM (*27, 29*). These findings highlight that an individual's genetic background is an important determinant of T2DM susceptibility.

Together, these observations suggest that TALK-1 channels serve an important functional role in the islet. However, prior to the studies described here, the physiological functions of TALK-1 channels were completely unknown. In many cells, K2P channels are important determinants of the V_m and electrical excitability; therefore, we hypothesized that TALK-1 channels are important for modulating islet cell electrical activity, controlling Ca^{2+}_c influx and hormone secretion. As TALK-1 is associated with T2DM, defining the physiological function and regulation of islet TALK-1 channels will advance our understanding of important mechanisms regulating islet cell function.

Mechanisms of islet cell hormone secretion

β-cells

In healthy individuals, insulin is released from β-cells in response to elevated glucose levels. Glucose enters β-cells through glucose transporters on the plasma membrane (Figure 1.3). Once in the cytoplasm, glucose is rapidly phosphorylated by glucokinase to glucose-6-phosphate (G6P) (*31*). Because the phosphorylation of glucose is rate-limiting for glycolysis and thus GSIS, glucokinase serves a pivotal role as a β-cell glucose sensor (*32*). G6P levels are also modulated by G6PC2, a glucose-6-phosphatase catalytic subunit expressed primarily in β-cells. G6PC2

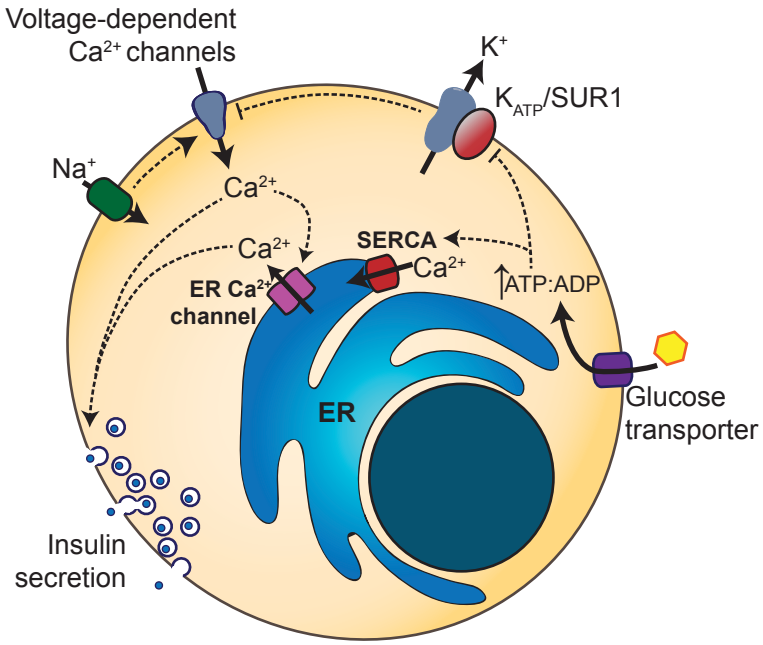

Figure 1.3. Consensus model of glucose-stimulated insulin secretion (GSIS). Glucose enters β-cells through glucose transporters (primarily GLUT1 and 3 in humans, Glut2 in rodents), where it is metabolized. Increased cellular ATP:ADP due to accelerated oxidative phosphorylation results in closure of K_{ATP} channels, leading to membrane potential (V_m) depolarization. This stimulates the opening of voltage-dependent Ca^{2+} channels (VDCCs), resulting in an elevation in cytosolic Ca^{2+} which triggers insulin granule exocytosis. Ca^{2+} uptake and release by the endoplasmic reticulum (ER) also serves an important role in shaping cytosolic Ca^{2+} handling.

dephosphorylates G6P in a cycle which reduces glycolytic production of pyruvate, tuning ATP production and GSIS (*33, 34*). Mutations and polymorphisms in these enzymes impair insulin secretion and can lead to diabetes (*33, 35, 36*).

Following its formation, G6P can enter anaerobic glycolysis, producing pyruvate and other metabolites important for β-cell glucose sensing (*37*). Pyruvate is oxidized through the tricarboxylic acid cycle in mitochondria, elevating cellular ATP levels. This increase in the β-cell ATP-to-ADP ratio is sensed by ATP-sensitive K^+ channels (K_{ATP}) and results in their closure, leading to V_m depolarization. Sufficient V_m depolarization triggers the activity of VDCCs, allowing Ca^{2+} to rush into the β-cell and interact with the exocytotic machinery of insulin granules, triggering insulin secretion.

K^+ channel regulation of β-cell electrical activity

K_{ATP} channels serve a central role coupling the β-cell V_m to glucose metabolism (*38, 39*). Functional K_{ATP} channels are composed of four pore-forming Kir6.2 subunits (encoded by *KCNJ11*), and four sulfonylurea receptor subunits (SUR1, encoded by *ABCC8*). As their name implies, K_{ATP} channels are gated by intracellular adenosine nucleotides. When cellular ATP levels are reduced (such as under low blood glucose conditions), K_{ATP} channels conduct K^+ currents which keep the V_m hyperpolarized. This prevents β-cell Ca^{2+} influx and inappropriate insulin secretion under low blood glucose conditions (*40*). K_{ATP} channels are the molecular target of the antidiabetic class of drugs known as sulfonylureas, which bind to SUR1 subunits and inhibit K_{ATP} channels, stimulating insulin secretion.

In addition to K_{ATP}, β-cells possess a number of K^+ channels which are very important for regulation of electrical activity. This includes (but is not limited to): inward-rectifying K^+ (K_{ir}) channels, which provide a tunable K^+ conductance separate from K_{ATP} (*25, 41, 42*); voltage-gated

K^+ (Kv) channels, which contribute to action potential repolarization and insulin granule exocytosis (*43-47*); Ca^{2+}-activated K^+ channels, which hyperpolarize the V_m, suppress action potential firing, and contribute to the regulation of pulsatile insulin secretion (*48-51*); and K2P channels, which are predicted to modulate the V_m both under resting states as well as during action potential firing (*52*). Although inhibition of K^+ conductance through any of these channels almost always results in increased insulin secretion, many of these channels are broadly expressed in many different tissues, limiting their therapeutic utility for treating diabetes.

Under high glucose conditions when K_{ATP} channels are closed, there is a residual K^+ conductance whose molecular determinants have not been conclusively determined (*53*). This K^+ conductance is essential for physiological hormone secretion because it stabilizes the V_m at a level needed for regenerative firing of action potentials (*53, 54*). K2P channels are a compelling candidate for explaining the molecular basis of these currents, as they are low-conductance K^+ channels predicted to be active when K_{ATP} channels are closed. β-cells have been shown to express TASK-1, TWIK-1, and TALK-1 K2P channels, all of which could conceivably mediate this current. The roles of K2P channels in β-cell electrophysiology are discussed in more detail below, and the contribution of TALK-1 channels to this current is examined in Chapter II.

Pulsatile insulin secretion and its underlying mechanisms

Circulating insulin levels show regular oscillations after meal ingestion as well as during fasting conditions (*55*). This is due to pulsatile insulin secretion from the pancreas, which is important for regulating hepatic glucose and lipid output as well as stimulating target tissue glucose uptake (*56*). Indeed, insulin administered in a pulsatile manner is much more effective at suppressing hepatic glucose production than continuous insulin delivery (*57*). This is especially important for post-prandial glycemic control and is related to the distinct biphasic insulin

secretion pattern which occurs after a meal. The first phase, consisting of a single pulse of insulin release, is triggered within a few minutes of nutrient ingestion and lasts for approximately 10-15 minutes. This is followed by the second phase of GSIS, which is oscillatory and continues until pre-prandial blood glucose levels are reestablished (*58*). The mechanistic basis of pulsatile insulin secretion lies in islet intrinsic oscillations of β-cell electrical activity, Ca^{2+} influx, and glucose metabolism.

Factors associated with glucose metabolism in β-cells exhibit regular oscillations, an effect which is believed to be an intrinsic quality of islet nutrient metabolism (*59*). These metabolic oscillations are believed to contribute to the oscillatory nature of electrical activity in β-cells: the V_m alternates between depolarized plateaus with superimposed action potential firing, separated by hyperpolarized silent periods (Figure 1.2). The termination of each period of excitability is thought to be due to a slowly activating, Ca^{2+}-sensitive K^+ current, termed the K_{slow} current (*60*). This current is potentiated by increasing Ca^{2+}_c levels which occur during periods of electrical excitability. Once sufficiently activated, K_{slow} hyperpolarizes the V_m and initiates an electrically silent period. Studies to determine the molecular identity of the channels mediating K_{slow} have revealed that this current reflects the composite activation of multiple β-cell K^+ channels. To date, intermediate-conductance K_{Ca} (SK4), apamin-insensitive small conductance (SK) K_{Ca}, and K_{ATP} channels have been shown to be part of K_{slow} (*48, 50, 61*). It is also known that ER Ca^{2+} release is critical for activation of the K_{slow} current. However, the molecular mechanisms which determine this ER Ca^{2+} release remain elusive. As studies of patients with T2DM have demonstrated that pulsatile insulin secretion is perturbed early in disease pathogenesis (*56*), defining how β-cells control oscillatory electrical activity may reveal novel mechanisms contributing to T2DM pathogenesis. The control of K_{slow}-activating ER Ca^{2+}

release and the relationship of TALK-1 channels to this process are further examined in this dissertation.

The role of ER Ca^{2+} in regulating β-cell function

Although extracellular Ca^{2+} influx is essential for insulin secretion, there are many intracellular channels and transporters, located primarily within the ER, which are essential for physiological Ca^{2+} handling. These mechanisms are important not only for controlling the Ca^{2+} fluxes required for hormone secretion but also diverse functions within islet cells including protein processing and metabolism. Sarco/endoplasmic Ca^{2+} ATPases (SERCAs) pump Ca^{2+} from the cytosol into the ER, helping to maintain ER Ca^{2+} as well as Ca^{2+}_c homeostasis. In order to maintain ER Ca^{2+} homeostasis, it is estimated that SERCAs account for 7-20% of cellular ATP consumption in the basal state (*219*). All cells within the islet express the high-Ca^{2+}-affinity SERCA isoform SERCA2b, which functions to maintain ER Ca^{2+} levels and helps set basal Ca^{2+}_c levels (*62*). The lower affinity SERCA3 is also selectively expressed in β-cells and serves an important role in shaping glucose-stimulated Ca^{2+}_c oscillations. β-cells lacking functional SERCA3 exhibit higher amplitude Ca^{2+}_c oscillations and lack the slowly descending "tail" of Ca^{2+}_c seen in control cells at the end of each oscillation (*63*). These observations indicate that SERCA3 is important for buffering Ca^{2+}_c influx due to VDCC activity.

All islet cells express inositol trisphosphate receptors (IP3Rs), ligand-gated Ca^{2+} channels localized almost exclusively to the ER membrane. IP3Rs are activated when bound by the plasma membrane-derived second messenger inositol 1,4,5-trisphosphate (IP3). Opening of IP3Rs typically results in a large release of Ca^{2+} from the ER into the cytosol, and the released Ca^{2+} can act as a co-agonist of IP3Rs to stimulate further ER Ca^{2+} release (*62*). Ca^{2+} release mediated by IP3Rs can have a range of effects on cellular function. For example, IP3R-mediated

Ca^{2+} release in most islet cells will increase hormone secretion and modulates electrical excitability (e.g., by activating plasma membrane Ca^{2+}-activated K^+ channels) (*64*). β-cells have also been shown to express ryanodine receptors (RyRs), Ca^{2+}-gated Ca^{2+} channels located on the ER membrane. Classically, RyRs mediate Ca^{2+}-induced Ca^{2+} release (CICR), a phenomenon in which an elevation of Ca^{2+}_c in the vicinity of RyRs triggers RyR opening. ER Ca^{2+} release through RyRs raises Ca^{2+}_c, potentiating the opening of nearby RyRs and sparking an increase in Ca^{2+}_c. In muscle cells, CICR is fundamental for excitation-contraction coupling; however, its existence in β-cells has been debated. For example, some groups have reported RyR-dependent amplification of GSIS (*65*) whereas other investigators have not observed these effects (*66*). The underlying molecular basis for these disparate observations has not yet been determined.

In alignment with the hypothesis that ER Ca^{2+} homeostasis serves a critical role in β-cell function, Tong and colleagues demonstrated that dysregulation of β-cell SERCA2b contributes to ER Ca^{2+} depletion and activation of the unfolded protein response (UPR) in a mouse model of T2DM (*67*). In human β-cells, it was also reported that patients with "leaky" RyR2 mutations (which result in an inability for RyR2s to close completely) exhibit diabetic phenotypes. Similarly, transgenic mice expressing these same RyR2 mutations demonstrate the same hyperglycemic phenotype, and islets from these mice show defective GSIS and activation of the UPR (*68*). Together, these observations demonstrate that normal ER Ca^{2+} handling is required for proper β-cell function. When compared to the relatively detailed comprehension of the mechanisms controlling plasmalemmal Ca^{2+} fluxes, we have only a rudimentary understanding of the mechanisms regulating β-cell ER Ca^{2+} homeostasis.

α-cells

Whereas low glucose levels suppress insulin secretion, α-cell glucagon secretion is stimulated under fasting conditions and is released at low levels in the non-fasted state (*69*). Glucagon elevates blood glucose levels by amplifying hepatic glycogenolysis and gluconeogenesis, sustaining blood glucose levels during conditions of increased glucose demand and fasting (*70*). The glucose-increasing effects of glucagon are potent; in humans, a dose of 0.5 ng/kg promptly induces long-lasting hyperglycemia (*71*).

Although it is clear that hypoglycemia stimulates glucagon secretion *in vivo* and *in vitro*, the mechanisms underlying glucose regulation of α-cell function remain controversial. In particular, the relative importance of intrinsic α-cell glucose-sensing mechanisms versus the many paracrine inputs of the islet in modulating glucagon secretion has been challenging to assign. In addition to α-cell autonomous mechanisms of glucose sensing and glucagon secretion, α-cells are under the control of numerous factors released from other cells in the islet, including insulin, GABA, and somatostatin, as well as input from the central nervous system (CNS) (*72, 73*). That normal α-cell function requires the intact islet environment is demonstrated by the observation that glucose inhibition of glucagon secretion disappears in purified preparations for α-cells (*7*). As hypoglycemia can be life-threating, perhaps it is not surprising that redundant mechanisms of controlling glucagon secretion evolved.

Electrical activity in α-cells

Like β-cells, α-cells exhibit glucose-sensitive electrical excitability; however, there are significant differences between β- and α-cell electrical activity. Under low glucose conditions which completely suppress β-cell electrical activity, α-cells exhibit large action potentials and oscillations in Ca^{2+}_c. Action potentials in α-cells are dependent on a different cohort of ion

channels than those found in β-cells. For example, α-cell glucagon secretion appears to be dependent on high-voltage activated P/Q-type VDCCs, unlike GSIS, which depends more on L-type VDCCs (*73*). Voltage-dependent Na^+ channels are also a major contributor to the upstroke of the α-cell action potential, and their activity in low glucose facilitates glucagon secretion (*74*). Interestingly, L-type VDCCs are present and mediate most (~80%) of Ca^{2+}_c influx in rodent α-cells, whereas in human α-cells L-type VDCCs are responsible for only ~20% of Ca^{2+}_c influx. L-type VDCCs appear to be critical for the α-cell response to epinepherine, during which glucagon secretion becomes much more sensitive to L-type VDCC inhibition (*75*). Consensus regarding the effects of glucose on the α-cell V_m has yet to emerge, however. Experimentally, both depolarizing as well as hyperpolarizing effects of glucose on the α-cell V_m have been reported. One model posits that α-cells share the K_{ATP}-dependent V_m depolarizing mechanism of β-cells. Thus, glucose metabolism would be predicted to depolarize the α-cell V_m, causing inactivation of voltage-dependent Na^+ channels and the P/Q-type VDCCs responsible for glucagon secretion in low glucose. Under low glucose conditions, α-cell K_{ATP} currents permit the hyperpolarized V_m needed for Na^+ channel-facilitated action potentials, allowing efficient P/Q-type VDCC opening to stimulate glucagon secretion (*76*).

A different model favoring a depolarizing effect of low glucose is based partially on observations that depletion of α-cell ER Ca^{2+} stores under low glucose conditions activates a depolarizing current called the store-operated current (SOC). At the molecular level, activation of the SOC involves ER-resident Ca^{2+} sensor STIM proteins interacting with and opening plasma membrane Orai Ca^{2+} channels in response to reduced ER Ca^{2+} levels. As Ca^{2+} influx through Orai depolarizes the V_m, the α-cell SOC amplifies Ca^{2+} influx and glucagon secretion in low glucose by activating VDCCs and triggering action potential firing (*72, 77, 78*). In support of this

model, Liu, Vieira and colleagues have demonstrated that pharmacological inhibition of SERCAs is sufficient to stimulate V_m depolarization and glucagon secretion (*77, 78*). The divergent observations of glucose's effects on the α-cell V_m may reflect slightly different experimental approaches, as well as the intrinsic heterogeneity of α-cells. Indeed, the recent finding that islet α-cells secrete GLP-1 (*79*) as well as observations of transcriptionally distinct α-cell subpopulations (*80*) suggests that the stimulus-secretion mechanisms may not be identical for all islet cells expressing protein products of the glucagon gene.

Although a unifying theory to describe the effects of glucose on α-cell electrical activity is still emerging, it is agreed that somatostatin signaling hyperpolarizes the α-cell V_m by activating G protein-coupled K_{ir} channels, or GIRKs (*42, 74, 81*). GIRK activation inhibits electrical activity and is predicted to inhibit Ca^{2+}_c influx, contributing to the suppressive effect of somatostatin on glucagon secretion. α-cells are under tonic control of somatostatin even at low glucose conditions, as inhibiting α-cell somatostatin signaling potently increases glucagon secretion in low glucose (*82*). However, the effects of somatostatin on α-cell Ca^{2+}_c dynamics in low glucose have not been determined, and the mechanisms regulating δ-cell somatostatin secretion are poorly understood.

δ-cells

As mentioned above, somatostatin released by islet δ-cells is a powerful inhibitor of glucagon as well as insulin secretion, an effect which is mediated by $G\alpha_i$ protein-coupled somatostatin receptors (SSTRs) expressed on the surface of α- and β-cells. Activation of SSTRs leads to cellular inhibition through a number of mechanisms, including Gαi-mediated suppression of cAMP production and cAMP-dependent signalling pathways (*83*), and Gβγ-dependent inhibition of VDCCs, activation of K^+ channels, and blockade of exocytosis (*41, 74*).

While insulin and glucagon serve essential roles in modulating peripheral tissue glucose handling, a role for somatostatin released from islet δ-cells outside of modulating islet-cell function has not been clearly established. Similar to insulin secretion, islet somatostatin secretion is augmented by increasing glucose levels. Glucagon and insulin secretion are enhanced in mouse islets with genetic ablation of somatostatin or SSTR2 (the predominant SSTR expressed in α-cells), and when treated with SSTR antagonists (*42, 84, 85*). These studies suggest that one of the primary physiological functions of islet δ-cells is to set the "tone" of islet insulin and glucagon secretion. However, very little is known about how δ-cells modulate islet function *in vivo*.

Electrical activity in δ-cells

Like insulin secretion, somatostatin release is accelerated by increasing glucose concentrations (*86*). Although δ-cells share similar transcriptional profiles to β-cells, there are significant differences in the molecular mechanisms which regulate δ-cell stimulus-secretion coupling. Somatostatin secretion is left-shifted relative to insulin secretion and is released at tonic levels as low as 1 mM glucose. The strong inhibitory effect of this small amount of somatostatin release on α-cells is revealed by blocking SSTR2 receptors at low glucose concentrations which greatly increases glucagon secretion (*82*). Islet δ-cells also show oscillations in Ca^{2+}_c and electrical excitability at low glucose concentrations below the threshold for insulin secretion (*87, 88*). At these low glucose concentrations, δ-cell K_{ATP} activity appears to be the primary modulator of somatostatin secretion. However, at higher glucose concentrations (>3 mmol/L glucose), secretion is less-dependent on K_{ATP} activity (*86*). Interestingly, inhibition of voltage-dependent K^+ channels stimulates somatostatin secretion four-fold at low glucose concentrations, but has no amplifying effect at higher glucose concentrations (*89*). These

observations suggest that action-potential dependent Ca^{2+} influx is more important for controlling somatostatin release in low glucose. Under elevated glucose conditions, it has been proposed that Ca^{2+}-induced Ca^{2+}-release (CICR) from the δ-cell ER amplifies somatostatin secretion.

By quantifying changes in membrane capacitance to assess exocytosis, it was observed that δ-cell exocytosis continues to increase after termination of the depolarizing stimulus (*86, 89*). This was found to be due to ER Ca^{2+} release triggered by opening of R-type VDCCs, potentiating somatostatin exocytosis. This effect could be blocked by pharmacologically depleting ER Ca^{2+} or antagonizing RyRs. In mouse δ-cells, CICR has been demonstrated to be due to a "loose-coupling" between R-type VDCCs and RyR3. However, although human δ-cells also exhibit the same delayed exocytosis kinetics as mouse δ-cells, they do not appear to express R-type VDCCs, nor do pharmacological blockers of RyRs impair this process (*89*). Thus, more work is clearly needed to understand the molecular mechanisms underlying somatostatin secretion in δ-cells.

PP- and ε-cells

Very little work has been done to define the stimulus-secretion mechanisms of PP- or ε-cells. PP-cells produce and secrete pancreatic polypeptide (PP), a 36-amino acid protein encoded by the *PPY* gene. The primary physiological functions of PP appear to be modulation of GI function and food intake. PP-cells exhibit oscillations in Ca^{2+}_c, but it does not appear that PP-cell Ca^{2+} influx is directly sensitive to glucose (*90*). Exogenous PP inhibits both insulin secretion and somatostatin secretion, suggesting that PP may serve an important role in facilitating glucagon secretion (*91*). However, in isolated islets, PP has been found to inhibit glucagon secretion at physiological concentrations while increasing glucagon secretion at supra-physiological concentrations (*92*). Interestingly, acetylcholine has been shown to stimulate increases in

circulating PP under hypoglycemic conditions, an effect which was lost by pancreatic denervation (*93*). More work is needed to understand whether islet PP-cells serve an important role in modulating glucose homeostasis.

Islet ε-cells produce and secrete ghrelin, a 28-amino acid peptide hormone which signals through GHSR, a $G\alpha_q$-coupled protein receptor. The physiological function of islet ghrelin is not well-understood, but it has recently emerged that intra-islet ghrelin signaling modulates δ-cell function (*94, 95*). It is also known that glucose infusion rapidly suppresses circulating ghrelin levels *in vivo* (*96*), but aside from the fact that ε-cells exhibit oscillations in intracellular cytosolic Ca^{2+} (Ca^{2+}_c) (*90*), the underlying mechanisms controlling ε-cell function are completely unknown.

Diabetes mellitus and islet dysfunction

Diabetes mellitus is characterized by chronic hyperglycemia (fasting blood glucose levels greater than 7.0 mM (*97*)), which if uncorrected causes several severe complications including diabetic ketoacidosis, retinopathy, peripheral neuropathies, and an increased risk for cardiovascular and kidney disease. In patients with type 1 diabetes mellitus (T1DM), hyperglycemia results from insulin deficiency due to autoimmune destruction of the insulin-producing β-cells. In patients with type 2 diabetes mellitus (T2DM), hyperglycemia is caused by increasing resistance of peripheral tissues to insulin action (insulin resistance) and β-cell dysfunction (Figure. 1.4). Diabetes mellitus can also arise from the increased insulin demand during pregnancy (gestational diabetes), as well as from autosomal dominant mutations in genes which are important for insulin production, secretion, or action (monogenic diabetes). Slightly over 9% of the US population currently has diabetes, and approximately 95% of these cases are

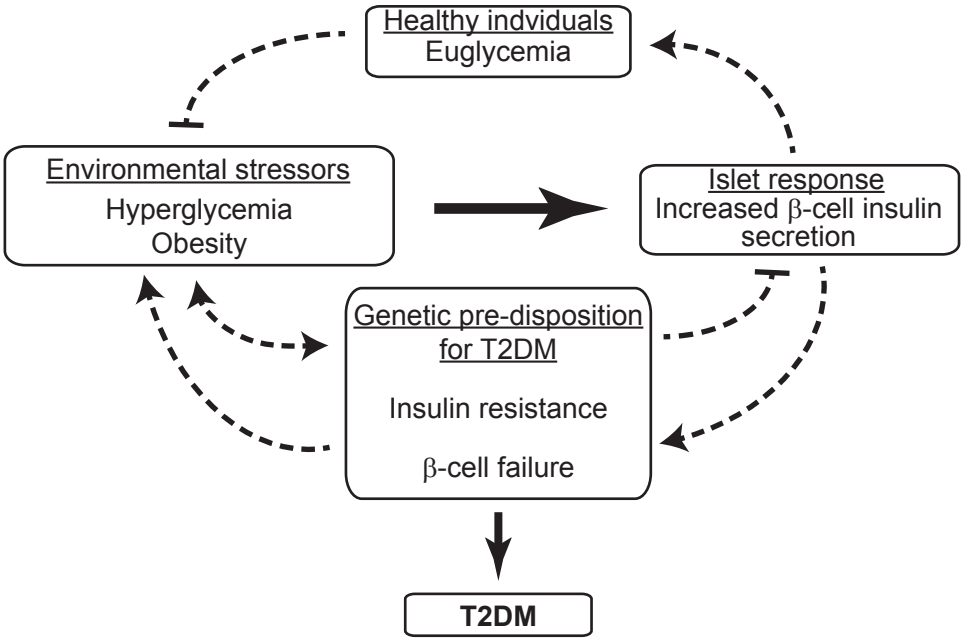

Figure 1.4. Hypothesized destructive feedback loop leading to T2DM. In healthy individuals, islets respond to hyperglycemia by secreting insulin, keeping blood glucose levels within a narrow range. However, in indivuals with increased genetic susceptibilty for T2DM, the β-cell secretory response to metabolic stressors may be inadequate, exacerbating hyperglycemia. Combined with increasing peripheral tissue insulin resistance, β-cells are unable to sustain sufficient insulin secretion needed to maintain euglycemia, leading to their failure and T2DM.

due to T2DM (*98*). With the prevalence of T2DM projected to increase throughout much of the world's population over the coming decades, defining the pathophysiological mechanisms which cause this disease will be essential for improving its diagnosis and treatment.

As mentioned above, there are at least two major causes of hyperglycemia in T2DM. One is insulin resistance, which arises when insulin-sensitive tissues such as muscle, adipose, and the liver fail to respond to normal insulin signaling. Insulin mediates its glucose-lowering actions through plasma membrane-localized insulin receptors, which stimulate increased cell surface expression of glucose transporters when activated (*99*). Although the molecular mechanisms of insulin resistance are incompletely understood, it is clear that physical inactivity an obesity are major risk factors (*100*). However, while environmental factors such as diet and sedentary lifestyle are key drivers of T2DM, many obese individuals do not develop T2DM, indicating that a patient's genetic background is a significant contributor to disease pathogenesis. In strong accordance with this possibility, T2DM heritability has been estimated at 40-70% (*101*). Interestingly, many of the genes which have been associated with T2DM risk are linked to islet-autonomous mechanisms which regulate insulin secretion, indicating that defects in islet function are a key driver of T2DM (*26*).

Islet dysfunction as a driver of diabetes mellitus

It has become clear that β-cell secretory defects are a core pathogenic mechanism in T2DM. Indeed, although peripheral tissue insulin resistance contributes to T2DM pathogenesis, many insulin resistant individuals fail to develop T2DM (*102, 103*). In individuals able to maintain euglycemia, increased systemic insulin demand causes a corresponding increase in β-cell insulin output and may also cause an expansion in functional β-cell mass. However, in individuals with a high susceptibility for developing T2DM, there may be existing defects in β-

cells that impact the capacity of β-cells to augment and sustain their function or increase in mass to meet the body's increased need for insulin, precipitating disease. In accordance with the hypothesis that islet dysfunction is a key driver of T2DM, many of the T2DM-linked genes identified in GWAS are implicated in β-cell function and insulin secretion. Accordingly, disrupted insulin secretion is a hallmark of T2DM (*56*).

Multiple mechanisms have been implicated in the loss of β-cell function in patients with T2DM. One pathogenic mechanism proposed to contribute to defective β-cell function is ER stress, which is caused by increased insulin secretory demands due to peripheral tissue insulin resistance (*102*). Prolonged and excessive elevations in insulin production can trigger the unfolded protein response (UPR), which can lead to further impairments in β-cell secretory capacity and eventual destruction. Another mechanism speculated to cause β-cell dysfunction is oxidative stress. β-cells express low levels of antioxidant enzymes, which may impair their ability to effectively clear toxic reactive oxygen species (ROS) under the chronic metabolically stressful conditions associated with T2DM (*104*).

Aberrant glucagon secretion from pancreatic α-cells has also long been suspected to contribute to hyperglycemia in T2DM. Although evidence of α-cell hyperplasia was first observed in some patients with T2DM as early as the 1950s (*105*), a clinical demonstration of inappropriate glucagon secretion in patients with T2DM did not occur until the 1970s (*106, 107*). However, the mechanisms underlying α-cell stimulus-secretion coupling under non-diabetic conditions remain controversial and very little is known about the causes of altered α-cell glucagon secretion in T2DM. In a mouse model of diabetes, it was shown that β-cell loss induces glucagon hypersecretion by increasing α-cell electrical excitability (*108*).

In humans, much less is known about the contributions of δ-cell dysfunction to the development and progression of T2DM. However, polymorphisms in the transcription factor HHEX have been linked to an increased risk for T2DM, and it has been found that an important role of this transcription factor is to maintain δ-cell number and function. Thus, in some patients, defective somatostatin signaling from islet δ-cells may contribute to increased glucagon secretion (*109*). Morphologic changes in δ-cells have been noted in islets from leptin-receptor deficient (db/db) (*110*) mice as well as patients with T1DM (*111*), suggesting that alterations in somatostatin signaling may contribute to islet dysfunction. As dysfunctional somatostatin secretion has been implicated in the etiology of T1DM and T2DM, more studies are needed to better understand the mechanisms controlling δ-cell function.

Defining the mechanisms which regulate islet cell hormone secretion could yield a more complete understanding of T2DM etiology and guide the design of rational therapies to treat islet dysfunction. Such therapies should address the underlying molecular defects causing reduced GSIS rather than simply augmenting insulin secretion. Indeed, certain therapeutics used to increase insulin secretion in patients with T2DM (i.e., sulfonylureas) may lead to β-cell exhaustion, exacerbating deterioration of β-cell function (*112*).

K^+ channels in T2DM

To date, polymorphisms in at least four K^+ channel genes have been associated with an increased risk for T2DM. These include *KCNJ11* (encoding Kir6.2, the K^+ channel subunit of K_{ATP}), *KCNQ1* (encoding a voltage-gated K^+ channel), *KCNJ15* (encoding Kir4.2), and *KCNK16* (encoding TALK-1). While it is well-known that K_{ATP} channels serve a critical role in controlling GSIS, the expression and functional roles KCNQ1, Kir4.2, and TALK-1 channels

within the islet are not as apparent, making biological investigation necessary to determine the mechanisms underlying their contributions to T2DM etiology.

Multiple single-nucleotide polymorphisms in K_{ATP} are associated with an increased risk for T2DM, highlighting its central importance in regulating β-cell function. Nearly all of the polymorphisms and mutations in K_{ATP} which increase diabetes susceptibility do so by increasing V_m-hyperpolarizing K^+ currents (*21*). Similarly, several mutations in Kir6.2 and SUR1 cause a gain-of-function in K_{ATP} channel activity, suppressing insulin secretion and causing neonatal diabetes mellitus (NDM) (*39*). Patients with NDM due to mutations in K_{ATP} can often be treated with a class of antidiabetic drugs known as sulfonylureas, which increase insulin secretion by inhibiting K_{ATP} channel activity (*113*).

The polymorphism in *KCNJ15* associated with an increased susceptibility for T2DM (rs3746876, a synonymous SNP suspected to influence mRNA processing) has been shown to increase *KCNJ15* mRNA abundance, which could increase T2DM risk by elevating hyperpolarizing K_{ir} currents that result in less β-cell VDCC activity and insulin secretion (*25*). Indeed, GSIS is significantly increased when $K_{ir}4.2$ channel expression is reduced in mouse islets. However, more work is needed to determine the physiological functions of $K_{ir}4.2$ channels in β-cells.

Although the rs2237895 SNP in *KCNQ1* is linked to an increased risk for diabetes, this channel does not appear to be expressed in human islets (*20, 80*). However, it has been reported that insulin exocytosis from islets from individuals carrying the *KCNQ1* risk allele is diminished under conditions when Ca^{2+} channel activity is experimentally clamped (*22*). These observations suggest that this polymorphism might be impacting the expression of other β-cell genes

important for insulin secretion, or influencing KCNQ1 function in another tissue. Accordingly, rs2237895 is located within an intron of *KCNQ1* which may influence gene expression.

Unlike *KCNQ1*, *KCNK16* mRNA is abundantly expressed in pancreatic islets. Moreover, the tissue expression pattern of *KCNK16* is primarily islet-restricted (*17, 18, 114*), although its mRNA is also present in gastric somatostatin-expressing cells (*115*). As the T2DM-associated SNP in *KCNK16* (rs1535500, encoding TALK-1 A277E) lies within the coding region of the gene, it is possible that this polymorphism could result in changes in TALK-1 channel activity which are detrimental to islet cell function. However, no physiological role had been reported for TALK-1 channels when my studies began, necessitating experimentation to determine its biological function. In the following section, I summarize the biophysical and physiological characteristics of K2P channels which provide the theoretical foundation for the studies presented herein.

Two-pore domain (K2P) channels

The existence of constitutively active K^+ channels controlling the resting V_m was predicted long before K2P channels were identified as molecular mediators of this current. In research which laid the groundwork for the study of ion channels, it was determined that a constant "leak" of K^+ and other ions was needed to account for the biophysics of electrically excitable membranes (*116, 117*). It took another 50 years to determine that K2P channels were responsible for conducting these background K^+ currents (*118*).

K2P channels are a major subclass of K^+ channels which can be found throughout the animal kingdom. The human genome encodes 15 K2P channels*, which can be classified into discrete groups based on their biophysical characteristics. Like all K^+-selective channels, K2P channels are transmembrane proteins possessing a K^+ selectivity filter created by the symmetrical assembly of four pore-forming domains around an ion-conducting pore. As implied by their name, functional K2P channels are a dimer of α-subunits, each containing four transmembrane segments with two pore-forming P-domains (Figure 1.5). This is unlike all other K^+ channels, tetrameric complexes composed of four α-subunits with each subunit containing a single P-domain. The membrane topology of K2P channels has been confirmed with multiple high resolution structures: K2P channels possess an extracellular "cap" domain which covers the pore region of the channel, and has two lateral fenestrations which allow K^+ flux into the pore domain. The cap domain is thought to be the molecular basis for the resistance of K2P channels to pharmacological blockade by inhibitors of most other K^+ channels (*119*).

As K2P channels conduct K^+ currents which are important for setting the resting V_m, modulation of K2P channel activity can regulate cellular electrical activity. Based on their functional characteristics, up- or downregulation of K2P channel activity should promote or limit V_m hyperpolarization, thus modulating Ca^{2+} influx. Accordingly, many regulatory signals target K2P channels to control the function of excitable cells. Among the many stimuli which influence K2P channel activity are intracellular and extracellular pH*, numerous lipids, plasma membrane

* HUGO nomenclature for K2P channels is "KCNK*x*"; the K2P channel literature tends to denote gene and mRNA using the "KCNK*x*" convention, whereas the protein product is referred to with a distinct name (e.g., the *KCNK16* gene encodes TALK-1 channels).

* Regulation by extracellular pH is a biophysical characteristic of many K2P channels and was used to describe the different K2P channels as they were cloned and characterized. Most K2P channels derive their name from TWIK-1 ("Tandem of P-domain in a Weak Inwardly rectifying K^+ channel"), the first K2P channel isolated in mammals. For example, the K2P channel TASK-1 is inhibited by extracellular acidification; thus, it was designated "**T**WIK-related **A**cid-**S**ensitive **K**$^+$ channel-1."

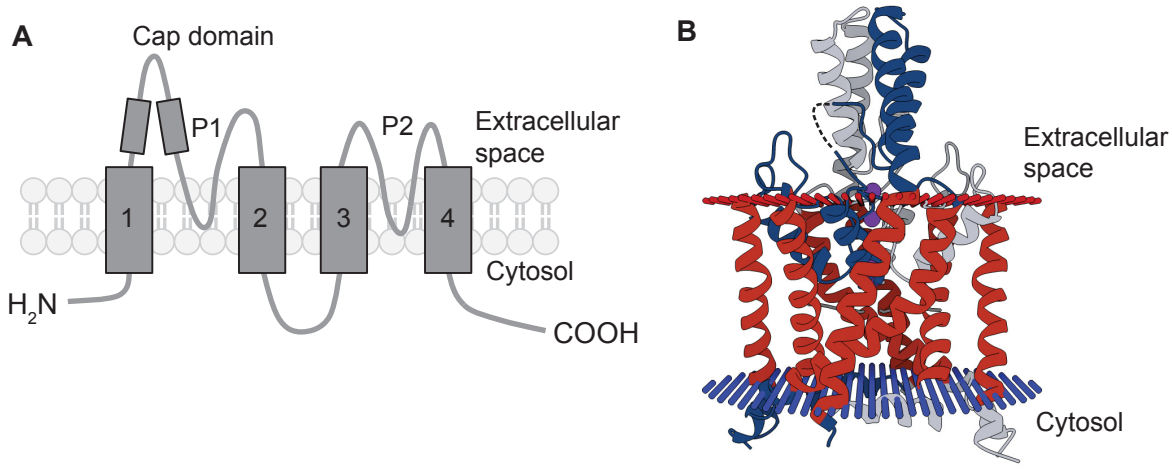

Figure 1.5. Membrane topology and quaternary structure of K2P channels. (A) Each α subunit of a K2P channel contains four transmembrane domains and two pore-forming P domains. (B) Transmembrane view of TWIK-1, a prototypical K2P channel, as determined from a 3.4-Å-resolution crystal structure. Note that extraceullar loop regions (shown as dashed lines) and intracellular N- and C-termini are absent in this structure. K^+ ions are depicted as purple spheres. Image from the RCSB PDB (www.rcsb.org) of PDB ID 3UKM (Miller, A.N., and Long, S.B. *Crystal structure of the human two-pore domain potassium channel K2P1*. (2012) Science 335: 432-436); image used in accordance with RCSB PDB policies.

stretch, post-translational modifications including phosphorylation, SUMOylation, palmitoylation [Jacobson lab observations], and a plethora of binding factors which control channel opening and trafficking. This wide array of modulators allow K2P channels to control a number of physiological processes, including hormone secretion, nociception, osmoregulation, and cardiovascular function (*120*). Most of these regulatory stimuli converge on the intracellular COOH-terminal tail (*Ct*) of K2P channels, and genetic deletion or functional uncoupling of the *Ct* precludes the regulatory effects of many of these stimuli.

Physiological roles of K2P channels in excitable cells

As there is presently a scarcity of K2P channel-specific pharmacology, the identification of the physiological functions of K2P channels has largely been determined from phenotypes observed in K2P channel knockout (KO) mice. K2P channel KO models have helped distinguish the contributions of different K2P channels in neurons, where they have been shown to regulate electrical excitability through their effects on the V_m. Studies of these mice led to the discovery that many K2P channels are a molecular target of volatile anesthetics. For example, mice lacking the K2P channel TREK-1 (encoded by *KCNK9*) are refractory to anesthesia (*121*).

In agreement with the hypothesis that K2P channels tune electrical excitability, both TREK-1 and TREK-2 (*KCNK10*) K2P channels are expressed at high levels in neurons of the dorsal root ganglia and are implicated in nociceptive sensitivity. Mice lacking these channels show increased responses to painful stimuli (*122, 123*), suggesting that these channels could be novel therapeutic targets for painful neuropathies (*124*). K2P channels have also been implicated in the regulation of thalamacortical relay (TC) neurons, which are important for the control of sleep-wake cycles. TASK-3 KO mice show altered electrical oscillations and disrupted sleep-wake patterns, consistent with a role for TASK-3 channels in controlling TC neuron function

(*125*). Interestingly, a mutation in TASK-3 causes Birk-Barel syndrome, a disease characterized by intellectual disability, hypotonia, and facial dysmorphism (*126*), suggesting that TASK-3 also serves important roles in development. The Ca^{2+}-activated K2P channel TRESK (encoded by *KCNK18*) regulates electrical excitability in trigeminal ganglion neurons (*127*), and mutations in TRESK have been identified in patients with severe migraine (*128*). Together, these observations broadly demonstrate that K2P channels modulate cellular function by controlling the threshold for electrical excitability.

K2P channels in the islet

TWIK-1 channels

Pancreatic islets express mRNA for several K2P channels; however, the physiological function of most of these channels is unclear. The first K2P channel identified in the pancreas was TWIK-1 (encoded by *KCNK1*) (*118*). This K2P channel exhibits intrinsically low K^+ channel activity at the plasma membrane due to its predominant localization to endosomes. Interestingly, it was demonstrated that the acidic pH of endosomes (~pH 6.0) causes a change in the ionic preference of TWIK-1 for Na^+ over K^+. This produces a transient Na^+ current at the plasma membrane which dissipates as TWIK-1 switches back to a K^+ conductance or is internalized (*129*). TWIK-1 is expressed in many tissues throughout the body and is present in both the exocrine and endocrine pancreas. However, a physiological function for TWIK-1 remains unclear. It has been suggested that cardiac TWIK-1 channels contribute to hypokalemia-induced cardiac arrhythmias through its Na^+-conducting properties (*130*). β-cells lacking functional TWIK-1 channels were found to be paradoxically hyperpolarized in high glucose, presumably due to the loss of depolarizing Na^+ currents through TWIK-1. However, the effect of TWIK-1 deletion on islet hormone secretion has not been examined.

TASK-1 channels

The next K2P channel found to be expressed in the pancreas was TASK-1 (encoded by *KCNK3*) (*131*). TASK-1 channels exhibit greater K^+ channel activity than TWIK-1, producing rapidly activating, voltage-independent currents that are highly sensitive to fluctuations in extracellular pH. However, the importance of the pH sensitivity of TASK-1 is uncertain, as a relationship between pH and the physiological functions of this channel has not been determined. In the adrenal glands, TASK-1 channels are important determinants of aldosterone secretion. Mice lacking TASK-1 exhibit hyperaldosteronism and hypertension. While the molecular mechanisms linking TASK-1 to aldosterone secretion are unclear, defects in adrenocortical cell Ca^{2+} signaling are suspected (*132*). In the islet, the role of TASK-1 in both β- and α-cells has been investigated. Treatment of β-cells with A1899, a selective TASK-1 antagonist, causes V_m depolarization and enhanced Ca^{2+}_c influx, indicating that TASK-1 channels control β-cell VDCC activity. β-cell specific knockout of TASK-1 channels produces similar effects on V_m and Ca^{2+}_c as A1899, leading to enhanced insulin secretion and improved glucose tolerance (*52*). In α-cells, the effects of A1899 on the V_m and Ca^{2+}_c influx are very similar to its effects on β-cells, causing V_m depolarization and augmenting Ca^{2+}_c influx. Interestingly, genetic deletion of α-cell TASK-1 shows a unique effect on glucagon secretion when compared to pharmacological inhibition of TASK-1. Whereas treatment of islets with A1899 increases glucagon secretion in high (11 mmol/L) glucose, α-cell TASK-1 KO islets show reduced glucagon secretion under this condition. Thus, mice lacking α-cell TASK-1 channels have improved glucose tolerance. As inhibition of TASK-1 channels has no effect on Ca^{2+}_c or glucagon secretion under low (1 mmol/L) glucose conditions, TASK-1 channels most likely modulate α-cell function specifically under high glucose conditions (*133*). Although the underlying molecular basis for the differential

effects of TASK-1 pharmacology compared to genetic deletion of TASK-1 on glucagon secretion have not been determined, it may relate to an intracellular function for TASK-1 channels. As detailed in Chapter III, TASK-1 channels are functionally present in the α-cell ER where they modulate ER Ca^{2+} fluxes; genetic deletion of TASK-1 channels may uncover this contribution to α-cell function, whereas TASK-1 pharmacologically would acutely affect primarily plasma membrane TASK-1 channels. Together, these findings indicate that TASK-1 channels modulate β- and α-cell electrical excitability and Ca^{2+}_c influx, controlling hormone secretion.

TALK-1 channels

In 2001, the Lesage group reported the cloning and characterization of TALK-1 (*KCNK16*), TALK-2 (*KCNK17*), and THIK-2 (*KCNK12*) (*114*). While all three of these K2P channels' mRNAs are expressed in the pancreas, only TALK-1 expression appeared to be restricted to the pancreas. Later studies by the Kim group also demonstrated that TALK-1 mRNA is abundant in the pancreas and is detectable at low levels in stomach tissue (*134, 135*). Whole-transcriptome studies of pancreatic tissue have revealed that TALK-1 mRNA is highly expressed in the pancreatic islets and is virtually undetectable in exocrine tissue (*16-20*). When compared to other tissues in the body, *KCNK16* expression was found to be among the most highly islet-restricted genes (*17*). Moreover, as described above, a non-synonymous polymorphism in *KCNK16* increases T2DM susceptibility.

KCNK16 shows strong sequence conservation in mammals. In humans, alternative splicing gives rise to at least five unique TALK-1 mRNAs, two of which encode functional TALK-1 channels differing only in their COOH-terminal tails (TALK-1a and TALK-1b). Interestingly, alternative splicing of TALK-1 mRNA is not found in rodents, which produce

TALK-1 channels homologous to human TALK-1b. The relative importance of the two different TALK-1 channel isoforms remains uncertain. When expressed in *Xenopus* oocytes, TALK-1 channels were found to be insensitive to most traditional regulators of K^+ channels, changes in Ca^{2+}_c, and activation of $G\alpha_i$ or $G\alpha_q$-coupled protein receptors (*114*). However, TALK-1 channels do show activation by alkaline extracellular pH, hence the name **T**WIK-related **AL**kaline pH-activated **K**$^+$ channel-1. By examining single-channel current recordings of TALK-1, the Kim group found that elevating extracellular pH increases the frequency rather than the unitary current amplitude of channel opening, enhancing aggregate whole-cell TALK-1 K^+ currents (*134*). Nitric oxide and reactive oxygen species have also been shown to activate TALK-1 channels, but the physiological relevance of these stimuli on TALK-1 channels has yet to be determined (*136*). Although the functional consequences on TALK-1 channel activity are unclear, protein interactome studies have also demonstrated that the majority (>60%) of proteins which interact with TALK-1 are ER resident proteins (*137, 138*). As similar studies with other K2P channels have not identified such a large percentage of interacting proteins which are ER residents, these observations suggest that TALK-1 channels could serve an intracellular function. Together, these findings provide a useful framework to investigate the physiological function of TALK-1 channels.

Goals of this thesis

The prominent expression of TALK-1 in the islet and its link with T2DM led us to hypothesize that one of the physiological functions of TALK-1 is to modulate islet hormone secretion. Moreover, the islet-restricted expression of TALK-1 suggests that it could be an attractive therapeutic target for the treatment of T2DM. However, the lack of knowledge regarding the physiological functions of TALK-1 channels presents a significant barrier to testing the validity of this hypothesis. Therefore, the central goal of this dissertation was to define the major functional roles of islet TALK-1 channels.

In the following chapters, I describe our investigations of islet cell electrical activity, Ca^{2+}_c handling, ER Ca^{2+} homeostasis, and hormone secretion in islets obtained from mice without functional TALK-1 channels as well as in primary human islet cells. In addition, I detail the effects of TALK-1 channel activity on islet health and the whole-animal glycemic response to high-fat diet (HFD) feeding, a paradigm of diabetes-inducing metabolic stress. First, we used mice lacking *Kcnk16* (encoding TALK-1) to identify the functional role of TALK-1 channels in β-cells and its contributions to systemic glucose metabolism. We found that TALK-1 forms a functional K^+ channel in mouse and human β-cells, where it limits electrical oscillations, Ca^{2+}_c oscillations, and insulin secretion. In addition, we discovered that TALK-1 channel activity is associated with impaired fasting glycemia after HFD feeding, and that the T2DM-associated SNP rs1535500 (encoding TALK-1 A277E) potentiates K^+ currents through TALK-1.

The finding that TALK-1 channels regulate β-cell Ca^{2+}_c oscillations inspired us to determine the underlying molecular mechanisms. In addition to our observation of prominent intracellular staining of TALK-1, reports of TALK-1 interacting predominately with ER proteins (*137*) prompted us to examine whether TALK-1 channels influence the ER Ca^{2+} handling which

controls islet Ca^{2+}_c oscillations. We found that ER-resident TALK-1 channels conduct a K^+ countercurrent which modulates ER Ca^{2+} stores, thus influencing ER Ca^{2+} release and islet Ca^{2+}_c oscillations. Moreover, we found that inhibiting TALK-1 channel activity protected islets from HFD-induced activation of ER stress, suggesting the exciting possibility that inhibiting TALK-1 channel activity could be a therapeutic strategy to ameliorate islet dysfunction in T2DM. Finally, we assessed the role of TALK-1 channels in islet δ-cell function. TALK-1 channels limit δ-cell CICR, controlling somatostatin secretion. TALK-1 KO islets secrete more somatostatin, causing a reduction in α-cell Ca^{2+}_c influx and glucagon secretion.

The observations presented here indicate that TALK-1 channels modulate insulin, somatostatin, and glucagon secretion. These findings suggest that a gain-of-function in TALK-1 channel activity could potentially impair insulin secretion and contribute to T2DM development or progression. In addition, our finding that TALK-1 channels serve an intracellular function in the ER represents a previously unidentified physiological function of K2P channels and improves our comprehension of the mechanisms controlling islet cell ER Ca^{2+} handling. Overall, the studies described in this dissertation have advanced our understanding of the mechanisms underlying islet cell physiology in health and disease.

CHAPTER II

TALK-1 CHANNELS MODULATE β-CELL ELECTRICAL EXCITABILITY, 2ND-PHASE INSULIN SECRETION, AND GLUCOSE HOMEOSTASIS*

Preface

This chapter explores the functional roles of TALK-1 channels in β-cells. Prior to the studies described here it was known that TALK-1 is abundantly expressed at the mRNA level in pancreatic islets. Moreover, it had been determined that a non-synonymous single-nucleotide polymorphism (SNP) in *KCNK16* (rs1535500, encoding TALK-1 A277E) increased susceptibility for T2DM. However, a functional role for TALK-1 channels in the islet had not yet been identified. Our data demonstrate that TALK-1 forms functional K^+ channels in mouse and human β-cells where it limits Ca^{2+} influx and insulin secretion. We discovered that TALK-1-deficient islets secrete more insulin *ex vivo* and that TALK-1 knockout (KO) mice are protected from high-fat diet-induced increases in fasting glycemia. Additionally, we found that the T2DM-associated TALK-1 A277E risk variant produces enhanced K^+ currents relative to the non-risk variant. These findings allowed us to make the prediction that rs1535500 may contribute to T2DM susceptibility by limiting GSIS. A recent study in human patients with T2DM supports this hypothesis, as it was found that those carrying the risk rs1535500 SNP show significantly reduced GSIS in response to an intravenous glucose challenge (*30*).

*The work presented in this chapter is adapted from: Vierra NC, Dadi PK, Jeong I, Dickerson M, Powell DR, Jacobson DA. Type 2 Diabetes-Associated K+ Channel TALK-1 Modulates beta-Cell Electrical Excitability, Second-Phase Insulin Secretion, and Glucose Homeostasis. Diabetes. 2015;64(11):3818-28. doi: 10.2337/db15-0280. PubMed PMID: 26239056; PMCID: PMC4613978.

Introduction

Pancreatic β-cell insulin secretion plays a central role in maintaining glucose homeostasis. GSIS is coupled to Ca^{2+} influx, which is modulated by the orchestrated action of several ion channels. The primary glucose-sensitive channel of the β-cell is the ATP-sensitive K^+ channel (K_{ATP}). K_{ATP} is active under low glucose conditions, limiting insulin secretion by hyperpolarizing the V_m and inhibiting voltage-dependent Ca^{2+} channels (VDCCs). Increased β-cell metabolism due to elevated glucose levels raises the intracellular ATP:ADP ratio, inhibiting K_{ATP} channels. The closure of K_{ATP} channels results in V_m depolarization to a plateau potential from which action potentials (APs) fire, allowing Ca^{2+} influx through VDCCs, resulting in insulin secretion (*139, 140*). During glucose-induced K_{ATP} inhibition, the plateau potential is stabilized by small conductance K^+ currents (*141, 142*), such as those mediated by two-pore domain K^+ (K2P) channels. For example, TWIK-related Acid Sensitive K2P (TASK-1) channels have been shown to polarize β-cell plateau potential suppressing Ca^{2+} entry through VDCCs and limiting GSIS (*52*). However, the physiological role of the most abundant β-cell K2P channel, TWIK-related alkaline pH-activated K2P channel (TALK-1), remains unexplored. Because TALK-1 channels may regulate β-cell Ca^{2+} influx and GSIS, defining their physiological roles may identify TALK-1 channels as a therapeutic target for T2DM.

TALK-1 was originally cloned from human pancreas (*114, 134*). *KCNK16*, the gene encoding TALK-1 channels, is the most abundant K^+ channel transcript in mouse and human β-cells (*17, 20, 143*). Moreover, *KCNK16* is the most islet-specific transcript in mice when compared to all other transcripts across six tissues assessed by transcriptome analysis (*17*). In humans, the *KCNK16* locus exhibits increased histone H3 methylation in islets compared to non-islet tissues, indicating that the locus is transcriptionally active in islets (*18*). While these

observations suggest that TALK-1 channels serve an important role in the islet, the physiological functions of TALK-1 remain to be determined.

The biophysical characteristics of TALK-1 have been defined in heterologous expression systems. These studies have revealed that TALK-1 channels produce outwardly rectifying, non-inactivating K^+ currents which are enhanced by elevations in extracellular pH (*114*). Additionally, reactive oxygen species such as singlet oxygen have been demonstrated to increase TALK-1 channel activity (*114, 134-136*). As TALK-1 currents resemble TASK-1 currents that modulate GSIS, TALK-1 may also play a role tuning β-cell V_m and GSIS. Nevertheless, to date there has been no examination of TALK-1 in primary cells, limiting our understanding of TALK-1 channel function.

Interestingly, genome-wide association studies have found that a non-synonymous polymorphism in TALK-1 (rs1535500) is associated with risk for T2DM (*27, 29, 144*). The rs1535500 polymorphism in TALK-1 results in a glutamate substitution at alanine 277 (A277E), in TALK-1's cytoplasmic C-terminal tail (*Ct*). Given the high expression of TALK-1 in the islet, it has been hypothesized that polymorphisms in TALK-1 might influence hormone secretion, contributing to T2DM predisposition (*27*). The A277E polymorphism may alter K^+ currents through TALK-1, potentially perturbing β-cell V_m, Ca^{2+} influx, and insulin secretion contributing to the pathogenesis of T2DM. Therefore, defining the islet cell functions of TALK-1 channels in physiological and diabetic states is required to understand the role of polymorphisms in *KCNK16* in the development of T2DM.

Here, we show that TALK-1 channels are key regulators of β-cell V_m, Ca^{2+} influx, and GSIS. We also reveal that rs1535500 increases TALK-1 channel activity, which may limit GSIS. These studies reveal that TALK-1 channels are important determinants of β-cell electrical

excitability, and suggest that changes in TALK-1 activity impact GSIS and contribute to the pathogenesis of T2DM.

Results

Pancreatic β-cells express functional TALK-1 channels.

We first determined whether TALK-1 channels are functionally expressed in mouse β-cells. Using immunofluorescence staining of mouse pancreatic sections for TALK-1 and insulin, we found that TALK-1 was specifically expressed in the islet and co-localized with insulin-positive β-cells, but not α-cells (Figure 2.1A). Although *Kcnk16*$^{-/-}$ (TALK-1 knockout, KO) sections exhibited a similar staining pattern as WT sections, this was due to the recognition of the truncated TALK-1 protein produced by the targeted *Kcnk16* allele by the TALK-1 antibody (Figure 2.2). Although the function of this truncated protein remains unknown, it may still enable protein interactions which occur at the amino-terminal portion of TALK-1. We next used patch clamp electrophysiology techniques to determine whether TALK-1 currents are present in β-cells. To specifically examine K2P channels, voltage gated K^+ (K_v) channels were blocked with TEA (10 mM), K_{ATP} channels were blocked with tolbutamide (100 μM), and Ca^{2+} was removed from the extracellular buffer to prevent activation of Ca^{2+}-activated K^+ (K_{Ca}) channels. In *Kcnk16*$^{+/+}$ (wildtype, WT) β-cells, an outwardly rectifying, non-inactivating K^+ current was observed (Figure 2.1B), indicating the presence of K2P channels as previously described (*52*). K2P currents recorded from TALK-1 KO β-cells were significantly reduced (pA/pF at +60 mV: WT, 18.3 ± 1.2, n = 23; vs. KO, 11.7 ± 1.0, n = 25; three mice per genotype; $P < 0.001$) (Figure 2.1C), indicating that TALK-1 forms a K^+ channel in mouse β-cells, and that K^+ channel function is not retained by the truncated TALK-1 protein expressed in the KO mouse β-cells.

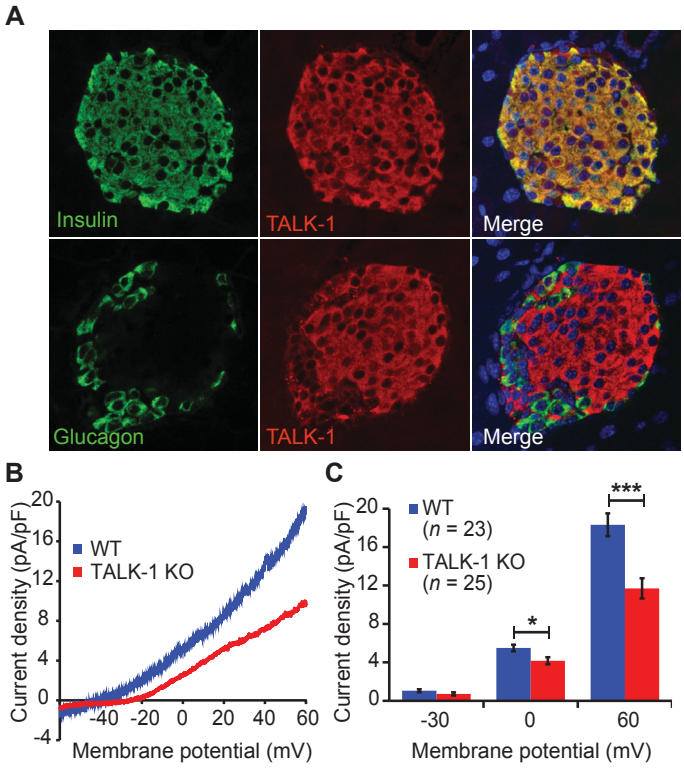

Figure 2.1. TALK-1 is functionally expressed in mouse β-cells. (A) Representative immunofluorescent stain of TALK-1 (red) and insulin (green, upper panels) or glucagon (green, lower panels) in mouse pancreas sections; nuclei (blue) are shown in the merge panel. (B) Voltage-clamp recordings of K2P currents from isolated WT and TALK-1 KO mouse β-cells. (C) Quantification of current density at -30, 0 and +60 mV in WT and TALK-1 KO mouse β-cells. Mean ± SEM; **P* <0.05; ****P* <0.001.

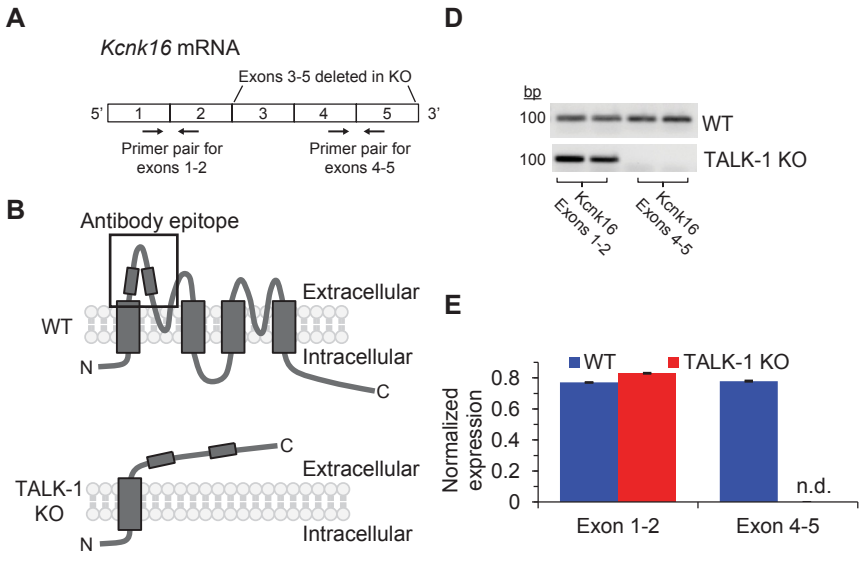

C

Primer	Sequence (5′ 3′)	Product size (bp)
Kcnk16 Exons 1-2 (Forward)	GACCAGCAGGCCCTGGAGCA	100
Kcnk16 Exons 1-2 (Reverse)	AGTCCCAGTTGCTGGGATTG	100
Kcnk16 Exons 4-5 (Forward)	AGCACCATTGGCTTCGGGGACTA	100
Kcnk16 Exons 4-5 (Reverse)	GTCCTAGGAGGATCCATATAGCT	100

Figure 2.2. Truncated TALK-1 mRNA in TALK-1 KO mice. (A) Diagram illustrating predicted structure of Kcnk16 (TALK-1) mRNA. Exons 3-5 are removed in the targeted allele. (B) Illustration of TALK-1 protein membrane topology in WT (top) mice, and the structure of the predicted truncated TALK-1 protein in TALK-1 KO mice. Note that the antibody epitope is retained in the truncated TALK-1 KO. (C) Primer pairs used to validate expression of Kcnk16 message in WT and TALK-1 KO islets, as illustrated in panel (A). (D) Gel images of RT-PCR products obtained using primers in (C) in WT (upper image) and TALK-1 KO (lower image) (E) TALK-1 transcript abundance in WT and TALK-1 KO islets, as assessed by real-time qRT-PCR; primers as in (D), expression normalized to GAPDH.

We next assessed TALK-1 channel expression and currents in human β-cells. In human pancreas sections, we found that TALK-1 exhibited strong islet expression which co-localized with insulin-positive cells but not with glucagon-positive cells (Figure 2.3A). Like mouse β-cells, human β-cells exhibit K2P currents (Figure 2.3B); the cells were recorded in extracellular solution that blocks most other K^+ channels (detailed above). To determine if the human β-cell K2P current includes TALK-1 currents we used a dominant-negative approach. A dominant-negative of TALK-1 (TALK-1 DN/P2A/mCherry) was designed by mutating the K^+ selectivity filter of TALK-1 (TALK-1 G110E), a strategy that has been used to create dominant-negative subunits for other K2P channels (*145*). The TALK-1 DN G110E point mutation prevents channel activity by dimerizing with endogenous TALK-1 subunits, disrupting the channel's K^+-selectivity filter and abolishing K^+ flux. Additionally, the bi-cistronic TALK-1 DN construct has a P2A cleavage sequence followed by a mCherry CDS downstream of TALK-1, which produces mCherry in all cells expressing the TALK-1 DN (*146*). Co-expression of TALK-1 DN/P2A/mCherry with WT TALK-1 in HEK293 cells resulted in near-complete suppression of TALK-1 currents, suggesting that the TALK-1 DN inhibits TALK-1 channel activity (Figure 2.4). We expressed the TALK-1 DN in dispersed human islet cells and recorded K2P currents from mCherry-positive cells. At the end of the recording, the cells were fixed and stained for insulin; only insulin-positive cells were analyzed. Expression of TALK-1 DN in human β-cells significantly reduced K2P currents when compared to cells expressing mCherry alone (pA/pF at +60 mV: mCherry, 36.7 ± 4.5, n = 10; vs. TALK-1 DN/P2A/mCherry, 22.1 ± 2.3, n = 11; P = 0.008; each construct was tested in β-cells from two donors) (Fig 2.3B,C). Together, these data strongly suggest that TALK-1 channels contribute to human β-cell K2P conductance.

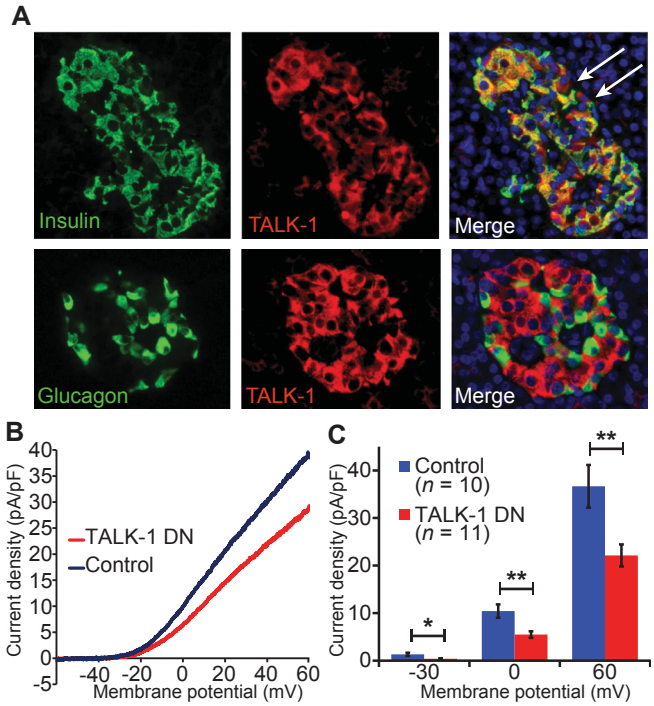

Figure 2.3. Human β-cells contain functional TALK-1 channels. (A) Representative immunofluorescent stain of TALK-1 (red) and insulin (green, upper panels) or glucagon (green, lower panels) in human pancreas sections; nuclei (blue) shown in the merge panel. White arrows indicate TALK-1-positive, insulin-negative cells. (B) K2P current obtained in human β-cells expressing either control (mCherry) or TALK-1 G110E-P2A-mCherry (TALK-1 DN) (C) Quantification of current densities at indicated membrane potentials. Mean values ± SEM; **P* <0.05; ***P* <0.005.

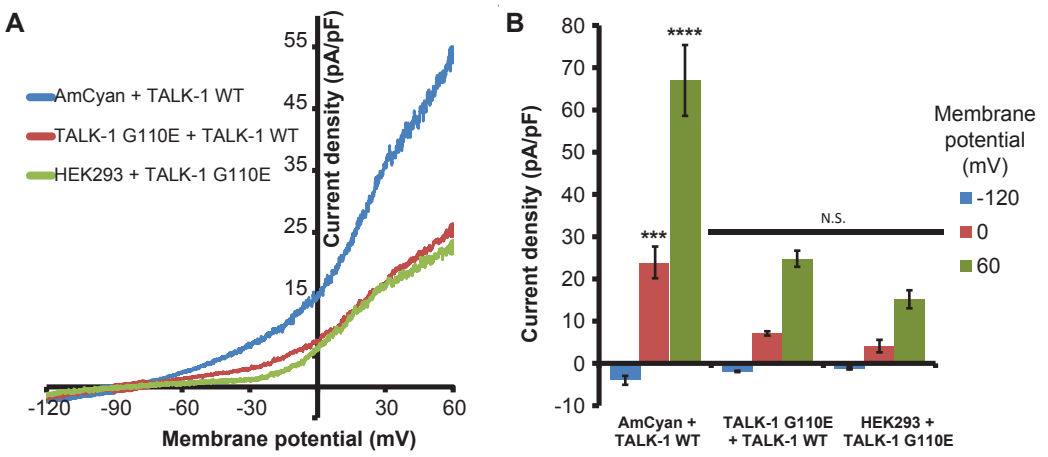

Figure 2.4. TALK-1 G110E (TALK-1 DN) suppresses TALK-1 WT-mediated whole-cell K^+ currents. (A) Whole-cell K2P currents in HEK293 cells expressing TALK-1 and TALK-1 G110E or a control plasmid (AmCyan) in response to a voltage ramp from -120 mV to +60 mV. Current densities are quantified in (B). Mean ± SEM; ***P<0.001; ****P<0.0001, Student's t-test.

TALK-1 channel activity and surface expression are sensitive to *Ct* charge

The polymorphism in *KCNK16* associated with T2DM risk (rs1535500) results in a glutamate substitution at alanine 277 in the *Ct* of TALK-1 (TALK-1 A277E) (Figure 2.5A,B). To assess how this substitution influences channel function, we used site-directed mutagenesis to insert the A277E polymorphism in cloned human TALK-1 channels and recorded their activity in CHO cells. We found that TALK-1 A227E produced significantly larger whole-cell currents than TALK-1 A277 (Figure 2.5C,D). Another non-synonymous polymorphism in strong linkage disequilibrium with rs1535500 is rs11756091 (*27*). This polymorphism is in transcript variant 2 of *KCNK16* (encoding TALK-1a), resulting in a proline substitution at histidine 301 (TALK-1a P301H). We recorded whole-cell currents of TALK-1a P301 and TALK-1a P301H, but found no significant difference in channel activity (Figure 2.6). Thus, rs1535500 may reduce GSIS through the gain-of-function TALK-1 A277E variant, increasing β-cell V_m polarization and reducing VDCC activity.

To further investigate the mechanism underlying the enhanced currents produced by TALK-1 A277E, we performed single-channel analysis of TALK-1 A277 and TALK-1 A277E channels expressed in HEK293 cells (Figure 2.5E). In cell-attached patches, we found that TALK-1 A277E exhibits enhanced open probability (P_o) (P_o at -30 mV: TALK-1 A277, 0.09 ± 0.008; vs. TALK-1 A277E, 0.15 ± 0.008; $P < 0.05$; n = 5-6) (Figure 2.5F). Unitary currents were not significantly different between TALK-1 A277 and TALK-1 A277E (Figure 2.7). We also assessed how the A277E polymorphism affects channel surface localization. Surface protein biotinylation of HEK293 cells expressing either TALK-1 A277-FLAG or the A277E-FLAG variant demonstrated that TALK-1 A277E channels exhibit greater cell surface localization than TALK-1 A277 channels (Figure 2.5G). These results indicate that TALK-1 A277E enhances

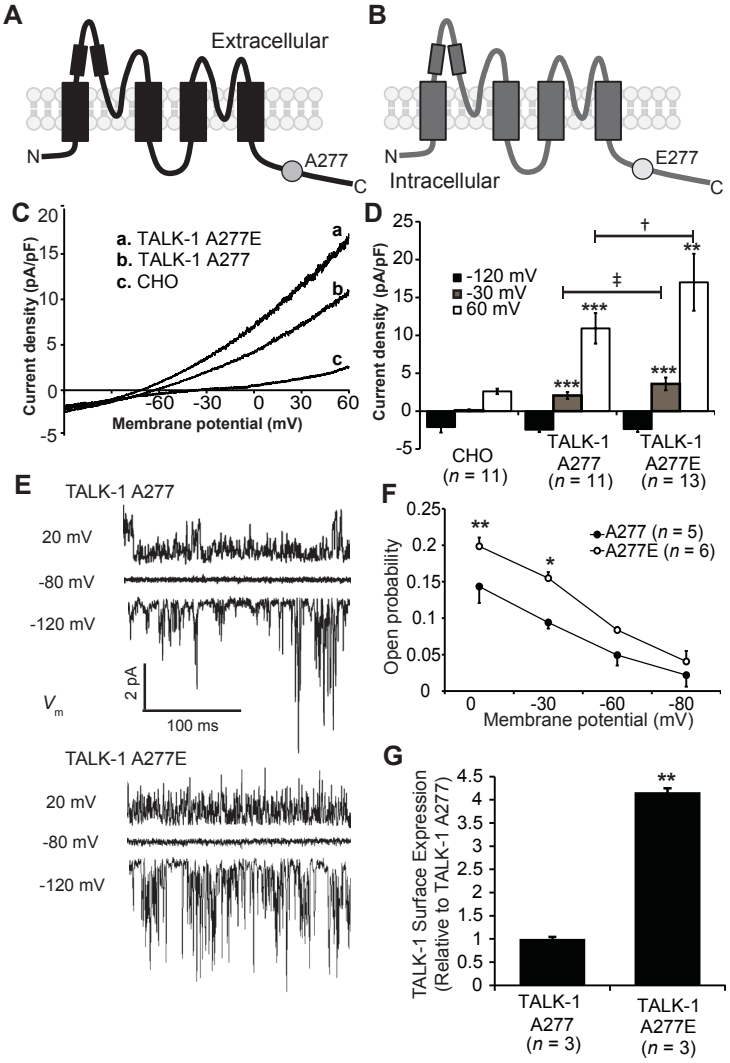

Figure 2.5. TALK-1 A277E exhibits increased open probability and surface expression. (A-B) Illustration of a TALK-1 A277 channel subunit (A) and a TALK-1 channel subunit showing the location of the rs1535500 polymorphism which results in an A277E substitution in the TALK-1 *Ct* (B). (C) Whole-cell TALK-1 current recordings from CHO cells expressing TALK-1 A277, TALK-1 A277E, or control (mCherry) in response to a voltage ramp from -120 mV to +60 mV. (D) Quantification of current density at selected membrane potentials in CHO cells expressing TALK-1 A277 or TALK-1 A277E. **P* < 0.05 vs. CHO; ***P* <0.005 vs. CHO; ****P* <0.001 vs. CHO; ‡*P*<0.001 vs TALK-1 A277; †*P* <0.0001 vs. TALK-1 A277. (E) Representative single-channel recordings from an attached patch of HEK293 cells expressing TALK-1 A277 or TALK-1 A277E in response to indicated voltage steps. (F) Quantification of P_o at indicated membrane potentials. (G) Quantification of FLAG-tagged TALK-1 A277 and E277 surface expression. Mean ± SEM; **P* < 0.05; ***P* <0.005.

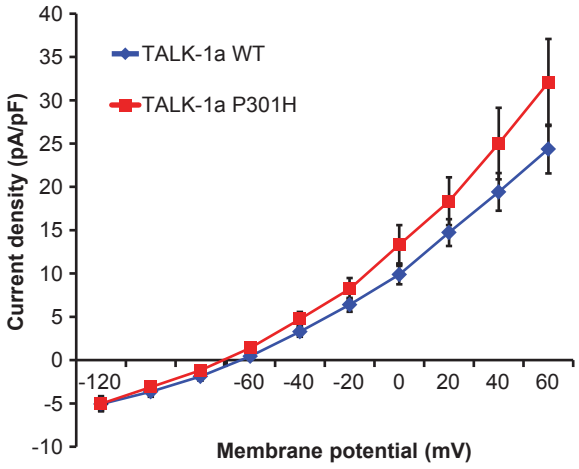

Figure 2.6. TALK-1a P301H does not exhibit changes in channel activity. Whole-cell current densities at selected membrane potentials for TALK-1a WT and TALK-1a P301H expressed in CHO cells. Mean ± SEM.

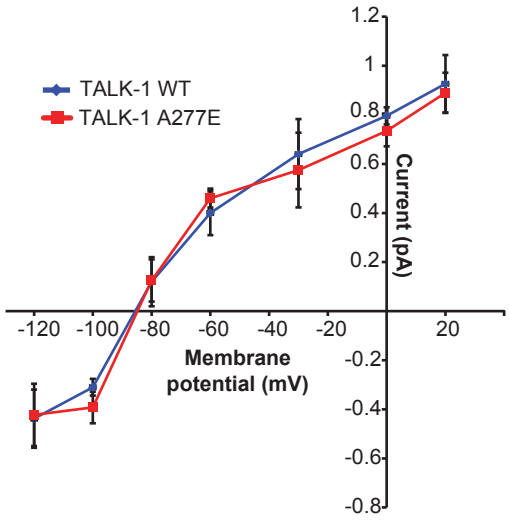

Figure 2.7. Unitary single channel currents measured from TALK-1 WT and TALK-1 A277E channels. Single channel currents measured in on-cell patches in HEK293 cells expressing TALK-1 WT or TALK-1 A277E at indicated membrane potentials. $N \geq 5$ for each point. Mean ± SEM.

channel activity through both elevated P_o and surface localization, which would be predicted to promote β-cell V_m polarization and oppose GSIS.

TALK-1 regulates β-cell electrical excitability and Ca^{2+} entry

To determine the physiological role of β-cell TALK-1 currents, we assessed how TALK-1 channels influence glucose-stimulated changes in β-cell V_m (Figure 2.8A,B). Loss of TALK-1 channels resulted in significant β-cell V_m depolarization over a range of glucose concentrations (Table 2.1). Furthermore, AP shape was altered in TALK-1 KO β-cells, with a tendency towards clustering of APs as well as reduced AP and after-hyperpolarization peak height when compared to WT β-cell APs (Figure 2.4C,D and Table 2.2). TALK-1 KO β-cells also showed a reduced interburst interval between oscillations compared to WT β-cells (seconds: WT, 144.4 ± 21.5; vs. KO, 51.4 ± 10.2; $P = 0.008$; $n = 7$) (Figure 2.8G). In agreement with the reduced interburst interval, the plateau fraction (the ratio of time spent in the active phase to the entire period (*147*)) was significantly increased in islets lacking TALK-1 at all stimulatory glucose concentrations examined (Figure 2.8H). Additionally, the average slope of repolarization at the termination of each burst was significantly less in β-cells lacking TALK-1 ($mV \cdot sec^{-1}$: WT, -3.95 ± 0.42; vs. KO, -1.25 ± 0.35; $P = 0.001$; $n = 21$) (Figure 2.8E,F,I), indicating that TALK-1 channels contribute to V_m repolarization at the end of each oscillation of electrical activity. Together, these data show that TALK-1 channels modulate β-cell glucose-stimulated electrical activity.

We next determined how changes in electrical activity caused by TALK-1 ablation influence glucose-stimulated islet Ca^{2+} entry. When exposed to increased glucose concentrations (2 mM to 14 mM), control and TALK-1 KO islets exhibited oscillatory increases in intracellular cytosolic Ca^{2+} (Ca^{2+}_c), (Figure 2.9A,B). We found that 2^{nd}-phase Ca^{2+}_c influx was increased

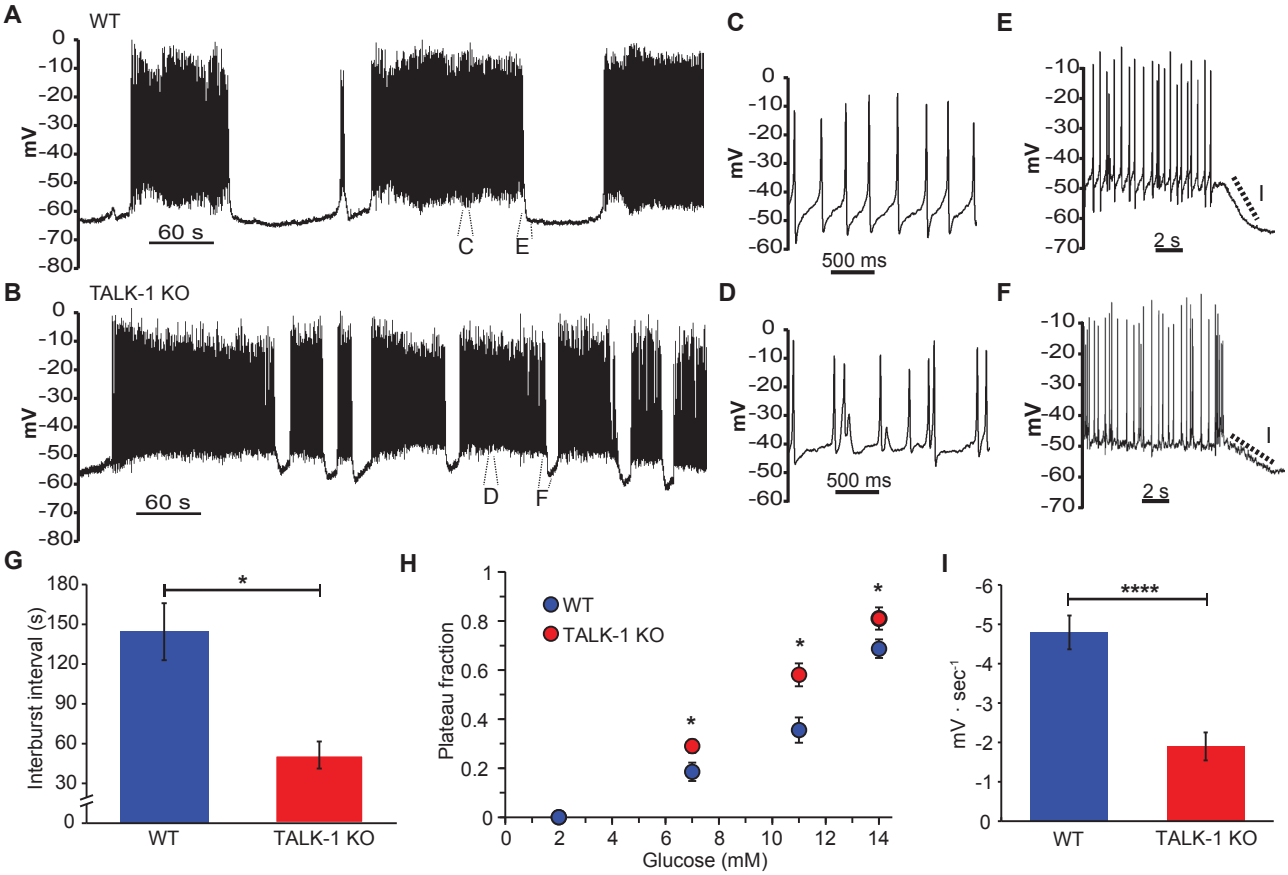

Figure 2.8. TALK-1 regulates β-cell electrical activity. (A) Representative V_m recording from a WT β-cell recorded in an intact mouse islet stimulated with 14 mM glucose. (B) Typical V_m recording from a TALK-1 KO β-cell in an intact islet in the presence of 14 mM glucose. (C-D) Enlarged view of APs recorded from WT (C) and TALK-1 KO (D) β-cells in 14 mM glucose. (E-F) Enlarged view showing the slope of V_m repolarization at the termination of an electrical oscillation in WT (E) and TALK-1 KO (F) β-cells. (G) Average length of the electrically silent interburst interval in WT and TALK-1-deficient islets, which was measured during the first 20 minutes of electrical excitability induced with 14 mM glucose. (H) Plateau fraction of electrical excitability in islets, determined as in G. (I), the mean slope of V_m repolarization at the termination of each oscillation of electrical activity in WT and TALK-1 KO β-cells, which was measured at the end of each oscillation in electrical excitability as in G. Mean ± SEM; *$P < 0.05$; **$P < 0.005$; ***$P < 0.001$.

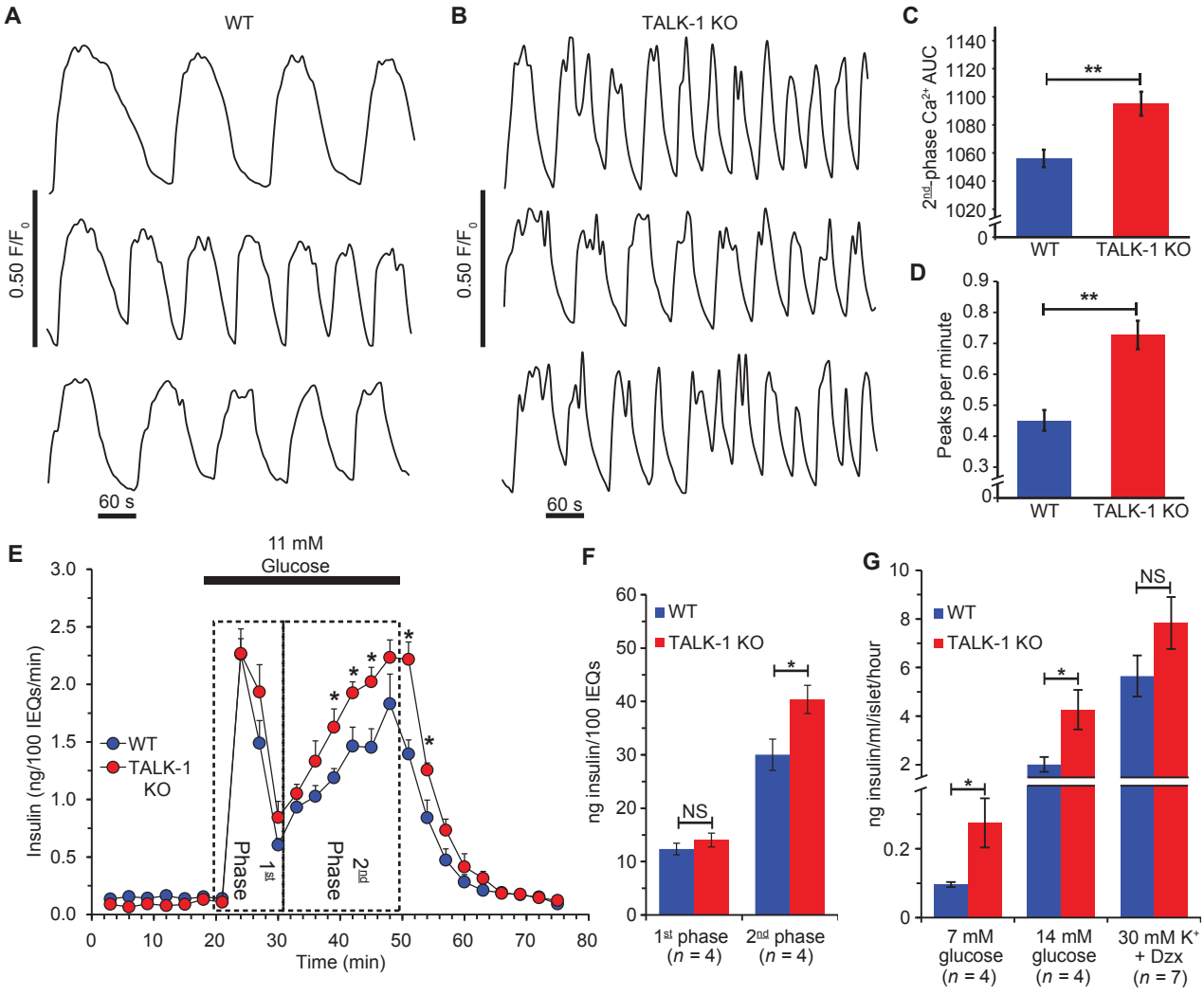

Figure 2.9. Ca^{2+}_c influx, oscillation frequency, and GSIS are increased in TALK-1 deficient islets. (A-B) Representative Ca^{2+}_c recordings in islets from WT (A) and TALK-1 KO (B) mice stimulated with 14 mM glucose. (C) Area under the curve (AUC) quantification of 2nd-phase Ca^{2+}_c influx in control and TALK-1 KO islets; Ca^{2+}_c AUC was calculated in the first 15 minutes of glucose-stimulated Ca^{2+}_c-influx after regular Ca^{2+}_c oscillations commenced (14 mM glucose). (D) Quantification of Ca^{2+}_c oscillation frequency in control and TALK-1 KO islets. (E) GSIS in isolated WT and TALK-1 KO islets. Islets were perifused with 1 mM glucose and stimulated with 11 mM glucose. (F) Area under the curve quantification of 1st- and 2nd-phase insulin secretion, for periods indicated on graph. (G) Insulin secretion from WT and TALK-1 KO islets in static incubation. *N* islet preparations per genotype are reported on the figure. Mean ± SEM; **P* < 0.05, ***P* <0.005.

Recording conditions	Interburst V_m (mV)	Plateau V_m (mV)
WT, 2 mM glucose	-72.7 ± 1.2 (N = 12)	n.a.
TALK-1 KO,2 mM glucose	-65.13 ± 0.66 (N = 13)	n.a.
Statistical significance	***	n.a.
WT, 7 mM glucose	-64.7 ± 2.4 (N = 9)	-49.7 ± 1.7 (N = 8)
TALK-1 KO, 7 mM glucose	-55.7 ± 1.1 (N = 6)	-47.3 ± 0.8 (N = 9)
Statistical significance	**	n.s.
WT , 11 mM glucose	-70.6 ± 2.5 (N = 9)	-51.2 ± 1.6 (N = 12)
TALK-1 KO, 11 mM glucose	-62.7 ± 2.1 (N = 12)	-44.2 ± 0.9 (N = 13)
Statistical significance	*	***
WT, 14 mM glucose	-63.1 ± 2.0 (N = 7)	-46.3 ± 2.2 (N = 7)
TALK-1 KO, 14 mM glucose	-54.6 ± 2.1 (N = 7)	-41.1 ± 0.9 (N = 7)
Statistical significance	*	*

Table 2.1. V_m values recorded in WT and TALK-1 KO β-cells. The V_m of β-cells in intact WT and TALK-1 KO was measured under the conditions described in the table. N observations were made from five islet preparations per genotype. Data is presented as mean ± SEM; *P < 0.05; **P < 0.005; ***P < 0.0005. n.a.: not applicable; n.s.: no significant difference.

(Figure 2.9C), and the frequency of Ca^{2+}_c oscillations in 14 mM glucose was accelerated in TALK-1 KO islets (peaks/minute: WT, 0.45 ± 0.03, N = 136; vs. KO, 0.73 ± 0.05, N = 126; **P <0.005; four islet preparations/genotype) (Figure 2.9D). These results indicate that TALK-1 channel activity is an important determinant of glucose-stimulated Ca^{2+}_c influx, and predict that inhibition of TALK-1 channels should increase Ca^{2+}_c influx and GSIS.

To assess how enhanced Ca^{2+}_c influx in TALK-1 KO islets impacts GSIS, we measured insulin secretion from isolated islets perifused with 11 mM glucose (Figure 2.9E). 1st-phase insulin secretion was not significantly different between WT and TALK-1 KO islets (Figure 2.9E,F). However, 2nd-phase insulin secretion, which occurs during the period of oscillatory

Parameter	WT ($N = 7$)	TALK-1 KO ($N = 7$)	P value
Peak amplitude (mV)	37.92 ± 2.24	30.69 ± 2.24	0.04
Antipeak amplitude (mV)	22.74 ± 1.02	18.38 ± 1.01	0.009
Time to peak (ms)	6.28 ± 0.66	7.91 ± 1.00	0.21
Half-width (ms)	11.77 ± 1.28	14.71 ± 1.85	0.24
Area (mV·ms)	395.94 ± 47.65	393.38 ± 44.53	0.96
Instantaneous frequency (Hz)	3.92 ± 0.30	7.93 ± 2.17	0.09
Interevent interval (ms)	323.50 ± 33.59	351.22 ± 50.45	0.66
Event frequency (Hz)	3.27 ± 0.30	3.17 ± 0.33	0.82
Maximum rise slope (mV/ms)	4.41 ± 0.77	3.09 ± 0.42	0.14
Maximum decay slope (mV/ms)	-5.59 ± 0.90	-3.75 ± 0.49	0.08

Table 2.2. Action potential characteristics in WT and TALK-1 KO β-cells. Action potential parameters were determined over a period of 30 seconds in the second oscillation of electrical activity in islets stimulated with 14 mM glucose using the "Threshold search" event detection function in Clampfit 10 (pCLAMP 10; Molecular Devices). Data is presented as mean ± SD; Student's *t*-test.

Ca^{2+}_c influx (*148*), was significantly increased in TALK-1 KO islets (ng insulin/100 islet equivalents: WT, 30.03 ± 2.65; vs. KO, 40.38 ± 2.92; $P < 0.05$; $N = 4$ islet preparations per genotype) (Figure 2.9E,F). In agreement with our observation of an increased plateau fraction in 7 and 14 mM glucose, at these glucose concentrations TALK-1 KO islets also secreted significantly more insulin than WT islets (Figure 2.9G).

Perturbations in the frequency of islet Ca^{2+}_c oscillation as well as total islet Ca^{2+}_c entry have been demonstrated to affect insulin secretion (*149, 150*). To examine the contribution of Ca^{2+}_c to the enhanced insulin secretion observed from TALK-1 KO islets, we "clamped" Ca^{2+}_c with a depolarizing concentration of KCl (30 mM) and activated K_{ATP} currents with diazoxide (200 μM). When 30 mM K^+ and diazoxide were applied in the presence of 14 mM glucose, insulin secretion from TALK-1-defiencient islets was comparable to WT islets (Figure 2.9G). These findings reveal that TALK-1 channel modulation of islet Ca^{2+}_c influx plays an important role in GSIS.

TALK-1 channels are critical for maintaining fasting glycemia

To assess how the increased insulin secretion caused by ablation of TALK-1 affects glucose homeostasis, we performed glucose tolerance tests (GTTs) in chow-fed TALK-1 KO mice. We observed slightly elevated serum insulin levels in TALK-1 KO mice; however, these changes were not statistically significant, and we did not observe altered glucose tolerance or insulin resistance (Figure 2.10A-C). We also observed that TALK-1 KO islet morphology was similar to WT islets (Figure 2.11), insulin content was comparable between WT and TALK-1 KO islets, and pancreatic insulin content was not different (Table 2.3). Therefore, we investigated whether the chronic metabolic stress of a high-fat diet (HFD) could reveal a role for TALK-1 channels in the maintenance of glucose homeostasis. After placing mice on a HFD, we observed protection from fasting hyperglycemia (three weeks on HFD; mg/dL: WT, 221.3 ± 8.4; vs. KO, 169.5 ± 5.6; $P < 0.0005$; $N = 10$ mice per genotype) (Figure 2.10D,F). We did not detect a difference in insulin tolerance in TALK-1 KO mice following exposure to a HFD (Figure 2.10E). Furthermore, pancreatic insulin content was not significantly different between WT and TALK-1 KO mice after 12 weeks on a HFD (Table 2.3), suggesting that the improved glycemia is not due to differences in β-cell mass.

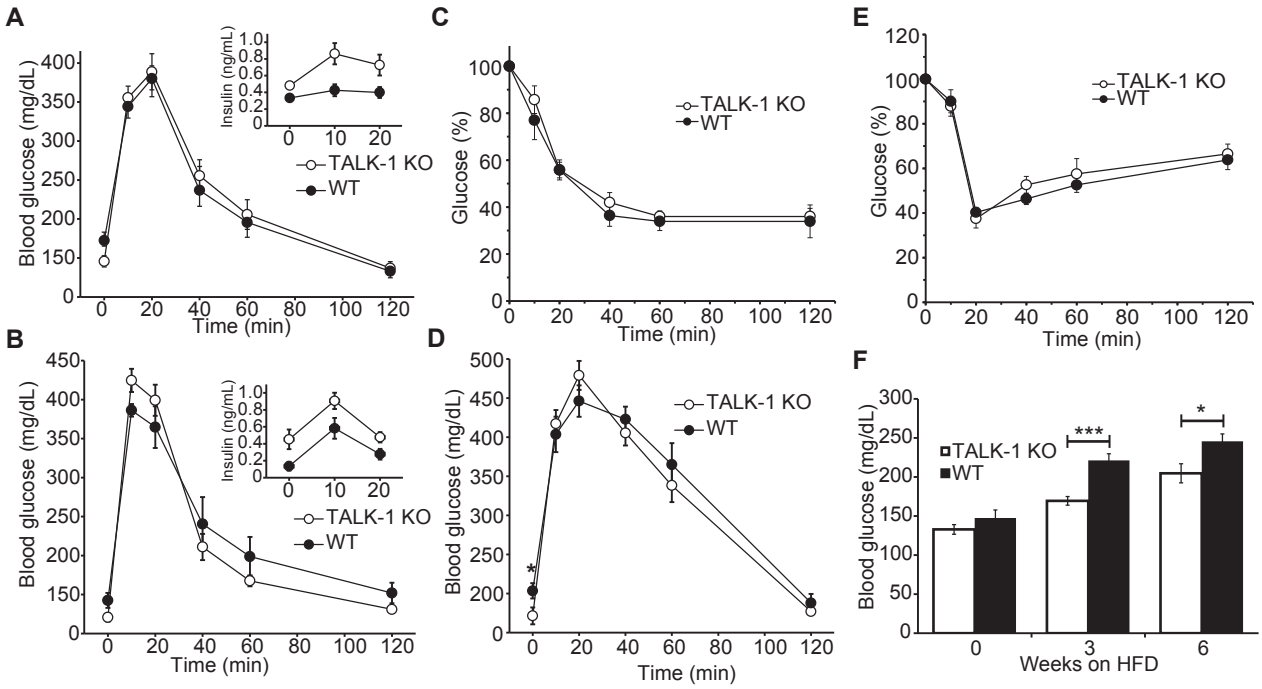

Figure 2.10. TALK-1 channels regulate fasting glycemia. (A-B) Glucose tolerance test (GTT) performed in chow-fed WT and TALK-1 KO male (A) and female (B) mice. Serum insulin levels from WT and TALK-1 KO mice are shown in the insets (A-B). (C) ITT performed in chow-fed WT and TALK-1 KO mice. (D) GTT performed in control and TALK-1 KO male mice after three weeks on a HFD (E) ITT performed in WT and TALK-1 KO mice after three weeks on a HFD. (F) Fasting blood glucose levels from control and TALK-1 KO mice after being placed on a HFD. Mean ± SEM; **P* < 0.05, ****P* < 0.0005.

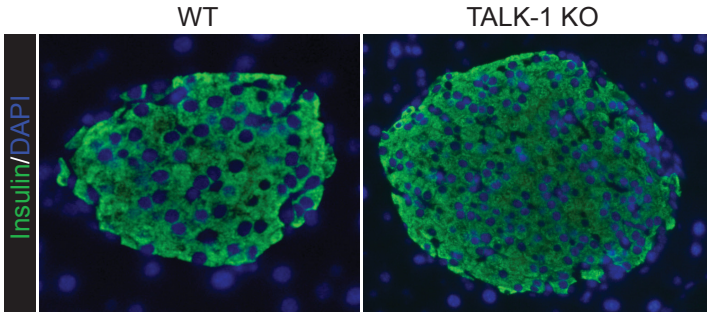

Figure 2.11. Representative islets in pancreas sections from TALK-1 WT and TALK-1 KO mice. Sections were stained for insulin, as described in Research Designs and Methods.

Parameter	WT	TALK-1 KO	*P* value
Islet insulin content (ng/IEQ)	37.24 ± 3.31 ($N = 4$)	38.87 ± 3.03 ($N = 4$)	0.73
Islet glucagon content (pg/IEQ)	912.10 ± 117.83 ($N = 4$)	718.42 ± 106.95 ($N = 4$)	0.27
Total pancreatic insulin (Chow diet) (ng/ml/mg tissue)	8.73 ± 3.43 ($N = 3$)	10.5 ± 4.89 ($N = 3$)	0.13
Total pancreatic insulin (HFD) (ng/ml/mg tissue)	15.56 ± 2.05 ($N = 4$)	11.49 ± 1.07 ($N = 4$)	0.16

Table 2.3. Islet and pancreatic hormone content of WT and TALK-1 KO mice. Islet hormone content was determined after perifusion experiments by RIA. Pancreatic insulin was extracted using acid ethanol, and quantified using a rodent insulin ELISA (ALPCO). Data is presented as mean ± SEM; Student's *t*-test.

TALK-1 channels modulate hepatic insulin sensitivity, food intake, and weight gain

When placed on a HFD, TALK-1 KO mice are protected from elevated fasting hyperglycemia. This effect may be caused in-part by an increase in basal pulsatile insulin secretion, as TALK-1 KO islets exhibit elevated electrical activity and insulin secretion at basal glucose (7 mmol/L) levels. Indeed, work from others has demonstrated that small increases in basal insulin release are sufficient to suppress hepatic glucose production without detectably increasing peripheral insulin concentrations (*57, 151, 152*). Consistent with these observations, we find significantly improved hepatic insulin sensitivity in TALK-1 KO mice without a change in adipose or muscle insulin sensitivity (Figure 2.12, A,B). Furthermore, serum insulin levels are significantly reduced in TALK-1 KO mice after prolonged HFD feeding, despite the increased insulin secretory capacity of TALK-1 KO HFD islets *in vitro* (Figure 2.12, C,D).

Chronic overnutrition, leading to obesity, is the most important environmental cause of hepatic and peripheral insulin resistance (*153, 154*). Moreover, hepatic insulin resistance is a major risk factor for T2DM (*155*). The relationship between visceral adiposity and hepatic insulin resistance is well-known (*156, 157*); however, the pathological processes underlying hepatic insulin resistance are poorly understood. Interestingly, we observe that TALK-1 KO mice are resistant to HFD-induced weight gain and adiposity (Figure 2.13, A,B). Similarly, basal insulin peglispro (BIL), an insulin analog which shows preferential action in the liver, produced weight loss in clinical study participants (*158, 159*). Together, these data indicate that TALK-1 channels play an important role in modulating fasting glycemia under metabolically stressful conditions that can lead to T2DM, and suggest a novel role for hepatic insulin signaling in the etiology of weight gain and obesity.

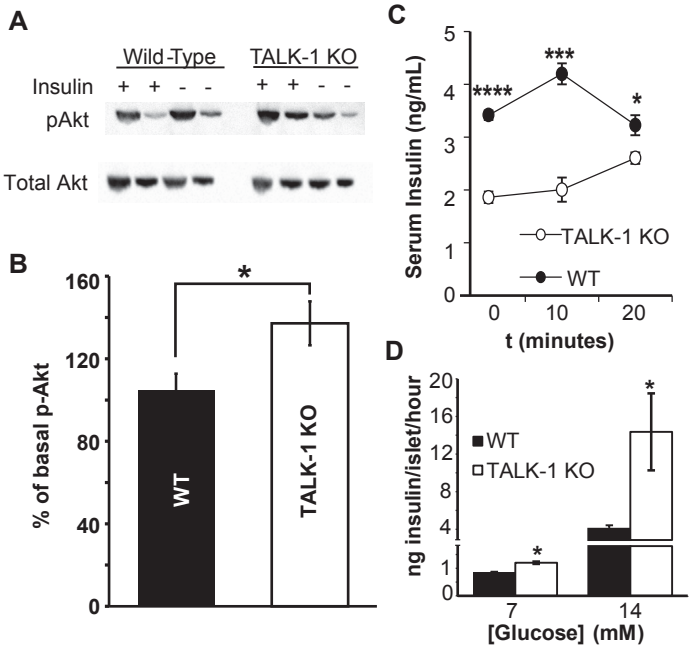

Figure 2.12. Enhanced hepatic insulin sensitivity and GSIS in TALK-1 KO mice fed a HFD for 8 weeks. 6-hour fasted WT and TALK-1 KO mice were injected with 5U/kg human recombinant insulin. Liver was harvested 15 minutes post-injection and processed for Western blot analysis of insulin-induced Akt phosphorylation (pAkt-Ser473). Representative blots are presented in (A). Quantification in (B); N =6 mice per genotype. (C) Serum insulin measurements from mice fed a HFD for 8 weeks taken at indicated times after an intraperitoneal glucose bolus (1g·kg-1). N = 5 mice per genotype. (D) Insulin secretion measured from WT and TALK-1 KO islets treated with indicated glucose concentrations. N = 3 mice per genotype. Mean ± SEM; *P < 0.05, ***P <0.001; ****P <0.0001; Student's t-test.

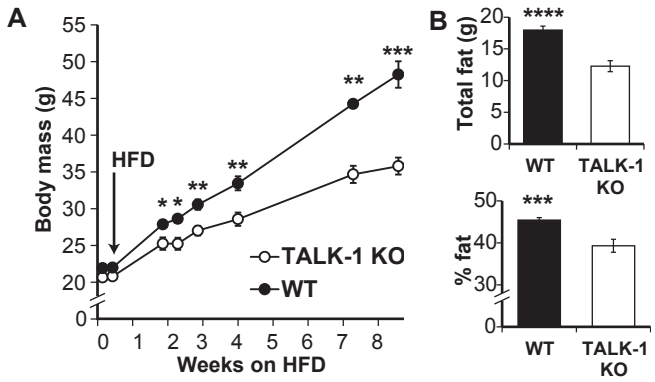

Figure 2.13. TALK-1 regulates weight gain and adiposity. (A) Male WT and TALK-1 KO mice placed on a HFD are resistant to obesity; $N = 10$ mice per genotype. (B) Adiposity measurements were performed after four weeks of HFD feeding; $N = 5$ mice per genotype. Mean ± SEM; * $P < 0.05$; ** $P < 0.005$; *** $P < 0.001$; **** $P < 0.0001$. Student's *t*-test.

Discussion

Physiological GSIS is dependent upon complex regulation of electrical activity by β-cell ion channels to control Ca^{2+} influx. The K2P channel TASK-1 stabilizes the β-cell plateau potential, which helps tune Ca^{2+} entry and GSIS (*52*). However, the role of TALK-1, the most abundant K^+ channel of the β-cell, has not been determined. The results presented here demonstrate the role of β-cell TALK-1 channels in regulating electrical activity, Ca^{2+}_c entry, and insulin secretion.

Stimulation of islets with glucose induces Ca^{2+}_c oscillations which underlie pulsatile insulin secretion (*50, 160*). The frequency and duration of Ca^{2+}_c oscillations is determined by alternating periods of electrical excitability (V_m depolarization) and inactivity (V_m hyperpolarization) (*161*). Periodic activation of a K^+ current interrupts regenerative AP firing by hyperpolarizing the V_m, giving rise to Ca^{2+}_c oscillations and pulsatile insulin secretion (*162*). Among the K^+ channels which have been shown to contribute to this current are K_{ATP} channels and the K_{Ca} channel of intermediate conductance, IK (*61, 163, 164*). K_{ATP} conductance fluctuates with oscillations in β-cell glucose metabolism and the ATP:ADP ratio, while IK is activated by elevated Ca^{2+}_c, contributing to the termination of the oscillation (*48, 141, 162*). However, β-cell V_m and Ca^{2+}_c oscillations persist in mouse islets lacking functional K_{ATP} or IK channels (*61, 165*). Furthermore, as IK is only briefly active following the reduction of Ca^{2+}_c at the termination of the oscillation, another K^+ conductance likely helps to keep the V_m hyperpolarized between each oscillation (*61*). Our data suggest that TALK-1 channel activity provides a hyperpolarizing influence that decreases islet Ca^{2+}_c oscillation frequency and plateau fraction. The greater V_m depolarization of TALK-1 KO β-cells during interburst phases may also explain the increased Ca^{2+}_c oscillation frequency and elevated plateau fraction in TALK-1-deficient islets. Indeed,

inhibition of K_{Ca} channels also results in interburst V_m depolarization and an increased oscillation frequency (*50*). Because the interburst V_m in TALK-1 KO β-cells is closer to the activation threshold for VDCCs, a smaller depolarizing stimulus would re-initiate AP firing. This is supported by recordings from brain neurons, where inhibition of TASK-1 K2P channels accelerates the frequency of AP bursting (*166*). Ca^{2+}_c oscillation frequency and pulsatile insulin secretion are perturbed in T2DM, which is believed to be pathogenic (*161, 167*). Thus, the influence of TALK-1 channels on β-cell Ca^{2+}_c oscillations could play an important role in modulating pulsatile insulin secretion.

The ion channels that increase Ca^{2+}_c influx during glucose-stimulated islet excitability also play a role in setting Ca^{2+}_c oscillation frequency. For example, Ca^{2+}-activated TRPM5 channels promote β-cell depolarization, enhancing Ca^{2+}_c oscillation frequency. Ablation of TRPM5 in mouse β-cells decreases glucose-stimulated Ca^{2+}_c oscillations, reducing GSIS (*150*). Conversely, β-cells lacking the Ca^{2+} channel β_3 subunit ($\beta_3^{-/-}$) show an increased Ca^{2+}_c oscillation frequency and enhanced GSIS (*149*). Similar to observations in $\beta_3^{-/-}$ mice, we find that the accelerated Ca^{2+}_c oscillation frequency in TALK-1 KO islets is associated with an increase in GSIS. The accelerated Ca^{2+}_c oscillation presumably increases GSIS; however, the increased plateau fraction may also amplify 2nd-phase insulin secretion in TALK-1 KO islets. It is well-known that the plateau fraction and insulin secretion increase concomitantly with elevated glucose concentrations (*147, 168-170*). Although the molecular mechanisms that modulate the plateau fraction are complex, it is generally accepted that fluctuations in K^+ conductance serve an important role (*171*). While the vast majority of information to this point has highlighted the importance of K_{ATP} and K_{Ca} channels in controlling the plateau fraction, our data demonstrate that K2P channels such as TALK-1 also serve an important role. The increase in oscillation

frequency and plateau fraction in TALK-1 KO islets is presumably involved in enhancing glucose-stimulated Ca^{2+}_c and 2nd-phase insulin secretion. A potential molecular mechanism regulated by TALK-1 channels underlying the change in Ca^{2+}_c oscillations is explored in Chapter III.

Our data establish that the T2DM risk polymorphism rs1535500 may reduce GSIS by increasing TALK-1 channel activity (*27, 144*). The A277E substitution in the *Ct* of TALK-1 resulting from rs1535500 increases channel P_o and channel surface localization. TALK-1 channels contribute to human β-cell K2P currents; thus, TALK-1 channels possessing the A277E substitution would be expected to augment β-cell K2P currents. Accordingly, A277E-containing TALK-1 channels would be predicted to promote V_m hyperpolarization and reduce β-cell excitability. Because TALK-1 channels limit mouse islet basal and 2nd-phase insulin secretion, we speculate that human islets with TALK-1 A277E would exhibit diminished basal and 2nd-phase insulin secretion. Although the A277E substitution increases TALK-1 channel activity, it is also possible that this substitution influences the mechanism(s) that modulate TALK-1 channels. Secretagogue-induced regulation of the V_m may differentially affect β-cells with TALK-1 A277E, which future studies will address. Together, these results also predict that gain-of-function mutations in TALK-1 channels may decrease β-cell Ca^{2+} entry, limiting insulin secretion and leading to glucose intolerance.

There is also the possibility that defects in TALK-1 channel function only elicit perturbations in glucose tolerance under the conditions of metabolic stress associated with T2DM. Indeed, TALK-1 KO mice show reduced fasting glucose levels when placed on a HFD. This diet-induced phenotype reveals that TALK-1 channels play a key role in adapting to metabolic stress. In T2DM, defects in insulin pulsatility contribute to impaired fasting glycemia

(*57, 172*), and it is thought that primary β-cell defects leading to reduced insulin pulsatility contribute to diabetes pathogenesis (*173*). We find an increase in plateau fraction and insulin secretion from TALK-1 KO islets at basal glucose levels (approximately 7 mM glucose in mice). Interestingly, small increases in basal portal insulin have been found to suppress hepatic glucose production (HGP), without producing a detectable increase in peripheral insulin concentrations (*151*). We postulate that enhanced insulin delivery through the portal vein decreases basal HGP (*57*) in TALK-1 KO mice. Mice fed a HFD show increased liver insulin resistance and HGP in as little as three days (*174*). As we observe no difference in insulin tolerance between chow- or HFD-fed WT and TALK-1 KO mice, the elevated basal insulin secretion from TALK-1 KO islets is not enough to exacerbate insulin resistance. In contrast, the increased basal insulin secretion from TALK-1 KO animals presumably suppresses HGP, leading to reduced fasting glycemia. This supported by our observation of elevated hepatic insulin sensitivity in TALK-1 KO mice after exposure to a HFD. Our findings also suggest that reduced liver insulin resistance in TALK-1 KO mice plays a reciprocal role in controlling islet insulin secretion *in vivo*. In the context of the diabetes-linked polymorphism, TALK-1 A277E may contribute to impaired fasting glycemia during the pathogenesis of T2DM by decreasing basal insulin secretion, which may lead to increased HGP during conditions of metabolic stress. Interestingly, human islets down-regulate TALK-1 expression in conditions of chronic metabolic stress (*175*), which our findings predict would increase insulin secretion. Future studies are required to determine how TALK-1 channels influence HGP during metabolic stress as well as in patients with rs1535500.

In summary, our findings demonstrate that TALK-1 is required for normal GSIS and glucose homeostasis. TALK-1 channel activity hyperpolarizes the β-cell V_m, controlling Ca^{2+} entry, GSIS, and fasting glycemia. Moreover, our data show that the TALK-1 A277E

polymorphism increases TALK-1 basal activity, predicting increased β-cell V_m hyperpolarization and reduced GSIS. This observation provides a molecular mechanism for rs1535500-linked increases in T2DM susceptibility, and suggests that inhibition of β-cell TALK-1 channels may be a therapeutic strategy to increase insulin secretion to reduce hyperglycemia in T2DM. Unlike sulfonylureas, which are suspected to accelerate β-cell exhaustion (*112*), inhibition of TALK-1 channels may also support aspects of islet function which would preclude this negative effect predicted to occur with sulfonylureas. These findings, as well as the molecular mechanisms underlying the increase in Ca^{2+}_c oscillations in TALK-1 KO islets, are further explored in Chapter III.

Research Design and Methods

Kcnk16$^{-/-}$ mouse preparation

A *Kcnk16* targeting vector was generated by inserting a 9.7 kb fragment containing exons 3-5 of the *Kcnk16* gene (accession: NM_029006.1) into a vector containing a floxed neomycin cassette. The targeting vector was transfected into Protamine-Cre 129S5 ES cells. Following recombination, 1707 bp of the *Kcnk16* gene corresponding to the 2nd base of the 119th codon to the 165th nt in the 3' intron after the 5th exon were removed (Figure 2.2). To identify correctly targeted ES cells, gDNA was isolated and digested with EcoRI, producing a 10.8 kb DNA fragment in WT alleles and an 8.7 kb DNA fragment in targeted alleles as assessed by Southern blot analysis. A correctly targeted ES cell was injected into 129S5 blastocysts, giving rise to germline transmission of the targeted *Kcnk16* allele. *Kcnk16*-deficient mice were backcrossed with congenic C57Bl6/J mice for nine generations. All mice used were 8 – 10 weeks of age. The

mice used for this study were handled in compliance with protocols approved by the Vanderbilt University Animal Care and Use Committee.

Islet and β-cell isolation

Islets were isolated from the pancreata of 8- to 10-week-old mice as previously described (*176*). Human islets from adult non-diabetic donors were provided by multiple isolation centers organized by the Integrated Islet Distribution Program (IIDP). Donor information is listed in Table 2.4. Some islets were dispersed into single cells with trituration in 0.005% trypsin and cultured for 12-18 hours. Cells were maintained in RPMI 1640 with 10% FBS, 100 $IU \cdot ml^{-1}$ penicillin, and 100 $mg \cdot ml^{-1}$ streptomycin in a humidified incubator at 37 °C under an atmosphere of 95% air–5% CO_2.

Donor	**1**	**2**
Sex	F	M
Age	32 yrs	52 yrs
BMI	39.4	22.5
Ethnicity	W	W
Type 2 Diabetes	No	No

Table 2.4. Islet donor characteristics for electrophysiology experiments using human islet cells.

Plasmids and transient expression

Cells were transfected with 4 μg DNA using Lipofectamine 2000 (Life Technologies). Cells were co-transfected with a plasmid encoding GFP and vectors containing the coding sequence for human TALK-1 (accession: NM_001135106.1), or TALK-1a (accession: NM_032115.3). The dominant-negative TALK-1 G110E, was created by site-directed

mutagenesis, and then cloned into a vector containing a P2A cleavage site followed by mCherry. Transfected cells were identified on the basis of mCherry fluorescence.

Electrophysiological recordings

TALK-1 channel currents were recorded in single cells using the whole-cell patch clamp technique with an Axopatch 200B amplifier and pCLAMP10 software (Molecular Devices). Cells were washed with a Krebs–Ringer-HEPES buffer (KRB) containing (in mM): 119 NaCl, 2 $CaCl_2$, 4.7 KCl, 25 HEPES, 1.2 $MgSO_4$, 1.2 KH_2PO_4, 11 glucose, adjusted to pH 7.35 with NaOH. Patch electrodes (3–5 MΩ) were loaded with intracellular solution containing (in mM) 140 KCl, 1 $MgCl_2 \cdot 6H_2O$, 10 EGTA, 10 HEPES, and 4 MgATP (pH 7.25 with KOH). Perforated patch recordings in intact islets were performed as previously described (*60*). To confirm recordings from human β-cells, cells were post-stained for insulin (*52*).

Surface expression analysis

HEK293 cells were transfected at 70% confluence with Lipofectamine 3000. After 72 hours, cell surface proteins were biotinylated and isolated using a Cell Surface Protein Isolation Kit (Pierce) according to manufacturer's instructions. TALK-1 E277-FLAG and A277-FLAG isolated from the plasma membrane and whole cell lysates were visualized on a western blot that was probed with anti-FLAG M2 (Sigma) followed with HRP secondary based detection with pierce chemiluminescent substrate (Thermo Scientific). Immunoblot band densitometry was performed using ImageJ software. Surface expression for each sample was calculated as the mean band intensity of biotinylated protein divided by total TALK-1-FLAG.

Measurement of cytoplasmic calcium

Following overnight culture, islets were incubated for 20 minutes at 37°C in RPMI supplemented with 2 μM Fura-2 AM (Molecular Probes), followed by incubation in KRB with 2 mM glucose for 20 minutes. Ca^{2+} imaging was performed as previously described (*52*).

Immunofluorescence analysis

Pancreata from 10-12 week-old mice or adult human donors (donor characteristics listed in Table 2.5) were fixed in 4% paraformaldehyde and embedded with paraffin. Rehydrated 5 μm sections underwent antigen retrieval using a citrate buffer according to the manufacturer's protocol (Vector Labs Inc), and stained with primary antibodies against insulin (1:500, Dako), glucagon (1:250, Sigma) and TALK-1 (1:175, Sigma), and secondary antibodies conjugated to Cy3 and DyLight488 (1:300; Jackson ImmunoResearch Laboratories). Nuclei were stained using Prolong Gold mountant with DAPI (Life Technologies). Sections were imaged with a Nikon Eclipse TE2000-U microscope and a Zeiss LSM 710 confocal microscope.

Donor	**1**	**2**
Sex	M	M
Age	31 yrs	58 yrs
Ethnicity	B	W
Type 2 Diabetes	No	No

Table 2.5. Human pancreas donor characteristics for immunofluorescence.

Insulin secretion measurements

For islet perifusion experiments, islets were allowed to recover for 24 hours following isolation in RPMI 1640 supplemented with 15% FBS and 11 mM glucose. GSIS was then determined by radioimmunoassay from perifused islets stimulated with 11 mM glucose (*177*).

Insulin secretion measurements from static incubations were performed as described elsewhere (*178*).

Glucose and insulin tolerance testing

Mice were placed either on standard chow diet or high-fat diet (60 kcal% fat; Research Diets, Inc.) Glucose tolerance testing (GTT) and insulin tolerance testing (ITT) was performed as previously described (*43, 178, 179*).

Statistical analysis

Data was analyzed using pCLAMP10 or Microsoft Excel and presented as mean ± SEM. Statistical significance was determined using Student's *t*-test.

CHAPTER III

TALK-1 CHANNELS CONTROL β-CELL ENDOPLASMIC RETICULUM Ca^{2+} HOMEOSTASIS*

Preface

Endoplasmic reticulum (ER) Ca^{2+} (Ca^{2+}_{ER}) handling serves critical roles controlling β-cell function and becomes perturbed during the pathogenesis of diabetes. Ca^{2+}_{ER} homeostasis is determined by ion movements across the ER membrane, including K^+ flux through K^+ channels. However, nothing is known about β-cell ER K^+ channels. Here, we demonstrate that K^+ flux through ER-localized TALK-1 channels facilitates Ca^{2+}_{ER} release. We find that β-cells lacking TALK-1 exhibit reduced basal cytosolic Ca^{2+}_{c} and elevated Ca^{2+}_{ER}, indicating diminished Ca^{2+}_{ER} leak. These changes in Ca^{2+} homeostasis are presumably due to TALK-1-mediated ER K^+ flux, as functional TALK-1 channels can be recorded on the nuclear membrane, which is continuous with the ER. Moreover, K^+-impermeable TALK-1 channels do not reduce Ca^{2+}_{ER}. Finally, we demonstrate that islets from mice lacking TALK-1 channels are resistant to ER stress induced by the metabolic stress of a HFD. Our data establish TALK-1 channels as key determinants of β-cell Ca^{2+}_{ER}, and suggest that TALK-1 may provide a novel therapeutic target to control β-cell Ca^{2+}_{ER} during the pathogenesis of diabetes.

*The work presented in this chapter is *in revision* as: Vierra NC, Dadi PK, Milian SC, Dickerson MT, Jordan KL, Gilon P, Jacobson DA. TALK-1 channels control β-cell endoplasmic reticulum Ca^{2+} homeostasis. Science Signaling. 2017.

Introduction

Pancreatic β-cell Ca^{2+} influx determines insulin secretion, and endoplasmic reticulum Ca^{2+} (Ca^{2+}_{ER}) handling plays a key role in this process (*62*). Ca^{2+}_{ER} serves many other essential functions in β-cells, such as controlling protein processing, metabolism, and the unfolded protein response (UPR) (*180*). The importance of precise β-cell Ca^{2+}_{ER} handling is evident in T1DM and T2DM, during which Ca^{2+}_{ER} homeostasis is disrupted, contributing to β-cell dysfunction and eventual destruction (*62, 176, 180-185*). Impaired Ca^{2+}_{ER} handling also causes defects in GSIS (*56, 181*). Therefore, treatments which reduce ER stress (such as those induced by the UPR) in the context of β-cell dysfunction improve glucose tolerance (*186-188*). While Ca^{2+}_{ER} concentrations are perturbed in diabetes, the molecular determinants that set β-cell Ca^{2+}_{ER} are poorly understood.

Maintenance of Ca^{2+}_{ER} homeostasis requires that Ca^{2+} movement across the ER membrane is balanced with a simultaneous K^+ flux in the opposite direction (*189-191*). Without the K^+ countercurrent, Ca^{2+} release from the ER would rapidly generate a negative charge on the luminal side of the ER membrane, inhibiting further Ca^{2+}_{ER} release. To date only a few ER K^+ channels have been identified, including TRIC-A channels, which regulate Ca^{2+}_{ER} stores in myocytes (*192, 193*); TRIC-B channels, which control Ca^{2+}_{ER} homeostasis in alveolar epithelial cells and osteoblasts (*194, 195*); and SK Ca^{2+}-activated K^+ channels, which modulate Ca^{2+}_{ER} uptake in neurons and cardiomyocytes (*196*). Genetic ablation or pharmacological inhibition of these channels impairs Ca^{2+}_{ER} handling. For example, knockout of TRIC-A or TRIC-B channels results in elevated Ca^{2+}_{ER} stores, presumably due to the loss of a K^+ countercurrent which regulates the ability of Ca^{2+} to exit the ER (*191, 192, 194*). Despite the importance of K^+

countercurrents in maintaining Ca^{2+}_{ER} homeostasis, nothing is known about the mediators or functions of β-cell ER K^+ countercurrents.

ER localization has been reported for several K2P channels, including TASK-1 (*197*), TASK-3 (*198*), TASK-5 (*199*), TWIK-2 (*200, 201*), and THIK-2 (*200*). Although the subcellular localization of TALK-1channels has not been reported, a protein interactome study determined that a majority (>60%) of the proteins interacting with TALK-1 are ER-resident proteins (*137*). Similarly, a human pancreatic islet cDNA library generated and screened in a membrane yeast-two-hybrid assay to identify islet TALK-1 interacting proteins identified multiple ER-resident proteins that interact with TALK-1 (*138*). In accordance with these observations, TALK-1 shows substantial intracellular staining in human and mouse pancreatic β-cells (*202*). Although these findings suggest that TALK-1 channels may serve an intracellular role, investigations of intracellular K2P channels have focused primarily on elucidating the factors that enable their functional expression on the plasma membrane, and an ER function for K2P channels has not been identified.

As demonstrated in Chapter II, β-cell TALK-1 channels contribute to V_m hyperpolarization, regulating Ca^{2+}_c influx and insulin secretion (*202*). TALK-1 is expressed in pancreatic islets as well as gastric somatostatin cells (*17, 18, 115*) and is the most abundant islet K^+ channel at the transcriptional level (*19, 20, 80*). One of the primary physiological functions of β-cell TALK-1 channels is to limit glucose-induced islet electrical and Ca^{2+}_c oscillations, controlling second-phase pulsatile insulin secretion (*202*). Furthermore, a non-synonymous polymorphism in TALK-1 (rs1535500) associated with T2DM (*27-29*) causes a gain-of-function in TALK-1 activity (*202*), which may impair Ca^{2+}_c oscillations and pulsatile insulin secretion. However, the molecular mechanisms underlying TALK-1 regulation of islet Ca^{2+}_c oscillations

remain unknown, and it remains unclear whether TALK-1 currents at the plasma membrane are responsible for the channel's effects on Ca^{2+}_{c} oscillations.

Here, we tested the hypothesis that TALK-1 channels are functional in the ER, mediating ER K^+ countercurrents which support β-cell Ca^{2+}_{ER} homeostasis. By measuring Ca^{2+}_{ER}, Ca^{2+}_{c}, and single-channel K2P currents on the ER membrane, we demonstrate that TALK-1 conducts ER K^+ countercurrents which enhance Ca^{2+}_{ER} leak in mouse and human β-cells. We find that TALK-1 control of β-cell Ca^{2+}_{ER} modulates islet Ca^{2+}_{c} handling, which has important implications for understanding the regulation of Ca^{2+} oscillations that underlie pulsatile insulin secretion. Moreover, we show that other ER-localized K2P channels, such as TASK-1, can function in an identical manner. Inhibition of K^+ currents through either TALK-1 or TASK-1 increased steady-state Ca^{2+}_{ER} concentrations, demonstrating that the K^+ channel function of these proteins is essential for their effects on Ca^{2+}_{ER} homeostasis. Moreover, islets from mice lacking TALK-1 channels resisted ER stress induced by the chronic metabolic stress of a HFD, suggesting that defects that increase TALK-1 channel activity can perturb ER health and contribute to islet dysfunction in T2DM. Overall, these findings identify an intracellular function of K2P channels, and reveal TALK-1 channels as a possible therapeutic target to modulate Ca^{2+}_{ER} homeostasis, which could reduce β-cell ER stress in diseases such as diabetes.

Results

TALK-1 activity promotes Ca^{2+}_{ER} leak

TALK-1's prominent intracellular staining pattern (*202*) together with its physical association with several ER-resident proteins (*137*) suggested that TALK-1 could be localized to the ER. To determine the subcellular localization of TALK-1, we performed immunofluorescence staining of mouse pancreas sections and detected the co-localization of TALK-1 and the ER marker calreticulin (Figure 3.1A). Additionally, co-expression of a TALK-1/mCherry fusion protein and an ER-targeted indicator (*203*) in mouse islet cells reveals TALK-1 in the ER (Figure 3.2).

While TALK-1 conducts K^+ currents on the plasma membrane in β-cells (*202*), it has not yet been determined whether K2P channels in the ER, such as TALK-1, are functional. To test if TALK-1 channel function could affect Ca^{2+}_{ER} homeostasis, we first directly measured β-cell Ca^{2+}_{ER} from control (wild-type, WT) and TALK-1 KO islets (*202*) with the ER-targeted, genetically encoded Ca^{2+} indicator D4ER (*204*) (Figure 3.1B). Under both low and high glucose conditions TALK-1 KO β-cells had significantly higher Ca^{2+}_{ER} concentrations (Figure 3.1B,C). Inhibition of sarco/endoplasmic Ca^{2+} ATPases (SERCAs) with cyclopiazonic acid (CPA) produced a greater decrease in Ca^{2+}_{ER} in KO β-cells compared with controls (Figure 3.1D). Absolute Ca^{2+}_{ER} levels in KO β-cells remained above WT β-cells after application of CPA, suggesting that inhibition of SERCAs was insufficient to completely empty β-cell Ca^{2+}_{ER} stores, as observed in neurons (*205*). Slight reductions in Ca^{2+}_{ER} stimulate β-cell proliferation (*206*); therefore, we tested if TALK-1 controls β-cell mass or proliferation. The absence of TALK-1 did not alter islet cellular composition, nor did it impair adaptive proliferation (as determined by BrdU incorporation) in response to a short term (one week) high-fat diet (HFD) stimulus (*207*)

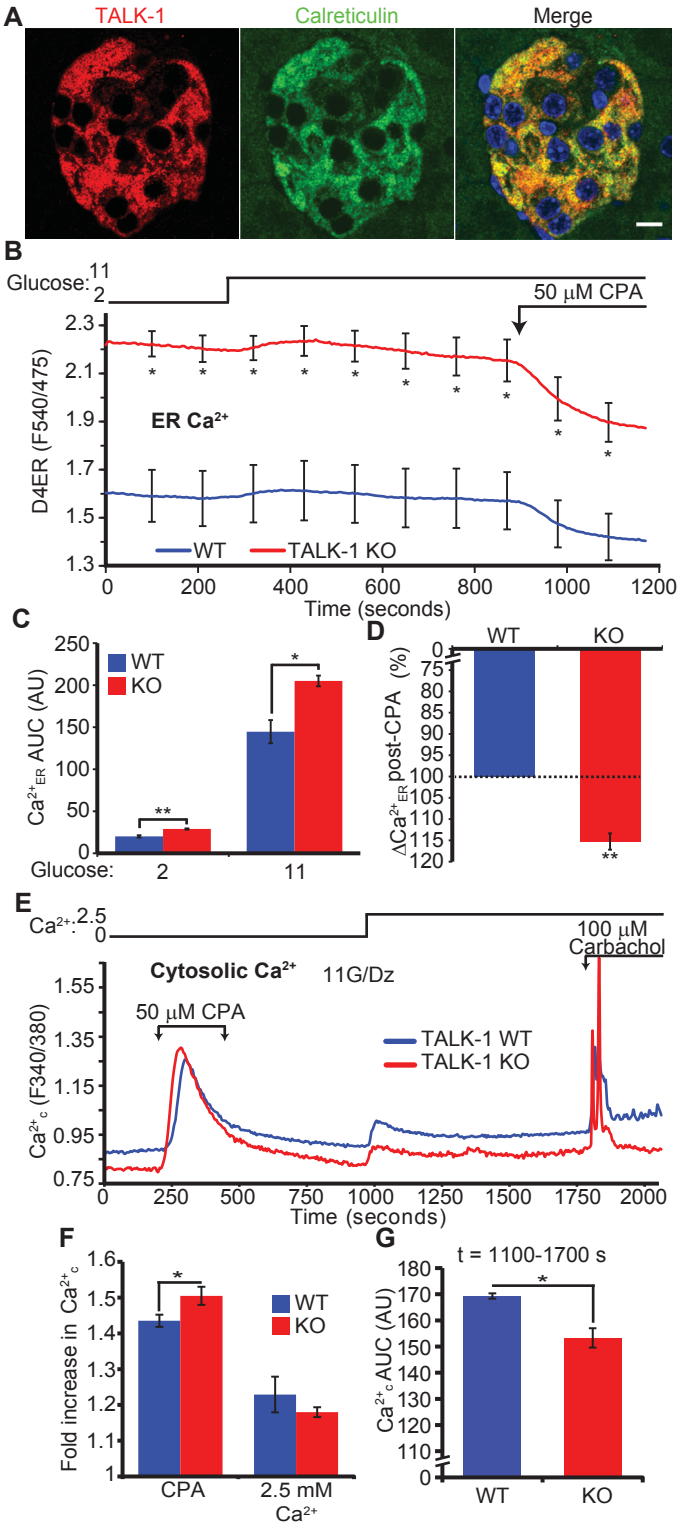

Figure 3.1. TALK-1 channels modulate β-cell ER Ca^{2+} homeostasis. (A) Representative images of a mouse pancreas section stained for TALK-1 and calreticulin. Scale bar is 10 μm. Images are representative of stain obtained from 3 mice. (B) β-cell Ca^{2+}_{ER} measurements made with the genetically encoded Ca^{2+}_{ER} indicator D4ER. Cells were perfused with solutions containing indicated glucose concentrations and 50 μM CPA, as indicated (N = 3 mice per genotype). (C) AUC analysis of Ca^{2+}_{ER} under low (2 mM) and high (11 mM) glucose conditions from (B). (D) CPA-induced reduction in Ca^{2+}_{ER}, presented as percent of maximum Ca^{2+}_{ER} of WT β-cells from (B). (E) WT and TALK-1 KO β-cells were perfused with the indicated solutions; 11 mM glucose and 125 μM diazoxide (Dz) were present throughout the experiment (N = 5 mice per genotype). (F) Fold increase in Ca^{2+} in response to the indicated treatments from (E). (G) Ca^{2+} AUC for the period following addition of 2.5 mM Ca^{2+} to the extracellular buffer (t=1000-1750 s) from (E). *P<0.05, **P<0.005; Student's t-test.

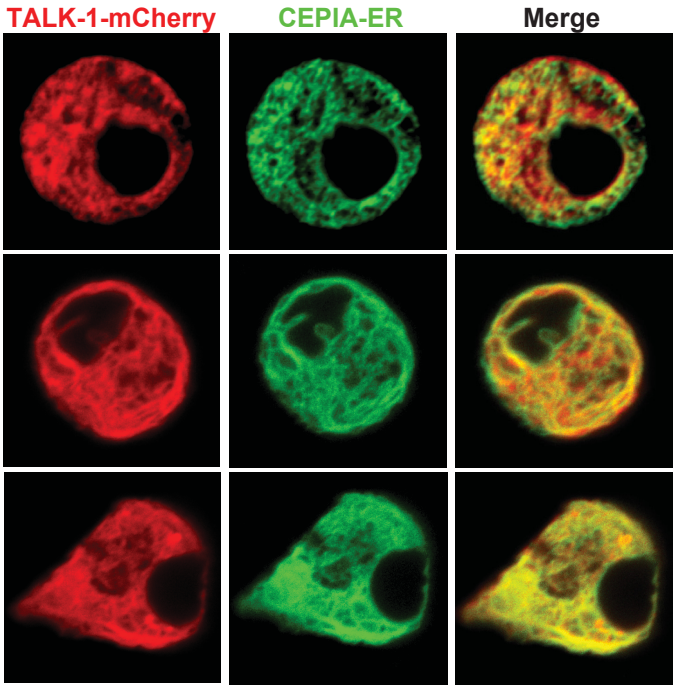

Figure 3.2. TALK-1 exhibits ER localization. Representative images of primary mouse islet cells co-transfected with mCherry-tagged TALK-1 and an ER-targeted fluorescent indicator (CEPIA-1er). Images are 0.9 μm optical sections representative of at least 3 tranfected cells from three indpendent mouse islet isolations.

(Figure 3.3A-F), indicating that inhibition of TALK-1 did not negatively impact β-cell mass or islet cell viability. These observations suggest that although slight reductions in β-cell ER Ca^{2+} concentrations can stimulate proliferation, modest increases in Ca^{2+}_{ER} stores under these conditions do not influence this adaptive response.

To further confirm that TALK-1 modulates Ca^{2+}_{ER} we quantified Ca^{2+}_{ER} indirectly in WT and KO β-cells by measuring Ca^{2+}_{c} in response to multiple stimuli. Treating β-cells with the Ca^{2+} ionophore ionomycin in the absence of extracellular Ca^{2+} resulted in more Ca^{2+} release from KO than WT β-cells (Figure 3.4 A,B), indicating elevated intracellular Ca^{2+} stores. We next perfused isolated WT and TALK-1 KO β-cells with Ca^{2+}-free buffer containing diazoxide to selectively monitor Ca^{2+}_{c} independent of Ca^{2+} entry through plasma membrane channels (Figure 3.1E). Under these conditions TALK-1 KO β-cells exhibited lower basal Ca^{2+}_{c} (Figure 3.1E) and addition of CPA produced a larger increase in Ca^{2+}_{c} (Figure 3.1E,F), suggesting reduced Ca^{2+}_{ER} leak and increased Ca^{2+}_{ER} stores. Following washout of CPA, addition of Ca^{2+} to the extracellular buffer led to a similar extent of Ca^{2+}_{c} influx in WT and TALK-1 KO cells, showing that activation of store-operated Ca^{2+} entry (SOCE) was not impaired in TALK-1 KO β-cells (Figure 3.1E,F). However, the reduced basal Ca^{2+}_{c} observed without external Ca^{2+} was maintained in the presence of extracellular Ca^{2+} in KO β-cells (Figure 3.1E,G).

We next examined whether TALK-1 is present in the ER of human β-cells. Immunofluorescent staining of human pancreas sections revealed co-localization of TALK-1 with the ER marker calreticulin (Figure 3.5A). To assess TALK-1 regulation of human β-cell Ca^{2+}_{ER}, we expressed a dominant-negative TALK-1 (TALK-1 DN) construct in β-cells and measured CPA-induced Ca^{2+}_{ER} release (Figure 3.5B). TALK-1 DN contains a pore mutation which inhibits K^{+} conductance when it interacts with endogenous TALK-1 (*202*). The TALK-1

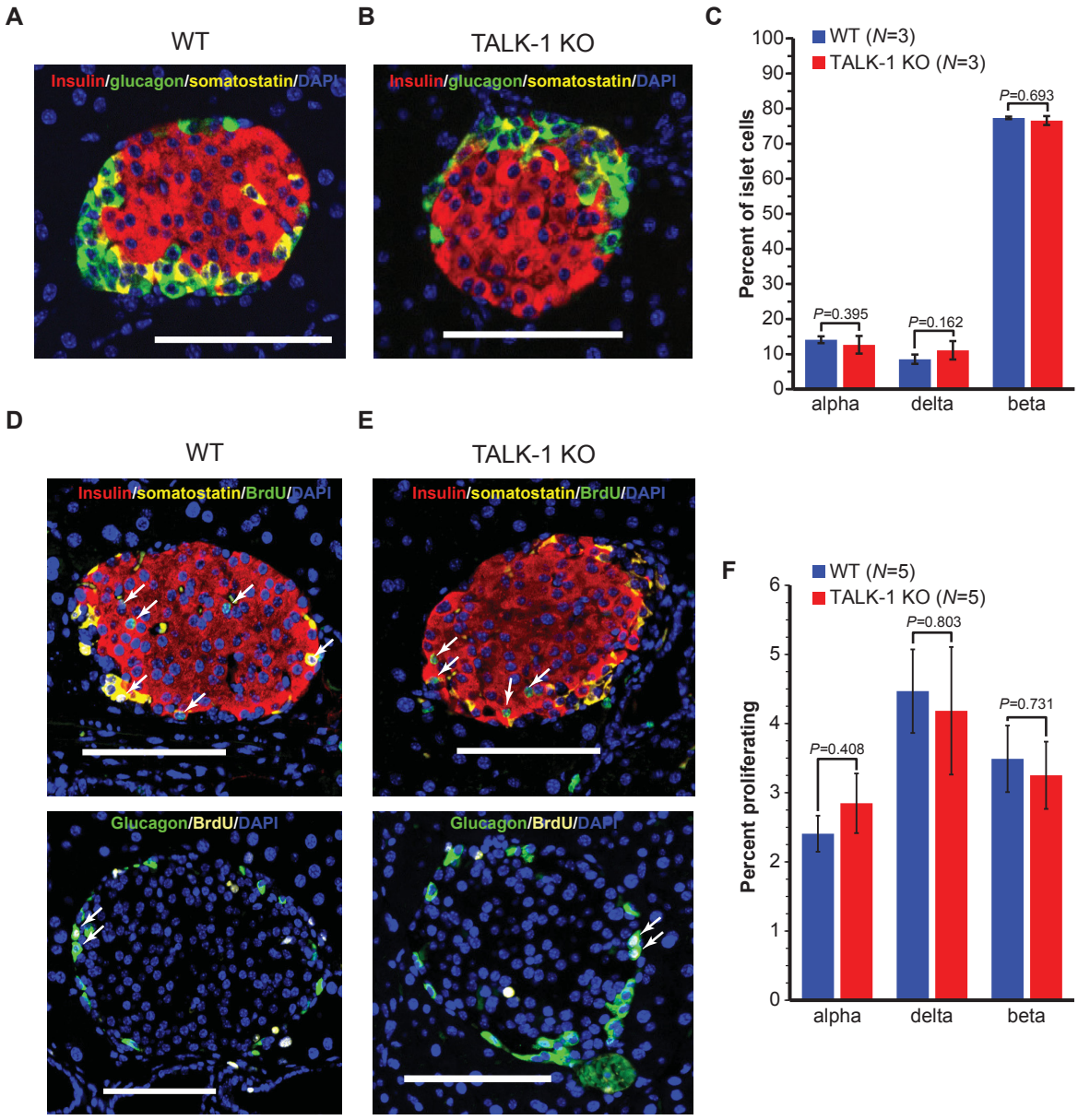

Figure 3.3. Islet cell number and proliferation are not modulated by TALK-1 activity. Islet in a pancreas section from a WT mouse (A) or a TALK-1 KO mouse (B) stained with antibodies against insulin, glucagon, and somatostatin. Scale bar is 100 µm. (C) The percentage of each islet cell type was calculated as the [(cell type number)/(β- + δ- + α-cell number)] (N = 3 pancreata per genotype). (D and E) Immunoflourescent images of an islet in a pancreas section from a WT mouse (D) or TALK-1 KO (E) fed a high-fat diet (60% kcal/fat) for one week stained by immunofluorescence with antibodies against insulin, somatostatin, and BrdU. Lower section: Islet in a pancreas section from a WT mouse fed a high-fat diet (60% kcal/fat) for one week stained by immunofluorescence with antibodies against glucagon and BrdU. Scale bar is 100 µm. (F) Quantification of proliferating cells in WT and TALK-1 KO islets, calculated as [(BrdU+ cell type number)/(β- + δ- + α-cell number)] (N = 5 pancreata per genotype); Student's t-test.

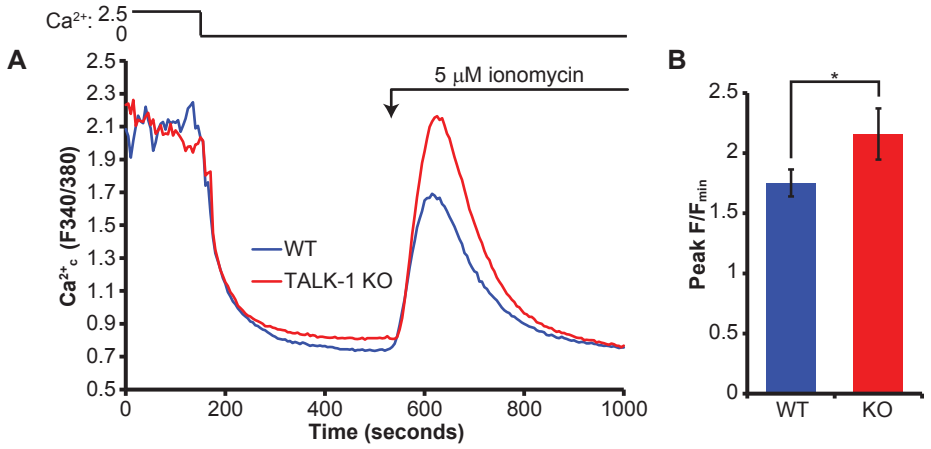

Figure 3.4. Intracellular Ca^{2+} stores are increased in TALK-1 KO islet cells. (A) Representative cytosolic Ca^{2+} measurements obtained from WT and TALK-1 KO islet cells treated with ionomycin. (B) Quantification of peak Ca^{2+} release in the presence of ionomycin (N = 4 mice per genotype); **P*<0.05; Student's *t*-test.

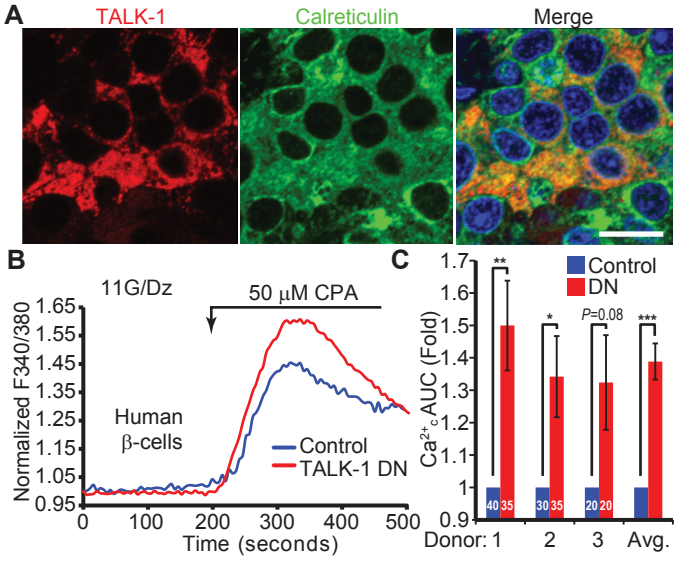

Figure 3.5. TALK-1 channels modulate human β-cell ER Ca^{2+} homeostasis. (A) Representative image of a human pancreas section stained for TALK-1 and calreticulin. Scale bar is 10 μm. (B) Representative recordings of intracellular Ca^{2+} in human β-cells transfected with either TALK-1 dominant-negative mutant (DN) or mCherry control. 11 mM glucose, 0 mM Ca^{2+}, and 1 mM EGTA were present throughout. (C) Quantification of the fold change in the Ca^{2+} AUC in response to treatment with CPA in human β-cells (The number of β-cells per donor is indicated on the graph). **P*<0.05, ***P*<0.005; ****P*<0.005; Student's *t*-test and one-way ANOVA.

DN construct also contains a P2A sequence between sequences encoding TALK-1 and an mCherry reporter, allowing us to detect cells expressing the TALK-1 DN by mCherry fluorescence; β-cells were identified by post-staining for insulin (*202*). Inhibition of TALK-1 with the TALK-1 DN caused a significant 34.7 ±5.1% increase in CPA-induced Ca^{2+}_{ER} release (Figure 3.5C), demonstrating that TALK-1 modulates human β-cell Ca^{2+}_{ER} homeostasis.

To test whether TALK-1 activity reduces Ca^{2+}_{ER} storage, we examined the effects of TALK-1 expression on Ca^{2+}_{ER} in HEK293 cells. First, to determine whether TALK-1 exhibits ER localization in HEK293 cells, we expressed two channel-forming isoforms of TALK-1 (1b and 1a) (*134*) and found that TALK-1 co-localized with an ER-targeted YFP marker (Figure 3.6A). We next assessed the consequences of TALK-1 expression on Ca^{2+}_{ER} homeostasis in these cells. To minimize potential deleterious effects of protein overexpression, we used the TALK-1 DN mutant as a control, which also permitted dissociation of the effects of K^+ conductance and protein-protein interactions on Ca^{2+}_{ER} homeostasis. Expression of wild-type TALK-1 yielded a significant elevation in basal Ca^{2+}_{c} (Figure 3.6B) and concomitant reduction in CPA-induced Ca^{2+}_{ER} release (Figure 3.6B,C), suggesting greater Ca^{2+}_{ER} leak due to TALK-1 channel activity. Addition of Ca^{2+} to the extracellular buffer produced a larger increase in Ca^{2+}_{c} in wild-type- compared to DN-expressing cells (Figure 3.6B,D), and similar to CPA-induced Ca^{2+}_{ER} release, stimulation of IP3-triggered Ca^{2+}_{ER} release elicited a greater response in cells expressing TALK-1 DN (Figure 3.6B,E). Thus, the K^+-channel function of TALK-1 is sufficient to alter Ca^{2+}_{ER} homeostasis.

To confirm the specificity of the effect of TALK-1 on Ca^{2+}_{ER}, we compared Ca^{2+}_{ER} storage in cells stably and inducibly expressing different K2P channels (*124*) (Figure 3.7A). Similar to transfected cells, TALK-1 induction reduced Ca^{2+}_{ER} stores (Figure 3.7A). We also

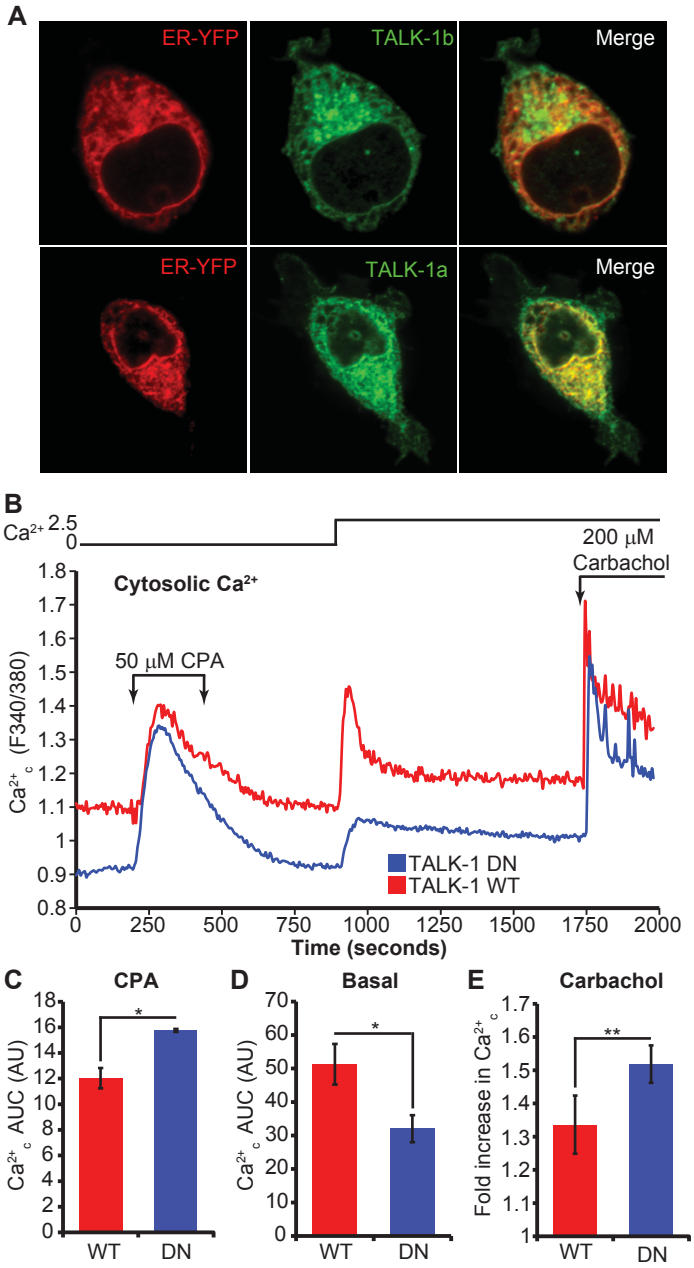

Figure 3.6. The K^+ channel function of TALK-1 contributes to its regulation of ER Ca^{2+} homeostasis. (A) TALK-1b and -1a co-localize with the ER marker ER-YFP. Images are representative of 3 independent experiments. (B) Representaive recordings of HEK293 cells expressing either WT TALK-1 or TALK-1 DN perfused with the indicated solutions; 10 mM glucose was present throughout the experiment. (C) Normalized Ca^{2+} AUC for the period during treatment with CPA (t=250-600 s).(D) Ca^{2+} AUC for the period following addition of 2.5 mM Ca^{2+} to the extracellular buffer (t=1000-1750 s). (E) Fold increase in Ca^{2+} in response to treatment with the muscarinic receptor agonist carbachol. ($N = 3$ independent experiments) *P<0.05, **P<0.005; Student's t-test.

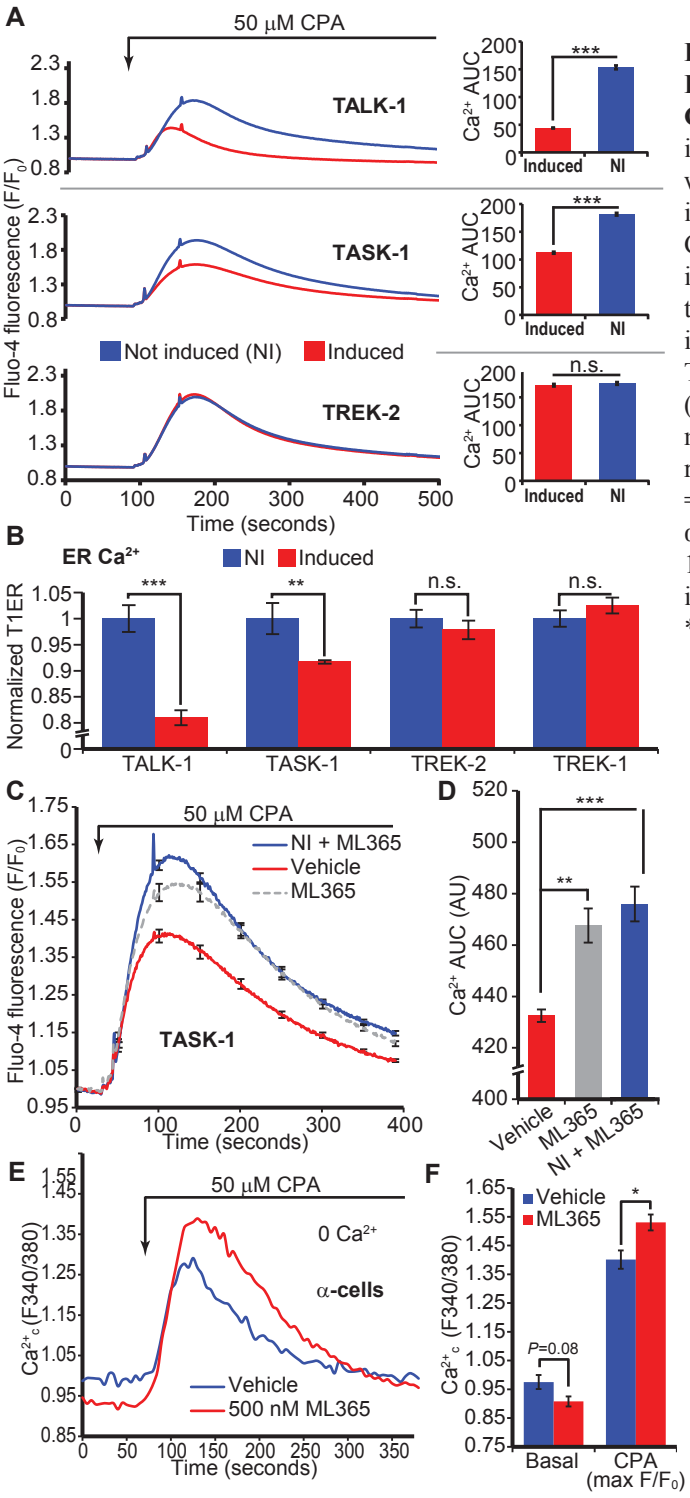

Figure 3.7. Pharmacological manipulation of K2P channel activity can alter steady-state Ca^{2+}_{ER} concentrations. (A) Representative recordings of CPA-induced ER Ca^{2+} release in cell lines with tetracycline-inducible expression of the indicated K2P channels. Ca^{2+} AUC in response to CPA is shown to the right (Representative of $N = 3$ independent experiments). (B) Direct quantification of Ca^{2+}_{ER} concentration in HEK293 cells with inducible expression of TALK-1, TASK-1, TREK-2, TREK-1 and the ER Ca^{2+} indicator T1ER ($N = 3$ independent experiments) (C and D) Treatment of TASK-1-expressing cells with ML365 restores Ca^{2+}_{ER} to pre-channel expression levels ($N = 3$ independent experiments) . (E and F) Mouse α-cells were treated with ML365 in the presence of 11 mM glucose and 125 μM diazoxide ($N = 3$ independent experiments) ;*P<0.05, **P<0.005, ***P<0.0005; Student's t-test.

found that expression of TASK-1 (Figure 3.7A) and TASK-3 (Figure 3.8A,B) channels (*197, 198*) also caused a reduction in Ca^{2+}_{ER}. We confirmed Ca^{2+}_{ER} reduction in TALK-1 and TASK-1 expressing cells by directly measuring Ca^{2+}_{ER} using the genetically encoded Ca^{2+}_{ER} indicator T1ER (*208*) (Figure 3.7B). However, not all K2P channels influence Ca^{2+}_{ER}, as demonstrated by the absence of a Ca^{2+}_{ER} phenotype following induction of TREK-2 or TREK-1 (Figure 3.7B, Figure 3.8C-F) channels.

This finding prompted us to examine whether pharmacological modulation of K2P channels could be used to manipulate Ca^{2+}_{ER} storage. Specific pharmacology for TALK-1 channels does not presently exist. Instead, we tested if selective TASK-1 inhibition with ML365 (a small molecule antagonist of TASK-1 (*209*), and partial TASK-3 inhibitor) could influence Ca^{2+}_{ER}. Inhibition of TASK-1 channel activity with ML365 treatment caused a significant replenishment of Ca^{2+}_{ER} loss caused by TASK-1 channel induction (Figure 3.7C-D). ML365 was without effect on cells expressing TREK-2 or TREK-1 (Figure 3.8C-F). As ML365 also partially blocks TASK-3, treatment of TASK-3-expressing cells with this compound caused a modest increase in Ca^{2+}_{ER} (Figure 3.8A,B). These data are further evidence in support of the hypothesis that K^+ flux through ER K2P channels enhances Ca^{2+}_{ER} leak.

We next tested whether pharmacological blockade of TASK-1 could alter Ca^{2+}_{ER} in primary islet α-cells, where they regulate glucagon secretion (*133*). ML365 treatment elevated α-cell Ca^{2+}_{ER} stores (Figure 3.7E,F), demonstrating that TASK-1 affects α-cell Ca^{2+}_{ER} homeostasis, and that pharmacological inhibition of Ca^{2+}_{ER}-modulating K2P channels can be used to control Ca^{2+}_{ER} in primary islet cells.

TASK-1 mutations have been implicated in pulmonary arterial hypertension (PAH), one of which (G203D) is a dominant-negative mutation that directly impairs TASK-1 K^+

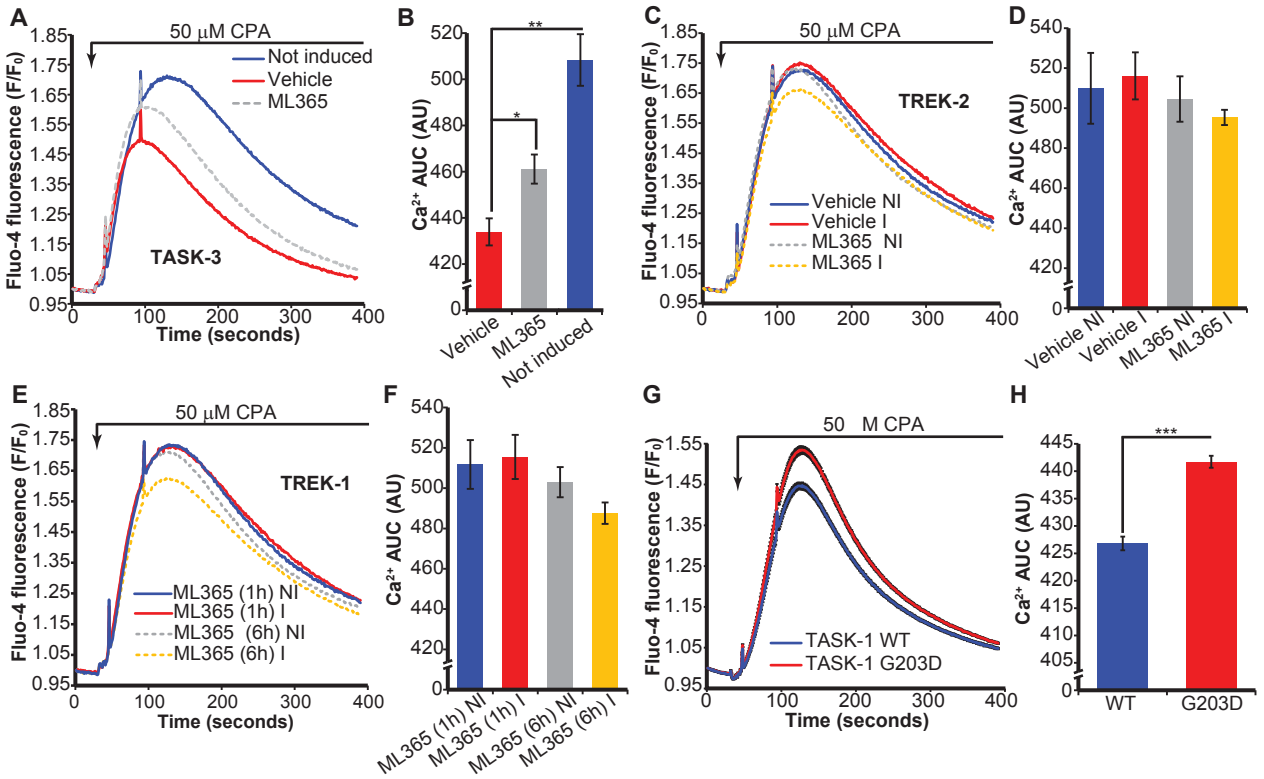

Figure 3.8. TASK-3 and TASK-1 K2P channel activity can alter Ca^{2+}_{ER} concentrations. (A, C, E) Representative recordings of HEK293 cells with inducible expression of TASK-3, TREK-2, or TREK-1 were treated with 500 nM ML365 or vehicle; ER Ca^{2+} stores estimated by treatment with CPA. Data are quantified in (B, D, F) ($N = 3$ independent experiments). (G, H) Representative recording of CPA-induced ER Ca^{2+} release in HEK293 cells expressing wild-type TASK-1 (WT) or TASK-1 G203D mutant channels.Data are quantified in (H) ($N = 3$ independent experiments). *P<0.05, **P<0.005, ***P<0.0005; Student's t-test.

conductance (*210*). Expression of TASK-1 G203D produced a significantly greater increase in Ca^{2+}_{ER} stores when compared to cells expressing control TASK-1 channels (Figure 3.8G,H). This was similar to the effect of expressing the TALK-1 DN mutant, which increased Ca^{2+}_{ER} stores compared to cells expressing wild-type TALK-1. These observations imply that defects in TASK-1 K^+ conductance may inappropriately increase Ca^{2+}_{ER} or impair physiologically important Ca^{2+}_{ER} fluxes.

TALK-1 and TASK-1 form functional channels across the ER membrane

During Ca^{2+}_{ER} release, K^+ moves across the ER membrane to maintain ER electroneutrality and sustain the driving force for ER Ca^{2+} release (*190, 192, 211, 212*). To directly assess whether TALK-1 functions as an ER K^+ channel, we used nuclear patch clamp electrophysiology (*213*) to measure channel activity on the outer nuclear membrane, which is continuous with the ER (Figure 3.9A,B). Nuclei from cells expressing TALK-1 (Figure 3.9D) or TASK-1 (Figure 3.9E) exhibited single-channel openings consistent with their respective biophysical profiles, suggesting that TALK-1 and TASK-1 form functional channels on the ER membrane. However, in nuclei from cells expressing TREK-2, which does not affect Ca^{2+}_{ER}, TREK-2 channel activity was undetectable (Figure 3.9C), similar to nuclei from HEK cells without induction of K2P channel expression.

These results suggest that TALK-1 and TASK-1 regulate Ca^{2+}_{ER} homeostasis by allowing K^+ flux across the ER membrane. We further tested whether TALK-1 modulation of Ca^{2+}_{ER} release depended on K^+ flux by manipulating the cytosolic K^+ concentration. Using digitonin-permeabilized HEK293 cells expressing TALK-1 WT or DN and the genetically encoded Ca^{2+}_{ER} indicator G-CEPIA1er (*203*), we examined Ca^{2+}_{ER} leak in response to SERCA inhibition with CPA. In the presence of K^+, Ca^{2+}_{ER} leak is faster in cells expressing TALK-1 WT

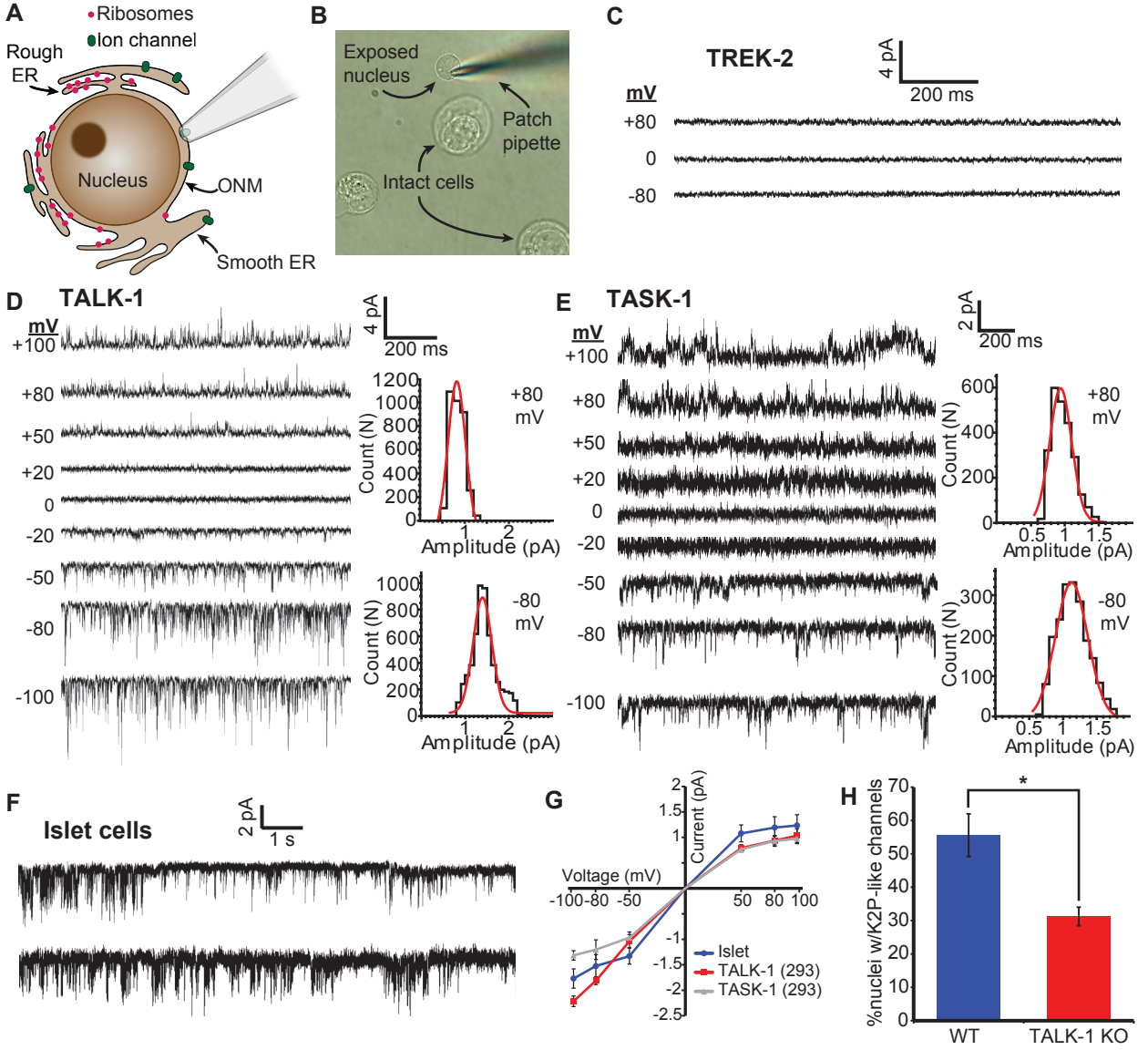

Figure 3.9. Functional TALK-1 and TASK-1 channels are present in the ER membrane. (A) Nuclear patch clamp of outer nuclear membrane permits detection of ER ion channels. (B) Representative image of isolated mouse islet nuclei with patch pipette positioned on nucleus. (C) Recordings obtained from nucleus of a TREK-2-expressing HEK293 cell (representative of 5 nuclei). (D) Current trace obtained from the nucleus of a TALK-1 expressing HEK293 cell. Representative current amplitude histograms at right (representative of 8 nuclei). (E) As in D, but recorded from the nucleus of a TASK-1 expressing cell (representative of 7 nuclei). (F) Representative current traces obtained from WT mouse nuclei; patches held at -50 mV (representative of 42 nuclei). (G) Single-channel current-voltage relationships from nucleus recordings obtained from TALK-1- ($N = 8$) and TASK-1- ($N = 7$) expressing HEK293 cells, and WT islet-cells ($N = 42$). (H) Percent of nuclei with K2P-channel-like channel activity detected in WT and TALK-1 KO β-cells. ($N = 42$ nuclei/4 mice per genotype) *$P<0.05$; Student's t-test.

compared to TALK-1 DN (Figure 3.10A-D). Therefore, K^+ flux through TALK-1 supports the movement of Ca^{2+} across the ER membrane. We also examined whether TALK-1 functions as an ER K^+ channel in primary cells by performing nuclear patch clamp recordings on nuclei isolated from WT and TALK-1 KO islets. We detected single channel openings (Figure 3.9F) with a current amplitude comparable to cloned TALK-1 in 55.6 ±6.3% of WT islet cell nuclei (Figure 3.9G). However, only 31.2 ±2.7% of nuclei from TALK-1 KO islets displayed K2P-like channel openings (Figure 3.9H). Taken together, our findings suggest that TALK-1 and TASK-1 form functional channels on the ER membrane, allowing for a K^+ countercurrent which supports Ca^{2+}_{ER} leak and helps to set Ca^{2+}_{ER}.

TALK-1 regulation of β-cell Ca^{2+}_{ER} handling modulates islet Ca^{2+} oscillations

To dissect the role of TALK-1 modulation of Ca^{2+}_{ER} during β-cell Ca^{2+} influx, we controlled β-cell Ca^{2+}_c influx with K^+-induced depolarization of diazoxide-treated cells in the presence or absence of the SERCA inhibitor thapsigargin (*214*) (Figure 3.11A). Under these conditions the role of plasma membrane TALK-1 channels was effectively dissociated from its intracellular functions: diazoxide precluded the depolarizing effects of glucose by activating K_{ATP} channels and K^+ depolarization activates VDCCs independent of K^+ channel activity (*215*). Subtracting the control trace from the thapsigargin-treated trace revealed the Ca^{2+}_{ER} contribution to the Ca^{2+}_c signal (Figure 3.11B). During Ca^{2+} influx, Ca^{2+}_{ER} uptake was observed (downward deflection, Figure 3.11B), whereas Ca^{2+}_{ER} release occured following the depolarizing K^+ pulse (upward component, Figure 3.11B). We found reduced Ca^{2+}_{ER} release in KO β-cells (Figure 3.11B,C), in accordance with our finding that TALK-1 promotes Ca^{2+}_{ER} release.

β-cell Ca^{2+}_{ER} release has been implicated in the activation of hyperpolarizing Ca^{2+}-activated K^+ currents (*49, 60, 216*). When stimulated with glucose, KO islets show accelerated

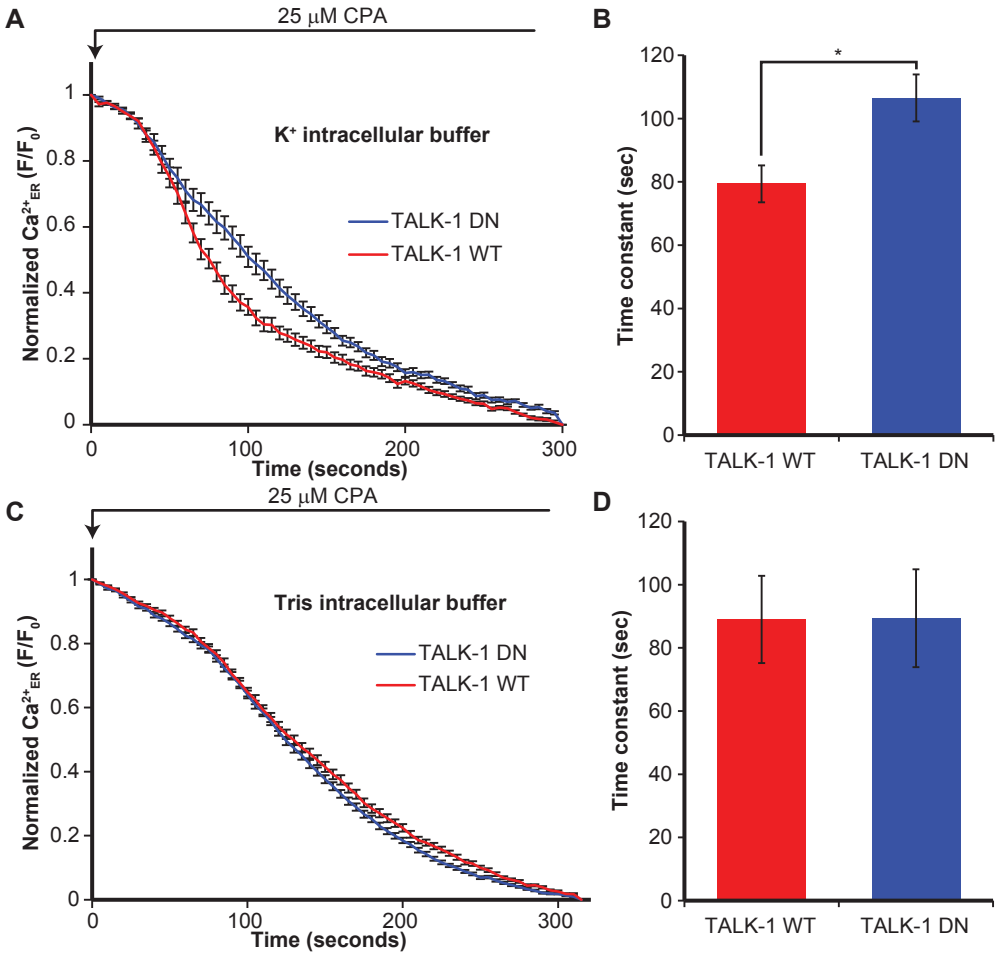

Fig. 3.10. ER Ca^{2+} leak is accelerated by TALK-1 channels. (A) Digitonin-permeabilized HEK293 cells expressing GCEPIA-1ER and wild-type TALK-1 (WT) or TALK-1 DN mutant were perfused with a K^+-containing intracellular buffer, and treated with CPA to induce ER Ca^{2+} leak. The time constant of CPA-induced ER Ca^{2+} leak is presented in (B) (N = 3 independent experiments). (C, D) As in A, but the K^+ in the intracellular buffer was substituted with an equimolar amount of $Tris^+$, a large, K^+ channel-impermeant cation (N = 3 independent experiments). *P<0.05; Student's t-test.

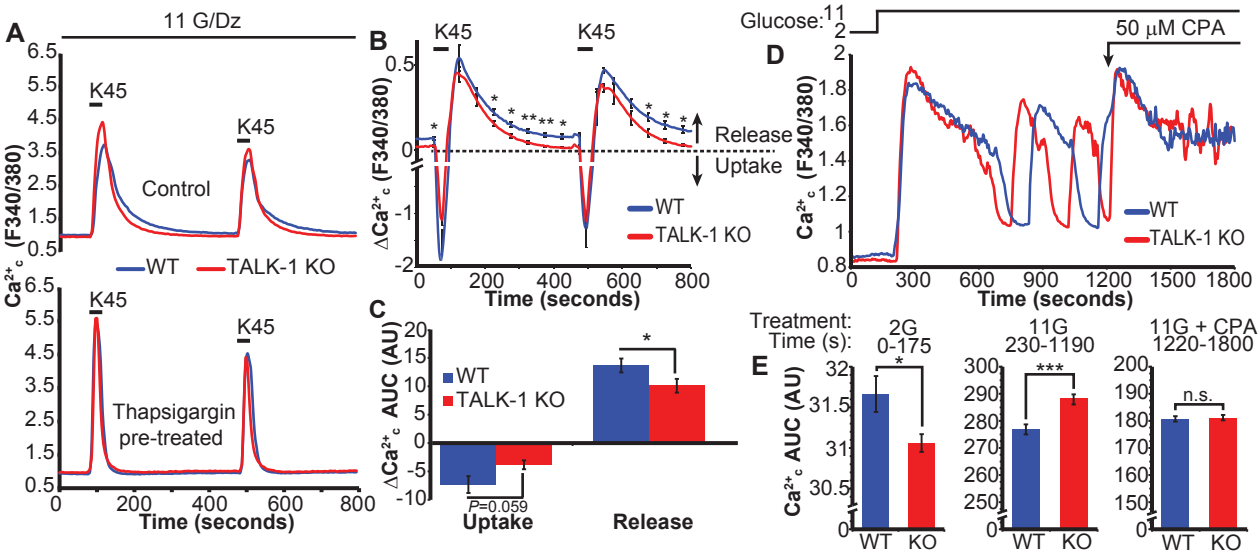

Figure 3.11. TALK-1 reglates ER Ca^{2+} handling during plasma membrane Ca^{2+} influx in β-cells. (A) Intracellular Ca^{2+} oscillations in response to pulses of 45 mM K^+ (K45) for 40 seconds in the presence or absence of thapsigargin (1.25 μM). Recordings were performed in the presence of 11 mM glucose (G), 2.5 mM Ca^{2+}, and 125 μM diazoxide (Dz). (B) Subtraction of the thapsigargin-treated trace from the control trace in A reveals the kinetics of ER Ca^{2+} uptake and release. (C) Quantification of average ER Ca^{2+} uptake and release in WT and TALK-1 KO β-cells ($N = 3$ mice per genotype). (D) Effect of CPA on glucose-stimulated Ca^{2+} influx in WT and KO islets. (E) Area under the curve (AUC) analysis of glucose-stimulated Ca^{2+} influx for periods corresponding to low glucose (2G), high glucose (11G), and CPA (11G + CPA) ($N = 49$ WT and 53 TALK-1 KO islets). *P<0.05, **P<0.005, ***P<0.0005; Student's t-test.

Ca^{2+} oscillations (*202*), which may be due to changes in Ca^{2+}_{ER} control of the membrane potential (V_m) and VDCC activity. We tested this by depleting Ca^{2+}_{ER} using CPA in WT and KO islets undergoing glucose-stimulated Ca^{2+} oscillations (Figure 3.11D). Under low glucose conditions basal Ca^{2+}_c levels were modestly lower in KO islets (Figure 3.11D,E). Upon stimulation with high glucose Ca^{2+} influx was significantly greater in KO islets (Figure 3.11D,E). However, Ca^{2+}_{ER} depletion with CPA normalized Ca^{2+}_c in KO islets to those of WT islets (Figure 3.11D,E). As depletion of Ca^{2+}_{ER} removes the contribution of the ER from the glucose-stimulated Ca^{2+}_c signal, this finding suggested that TALK-1 influences β-cell Ca^{2+}_c by modulating Ca^{2+}_{ER} handling, which in turn regulates plasma membrane currents. Therefore, we proceeded to test the relationship between TALK-1 regulation of Ca^{2+}_{ER} release and β-cell Ca^{2+}-activated K^+ currents.

The termination of each electrical oscillation is triggered by a slowly activating, Ca^{2+}-dependent K^+ current termed K_{slow}, which is mediated by intermediate-conductance K_{Ca} channels (SK4), apamin-insensitive small conductance (SK) K_{Ca} channels, and K_{ATP} (*50, 61, 216*). The β-cell ER can release Ca^{2+} close to the plasma membrane (*217*), and K_{slow} activity is sensitive to Ca^{2+}_{ER} release (*49, 60, 216*). In KO islets, V_m repolarization is reduced by ~50% at the termination of each electrical oscillation (*202*), suggesting that K_{slow} may be impaired in KO islets. We tested this notion by measuring K_{slow} in WT and KO β-cells. K_{slow} amplitude (inset, Figure 3.12A,B) was reduced in KO β-cells by 48 ±17% relative to WT (Figure 3.12C). As TALK-1 is not activated by Ca^{2+}_c in oocytes (*114*), and we also found that TALK-1 activity in HEK293 (Figure 3.12D) or β-cells (Figure 3.12E) was not activated by Ca^{2+}_c, it is unlikely that TALK-1 is a constituent channel of K_{slow}. These findings suggest that TALK-1 may modulate β-cell K_{slow} indirectly through control of Ca^{2+}_{ER} homeostasis. To assess whether modulation of

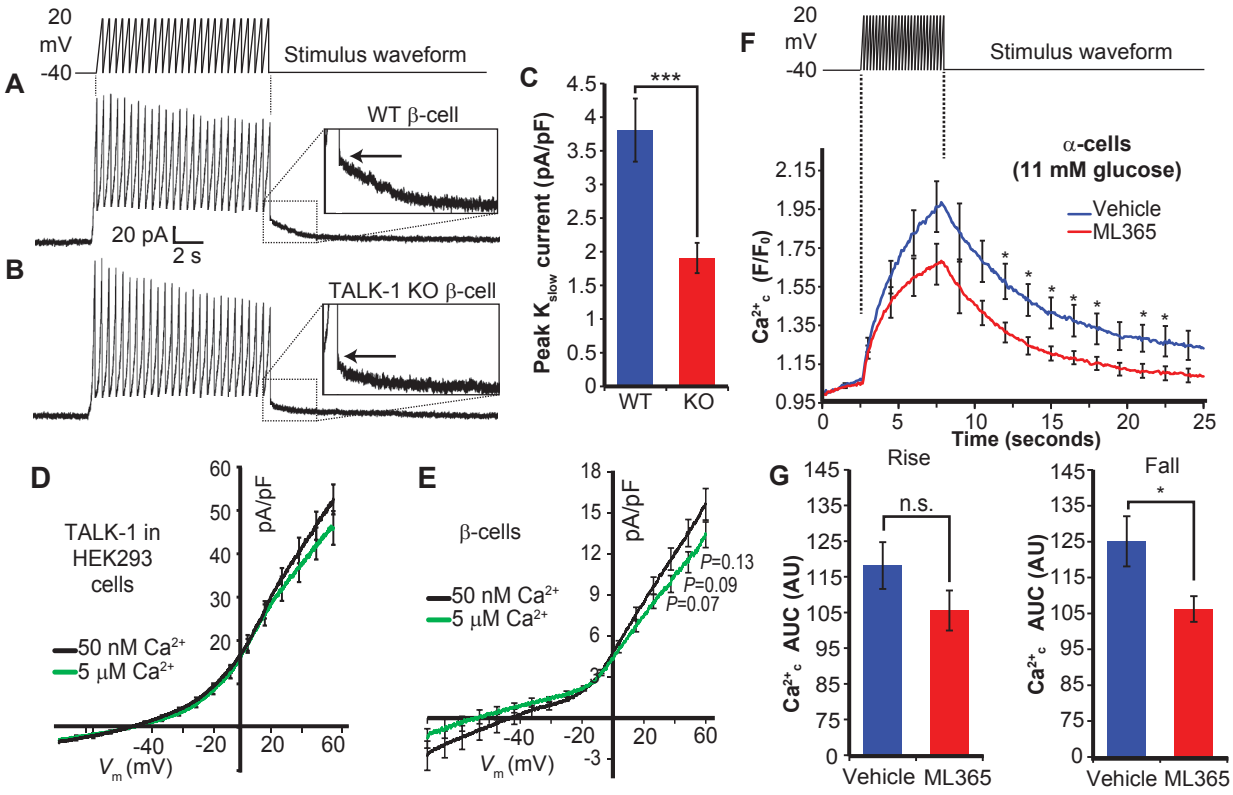

Figure 3.12. Reduced K_{slow} currents are associated with altered ER Ca^{2+} dynamics. (A, B) Representative K_{slow} currents recorded from WT (A) and TALK-1 KO (B) β-cells. The peak of the K_{slow} tail current is indicated by the arrow. (C) Quantification of K_{slow} currents recorded from WT and TALK-1 KO β-cells ($N = 26$ cells; 4 mice per genotype). (D, E) Average whole-cell currents recorded in HEK293 cells expressing TALK-1 with intracellular buffer containing low Ca^{2+} (50 nM, black line) or high Ca^{2+} (5 μM, green line) in HEK293 (D, $N = 11$ cells per condition) and mouse β-cells (E, $N = 15$ (50 nM Ca^{2+}) and 13 cells (5 μM)) (F) Depolarization-induced Ca^{2+} influx in mouse α-cells treated with vehicle or ML365. (G) AUC analysis of rising (rise) and decaying (fall) phase of Ca^{2+} influx in α-cells in vehicle and ML365-treated α-cells ($N = 11$ cells per condition). *P<0.05, ***P<0.0005; Student's t-test.

K2P channels activity affects depolarization-induced Ca^{2+}_{ER} uptake and release, we inhibited TASK-1 in α-cells with ML365. We found reduced Ca^{2+}_{ER} release induced by V_m depolarization (*214*) when TASK-1 channels are inhibited (Figure 3.12F,G), suggesting that TASK-1 facilitates α-cell Ca^{2+}_{ER} release.

TALK-1 channel activity exacerbates islet ER stress

Reduced β-cell ER Ca^{2+} content is associated with ER Ca^{2+} stress and islet dysfunction in diabetes (*67, 103, 182, 218, 219*). Our results indicated that TALK-1 channels are a determinant of β-cell ER Ca^{2+} levels, and suggested that TALK-1 channel activity could exacerbate ER Ca^{2+} depletion which leads to ER stress. Therefore, we determined whether the absence of functional TALK-1 channels impacted islet responses to the metabolic stress of a HFD. After one week of HFD feeding, the expression of genes involved in ER stress signaling was not different between wild-type and TALK-1 KO islets (Figure 3.13A). As SERCA expression is reported to change as a function of ER Ca^{2+} content (*220, 221*), we also examined the expression of mRNA encoding SERCA2b and SERCA3 in wild-type and TALK-1 KO islets, but detected no significant difference. However, after prolonged (20 weeks) of HFD feeding, TALK-1 KO islets exhibited broadly lower expression of multiple ER stress genes, as well as significantly downregulated expression of mRNA encoding SERCA2b and SERCA3 (Figure 3.13B).

We also assessed whether the T2DM-linked gain-of-function polymorphism (rs1535500) encoding TALK-1 A277E (*202*) negatively impacts ER function. We chose to measure ATF6 transcriptional activation, a well-established cellular response to ER Ca^{2+} depletion and protein misfolding (*221, 222*), by using a luciferase reporter containing five tandem repeats of ATF6 binding sites (*223*) co-expressed with wild-type TALK-1 (A277), TALK-1 A277E, or the TALK-1 DN mutant in INS-1 cells (*224*). ER stress was induced with tunicamycin, which

inhibits protein glycosylation and causes protein misfolding. INS-1 cells expressing wild-type TALK-1 or TALK-1 A277E were significantly more susceptible to tunicamycin-induced ATF6 activation than cells expressing the non-conducting TALK-1 DN, and TALK-1 A277E caused significantly more ATF6 activation than wild-type TALK-1 (Figure 3.13C). However, co-expression of TALK-1 A277E with the TALK-1 DN could reduce ATF6 activation to levels comparable to expression of TALK-1 DN alone (Figure 3.13C). Finally, we examined the effects of TALK-1 A277E on INS-1 ER Ca^{2+} levels, and found that it caused a reduction in ER Ca^{2+} when compared to cells expressing wild-type TALK-1 (Figure 3.13D). Taken together, our findings indicate that TALK-1 channels control Ca^{2+}_{ER} fluxes in the islet, which may regulate plasma membrane ion channel activity and electrical excitability as well as ER Ca^{2+} levels important for protein processing. A model depicting the possible mechanisms by which TALK-1 channels modulate β-cell Ca^{2+} influx is presented in Figure 3.14.

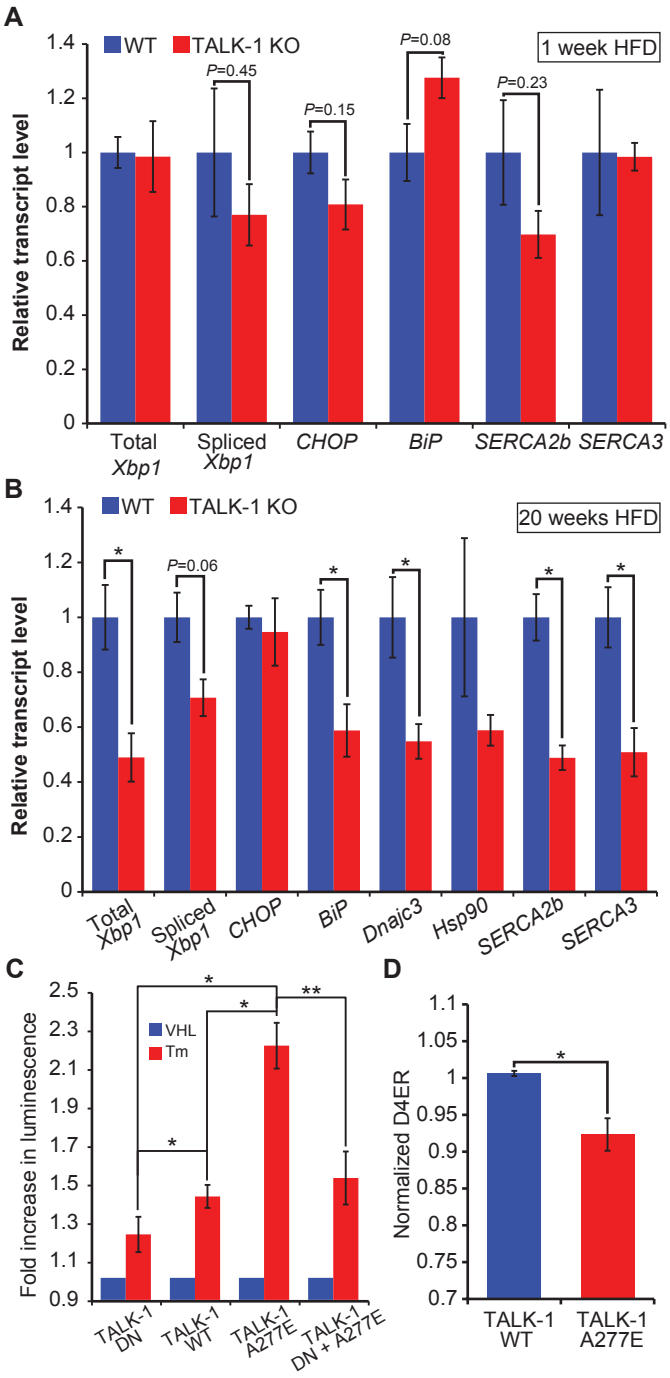

Figure 3.13. TALK-1 channel activity exacerbates ER stress. (**A**) Reverse-transcribed RNA from islets isolated from wild-type (WT) and TALK-1 KO mice fed a HFD for 1 week was subjected to quantitative real-time PCR (qRT-PCR) to measure total *Xbp1*, spliced *Xbp1*, *CHOP*, *BiP*, *Atp2a2* (SERCA2b), and *Atp2a3 (*SERCA3) transcript abundance (N = 4-5 mice per genotype). (**B**) Reverse-transcribed RNA from islets isolated from wild-type (WT) and TALK-1 KO mice fed a HFD for 20 weeks was subjected to qRT-PCR to measure total *Xbp1*, spliced *Xbp1*, *CHOP*, *BiP*, *Dnajc3*, *Hsp90*, *Atp2a2* (SERCA2b), and *Atp2a3 (*SERCA3) transcript abundance (N = 3-4 mice per genotype). (**C**) INS-1 cells co-transfected with TALK-1 DN mutant, wild-type TALK-1 (WT), or TALK-1 A277E and an ATF6 promoter luciferase reporter (p5xATF6-GL3) were treated with vehicle (Vhl) (DMSO, 0.0125% *v*/*v*) or tunicamycin (Tm) (0.25 μg/mL) for 16-20 hours prior to cell lysis and luciferase assay (N = 4 independent experiments). (**D**) INS-1 cells were co-transfected with TALK-1 WT or TALK-1 A277E and pCMV-D4ER to measure basal ER Ca^{2+} levels in 11 mM glucose (N = 3 independent experiments). Statistical significance was determined by Student's *t*-test; **P*<0.05, ***P*<0.01.

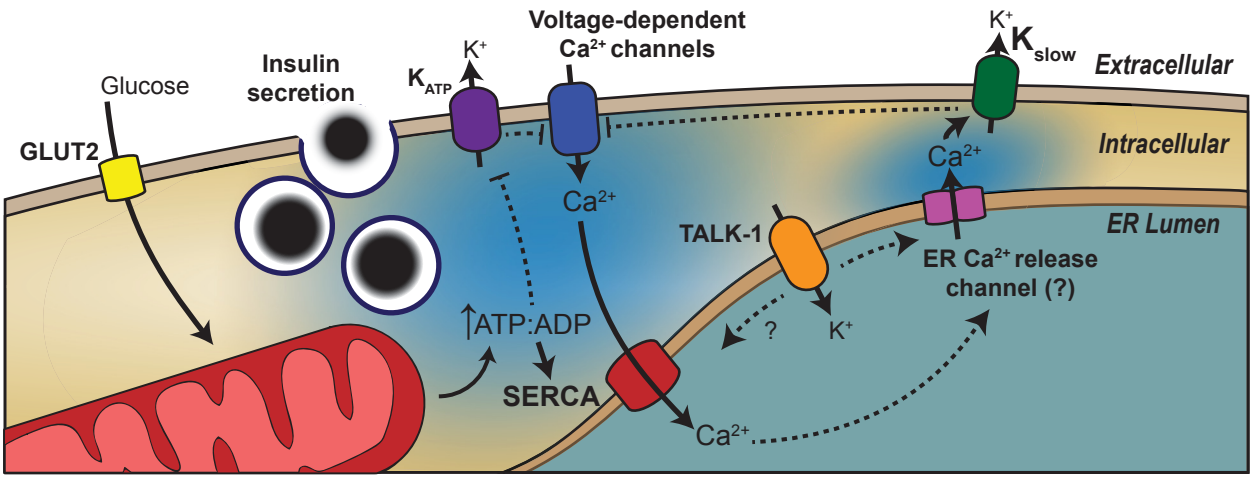

Figure 3.14. Hypothetical model depicting potential molecular mechanisms of TALK-1 channel modulation of β-cell Ca^{2+}_{ER} handling and cytosolic Ca^{2+} oscillations. As glucose is taken up and metabolized, SERCA is energized, increasing Ca^{2+}_{ER}. The increase in the ATP/ADP ratio also leads to K_{ATP} closure and V_m depolarization, activating voltage-dependent Ca^{2+}channels (VDCCs). Plasma membrane TALK-1 channels are predicted to stabilize the V_m at a value which will sustain efficient VDCC activity. As Ca^{2+} influx through VDCCs triggers insulin secretion, the ER rapidly takes up cytosolic Ca^{2+}, further increasing Ca^{2+}_{ER}. Stimulation of Ca^{2+} release from the ER likely contributes to activation of the K_{slow} current, hyperpolarizing the V_m and terminating VDCC activity. TALK-1 channels in the ER potentiate Ca^{2+}_{ER} release, which we hypothesize contributes to K_{slow} activation; thus, loss of ER TALK-1 channel activity impairs K_{slow} -activating Ca^{2+}_{ER} release, inhibiting the K_{slow} current. A reduction in K_{slow} currents would be predicted to increase cytoplasmic Ca^{2+} oscillations and pulsatile insulin secretion.While TALK-1 channels regulate Ca^{2+}_{ER} release, they may also affect Ca^{2+}_{ER} uptake through modifying the activity of SERCAs, either directly or indirectly (see discussion for details).

Discussion

Tight regulation of β-cell Ca^{2+}_{ER} is required to sustain insulin synthesis, metabolism, as well as intracellular Ca^{2+} signaling, and perturbations in Ca^{2+}_{ER} handling contribute to diabetes pathogenesis. β-cell Ca^{2+}_{ER} is controlled by several proteins including SERCAs (*67, 204*), IP3Rs (*225*), RyRs (*180, 225*), and the translocon (*226*). However, the ubiquitous distribution of most Ca^{2+}_{ER} handling proteins precludes their clinical use in treating diabetes. Here, we demonstrate that pharmacological manipulation of K2P channels can be used to control primary cell Ca^{2+}_{ER}. Moreover, our data indicate that inhibiting TALK-1 channel activity can protect islets from ER stress induced by chronic metabolic stress. This opens the exciting potential of utilizing K2P channels such as TALK-1 for therapies that target islet ER dysfunction with minimal off-target effects.

Ca^{2+}_{ER} is determined by a balance of SERCA activity, Ca^{2+}_{ER} release, and Ca^{2+}_{ER} buffering. Ca^{2+}_{ER} release shifts the ER membrane potential ($V_{m(ER)}$) towards the ER Ca^{2+} reversal potential ($E_{Ca^{2+}(ER)}$), where net ER Ca^{2+} efflux would stop. However, the K^+ countercurrent across the ER membrane maintains $V_{m(ER)}$ positive of $E_{Ca^{2+}(ER)}$, facilitating Ca^{2+}_{ER} release (*192, 196*). Our data indicate that ER TALK-1 K^+ currents support the electrochemical driving force for Ca^{2+}_{ER} release. This fits with our finding that TALK-1 overexpression decreased Ca^{2+}_{ER} storage by increasing Ca^{2+}_{ER} leak. Conversely, inhibition of TALK-1 should move the $V_{m(ER)}$ closer to $E_{Ca^{2+}(ER)}$, resulting in reduced Ca^{2+}_{ER} leak and elevated Ca^{2+}_{ER} (*191*), a prediction in accordance with the phenotype of TALK-1 KO β-cells. As insulin secretion is largely dependent on Ca^{2+} influx through VDCCs, the effect of reduced ER Ca^{2+} leak on insulin secretion in TALK-1 KO β-cells is likely minimal. Previous studies demonstrate that ER Ca^{2+} release *per se* does not strongly stimulate insulin secretion (*64, 227*). Indeed, depletion of ER Ca^{2+} increases

average Ca^{2+}_c and insulin secretion (*228*), highlighting the role of ER Ca^{2+} homeostasis in modulating the plasma membrane Ca^{2+} influx which controls insulin release.

TALK-1 KO islets exhibit increased insulin secretion, an elevated frequency of Ca^{2+}_c oscillations, and greater plateau fraction (i.e., the fraction of time spent in electrically excitable periods) (*202*). The present study helps resolve the molecular mechanisms underlying these phenotypes. A rationale for the increased plateau fraction and oscillation frequency in TALK-1 KO islets is that ER TALK-1 channels sustain V_m-hyperpolarizing, K_{slow}-activating ER Ca^{2+} release. Because this ER Ca^{2+} release is reduced in TALK-1 KO β-cells, K_{slow} activation is diminished, resulting in an increased plateau fraction. This is in accordance with observations that depletion of ER Ca^{2+} inhibits K_{slow} (*49*). Despite reduced K_{slow} amplitude in β-cells lacking TALK-1, the frequency of K_{slow} activation appears to be increased. This may reflect an interesting feedback in TALK-1 KO β-cells between increased ER Ca^{2+} levels stimulating activation of the ER Ca^{2+} release mechanism, combined with an inability to sustain ER Ca^{2+} release due to the shifted $V_{m(ER)}$. Indeed, the open probability of IP3 receptors and RyRs is increased by elevated ER Ca^{2+} levels (*229, 230*), and increasing β-cell IP3 levels potently accelerates electrical and Ca^{2+}_c oscillations (*64, 149*). Future investigations are needed to define the molecular identity of β-cell ER Ca^{2+} release channels and how they modulate plasma membrane currents.

Treatment of islets with SERCA inhibitors accelerates Ca^{2+}_c and electrical oscillations (*231-233*), presumably due to inhibition of K_{slow} and activation of SOCE. However, islets lacking SERCA3 show a decreased frequency of Ca^{2+}_c oscillations (*63*). One conceivable explanation for this paradoxical phenotype is that SERCA3 is necessary for K_{slow} activating ER Ca^{2+} release, which is suggested by the findings that slow ER Ca^{2+} release (*215*) and rapid V_m

oscillations (*234*) are largely abolished in SERCA3 KO β-cells. These observations highlight that SOCE serves an important role in shaping islet Ca^{2+}_c oscillations, and future studies are required to dissect the relationship between TALK-1 modulation of ER Ca^{2+} stores, SOCE, V_m and Ca^{2+}_c oscillations, and insulin secretion.

ER K^+ channels are also important for Ca^{2+}_{ER} uptake, as demonstrated by the influence of ER-localized SK channels in regulating neuronal and cardiomyocyte ER/SR Ca^{2+} uptake (*196*). SK channels are predicted to preserve ER pH homeostasis through activation of an ER K^+/H^+ antiporter that promotes ER H^+ entry to balance SERCA-mediated H^+ loss during Ca^{2+} uptake (*196*). Although we cannot exclude a role for K2P channels in modulating SERCA function, we find reduced basal Ca^{2+}_{ER} when TALK-1was heterologously expressed, and increased Ca^{2+}_{ER} in KO β-cells. These findings suggest that if TALK-1 controls Ca^{2+}_{ER} uptake, it would presumably do so by inhibiting SERCA function, in contrast to SK channels, which enhance SERCA function. Thus, any effects of TALK-1 on SERCA could be through indirect mechanisms that Ca^{2+}_{ER} modulates, such as mitochondrial ATP production which energizes the β-cell SERCA pump (*235*). Interestingly, we find that SERCA2b and SERCA3 mRNA are reduced in TALK-1 KO islets after prolonged HFD feeding, which may represent a compensatory mechanism to reduce ER Ca^{2+} overloading and maintain ER Ca^{2+} levels in an optimal range.

Our observations suggest that TALK-1 activity contributes to the unique features of β-cell ER function. For example, TALK-1 control of Ca^{2+}_{ER} potentiates K_{slow} currents, limiting the islet Ca^{2+} oscillations which underlie pulsatile insulin secretion. Another essential function of β-cell Ca^{2+}_{ER} handling is to maintain insulin production and processing. Ca^{2+}_{ER} homeostasis is impaired under conditions of β-cell stress induced by insulin resistance or decreased β-cell mass, and a hallmark of ER stress is increased Ca^{2+}_{ER} leak (*180*). This can be caused in β-cells by

reductions in expression of proteins which affect Ca^{2+}_{ER} such as SERCA2b (*67*) or sorcin (*224*). Our data indicate that TALK-1 activity negatively contributes to ER stress during metabolic stress. Moreover, our finding that T2DM-associated TALK-1 A277E channels exacerbate Ca^{2+}_{ER} leak and ER stress responses suggests that TALK-1 activity can contribute to islet Ca^{2+}_{ER} defects in diabetes. Interestingly, TALK-1 transcript abundance is downregulated under conditions that cause ER stress in diabetes (such as palmitate or inflammatory cytokine treatment (*175*)), which may be a protective mechanism to preserve β-cell Ca^{2+}_{ER} homeostasis. It will be imperative to determine how TALK-1 participates in the cellular response to other diabetes-associated ER stressors.

Dominant-negative mutations in TASK-1 and TASK-3 cause PAH and Birk-Barel syndrome, respectively (*210*). We found that a PAH-linked mutation in TASK-1 (G203D) enhanced Ca^{2+}_{ER} stores relative to WT TASK-1. Thus, in patients with the TASK-1 G203D mutation, disruptions in ER/SR Ca^{2+} handling may contribute to PAH (*236-238*). TASK-3 also controls Ca^{2+}_{ER}, and a mutation in *KCNK9* (which encodes TASK-3, G236R) causes Birk-Barel syndrome, which is characterized by intellectual disability, hypotonia, and facial dysmorphism. Importantly, we observe that pharmacological regulation of TASK-1 can be used to control primary cell Ca^{2+}_{ER} (i.e., in pancreatic α-cells). This opens the exciting potential of utilizing K2P channels such as TASK-1, TASK-3 or TALK-1 for cell-selective therapies that target ER dysfunction.

Not all K2P channels regulate Ca^{2+}_{ER}, as demonstrated by our finding that neither TREK-1 channels nor TREK-2 channels affected Ca^{2+}_{ER} homeostasis. This could be due to localization of these channels; TREK-1 channels are found primarily on the plasma membrane (*239*), whereas the subcellular localization of TREK-2 channels has not been examined. However, all

K^+ channels are assembled in the ER prior to their delivery to the plasma membrane. Some K^+ channels, such as K_{ATP}, require a physical interaction with the plasma membrane lipid phosphatidylinositol 4,5-bisphosphate (PIP_2) in order to conduct K^+, K2P channels that are dependent on PIP_2 for activity may not function in the ER membrane. This is due to intrinsically low PIP_2 levels on the ER membrane, which limits most K^+ channel activity until they are transported to the plasma membrane. TREK-1 is highly sensitive to PIP_2, whereas both TASK-1 and TASK-3 channels, both of which affect Ca^{2+}_{ER}, are insensitive to PIP_2 (*240*). Future studies are needed to better understand the regulatory mechanisms underlying K2P channel activity in the ER, and how these affect Ca^{2+}_{ER} homeostasis.

In conclusion, we demonstrate that TALK-1 is functionally expressed in the ER where it regulates Ca^{2+}_{ER} handling, thus controlling K_{slow} activity, Ca^{2+} influx and insulin secretion. These findings highlight a physiological function of K2P channels in the regulation of Ca^{2+}_{ER}. K2P channels may provide cell-selective targets to modulate Ca^{2+}_{ER} to treat the many diseases characterized by dysfunctional Ca^{2+}_{ER} handling.

Research Design and Methods

Mouse models

The mice used in this study were 8-12 week-old males on a C57Bl6/J background. The generation of *Kcnk16*$^{-/-}$ (TALK-1 KO) mice has been previously described (see Chapter II) (*202*). For experiments using mouse α-cells, transgenic mice expressing tdRFP specifically in α-cells were used (*133*). All mice used in this study were handled in compliance with protocols reviewed and approved by the Vanderbilt University Institutional Animal Care and Use Committee, according to guidelines set forth by the NIH.

Islet isolation and culture

Mouse islets were isolated using collagenase P (Roche) digestion of the pancreas and density gradient centrifugation (*176*). Human islets from adult nondiabetic donors (donor information is provided in Table 3.1) were obtained through isolation centers organized by the Integrated Islet Distribution Program. In experiments using D4ER, cells were transduced with Ad-D4ER (*204*) 48 hours prior to imaging. In human β-cell experiments, cells were transfected with TALK-1 DN- or mCherry-expressing plasmids (*202*). Islets and dispersed cells were cultured for 24-48 hours prior to experimentation (*202*).

Donor	**1**	**2**	**3**
Sex	F	F	F
Age (years)	37	54	64
BMI	25.1	30.1	27.4
Ethnicity	Hispanic/Latino	W	W
HbA1c	5.5%	5.8%	5.5%
Type 2 Diabetes	No	No	No

Table 3.1. Human islet donor characteristics

Cell culture and luciferase assays

The development of TREx-293 cells with inducible expression of K2P channels has been previously described (*124*). To determine the levels of TALK-1 and TASK-1 expression in induced cells, lysates from TALK-1- or TASK-1-TREx-293 cells treated for 24 hours with or without tetracycline induction (1 μg/mL) were run on 4−12% Bis-Tris polyacrylamide gels (Invitrogen). The protein was then transferred to a nitrocellulose blotting membrane (BioRad) which was probed with TALK-1 (Novus Biologicals #NBP1-83071) or TASK-1 (Abcam #49433) antibodies. Equal loading of wells was assessed by stripping and reprobing membranes with a β-actin antibody (Cell Signaling Technologies #4970). Representative blots are shown in

Fig. S7. For experiments comparing the effects of wild-type TALK-1 and TALK-1 DN on Ca^{2+}_{ER} handling, HEK293 cells were transfected with pCDNA3.1 plasmids encoding these channels using Lipofectamine 3000 (Thermo Fisher) according to the manufacturer's instructions, and imaged 48 hours post-transfection.

INS-1 (832/13) cells were cultured in RPMI 1640 supplemented with 15% FBS and penicillin-streptomycin. INS-1 cells were transfected with p5xATF6-GL3 (Addgene #11976) and plasmids encoding wild-type TALK-1, TALK-1 A277E, or TALK-1 DN (*202*). Cells were incubated overnight with vehicle (DMSO) or tunicamycin (0.25 µg/mL) for 16-20 hours prior to performing a luciferase assay using the Steady-Glo Luciferase Assay System (Promega) according to the manufacturer's instructions.

Patch clamp electrophysiology

An Axopatch 200B amplifier (Molecular Devices) was used to measure whole-cell K^+ channel currents in the voltage-clamp mode; currents were digitized using a Digidata 1440, lowpass filtered at 1 kHz and sampled at 10 kHz. For K_{slow} recordings, pipettes were filled with an intracellular solution (*50*) containing (in mM) 28.4 K_2SO_4, 63.7 KCl, 11.8 NaCl, 1 $MgCl_2$, 20.8 HEPES, 0.5 EGTA (pH 7.22 with KOH) and ~0.05 $mg{\cdot}ml^{-1}$ amphotericin B. Nuclear patch clamp experiments were preformed using the approach described by Mak and colleagues (*213*). Nuclei were patched in a solution containing (in mM): 150 KCl, 10 HEPES, 0.5 EGTA, 0.36 $CaCl_2$ (pH 7.3 with KOH). Patch electrodes were pulled to a resistance of 8-10 MΩ , loaded with recording solution, and coated with Sigmacote. Single-channel currents were lowpass filtered at 1 kHz and sampled at 50 kHz.

When intracellular [Ca^{2+}] was clamped, cells were recorded using the whole-cell configuration using electrodes filled with a solution containing (in mM) 140 KCl, 5 HEPES, 4

Mg·ATP, 1 EGTA, 137 μM (for 50 nM Ca^{2+} final) or 946 μM (for 5 μM Ca^{2+} final) $CaCl_2$, (pH 7.22 with KOH). [Ca^{2+}] was determined using MAXCHELATOR software. The extracellular buffer used for islet-cells (A modified Krebs-Ringer buffer, KRB) contained (in mM) 119 NaCl, 2.5 $CaCl_2$, 4.7 KCl, 25 HEPES, 1.2 $MgSO_4$, 1.2 KH_2PO_4, 11 glucose (pH 7.35 with NaOH). The extracellular buffer used for HEK293 cells (HEK buffer) contained (in mM) 150 NaCl, 5 KCl, 2 $MgCl_2$, 2.5 $CaCl_2$, 10 HEPES, and 10 glucose (pH 7.35 with NaOH). When assessing the Ca^{2+} sensitivity of TALK-1 in β-cells, the extracellular buffer was supplemented with a cocktail of K^+ channel inhibitors including 200 μM tolbutamide (MP Biomedicals), 10 mM tetraethylammonium chloride (Acros Organics), 100 nM apamin (Alomone Labs), 100 nM iberiotoxin (Alomone Labs), 100 nM TRAM-34 (Alomone Labs), and 10 μM nifedipine to inhibit voltage-gated Ca^{2+} channels. Cells were recorded with a voltage-clamp protocol used to assess K2P channel currents (*202*). Recordings were analyzed using Clampfit 10 (Molecular Devices) and Microsoft Excel software.

Calcium imaging

Mouse and human β-cells were loaded with 2 μM Fura-2 AM (Molecular Probes) and imaged as previously described (*52*). Cyclopiazonic acid (CPA; Alomone Labs) was used at a concentration of 50 μM; ionomycin was used at a concentration of 5 μM (Alomone Labs). Human β-cells were post-stained for insulin (*52*). In all experiments, cells were perifused with a flow of 2 mL·min^{-1} at 37 °C. Detailed methods describing Ca^{2+} imaging in stably transduced TREx-293 cells and high-speed Ca^{2+} imaging can be found in the supplementary material. For analysis of mouse β-cell ER Ca^{2+} uptake and release (*214*), Fura-2 loaded cells were incubated for 10 minutes in KRB supplemented with 11 mM glucose, 125 μM diazoxide (Enzo) and 1.25 μM thapsigargin (Alomone Labs) or vehicle. In high-[K^+] stimulus buffer, NaCl was reduced

accordingly to maintain osmolarity. For experiments using D4ER, cells were incubated for 20 minutes in KRB containing 2 mM glucose prior to imaging.

For assays comparing the effects of expression of K2P channels in stably transduced TREx-293 cells, 30,000 cells/well were seeded to 384-well black-wall, clear-bottom, amine-coated plates (BD Biosciences). Channel expression was induced with 1 $\mu g \cdot ml^{-1}$ tetracycline in culture medium, and the cells were cultured overnight in a 5% CO_2 incubator at 37 °C. The cells were washed with HEK buffer (10 mM glucose) using an ELx405CW plate washer (Bio-Tek Instruments, Inc.), and loaded with 4 μM Fluo-4 AM (Molecular Probes) in HEK buffer for 45 minutes in a 5% CO_2 incubator at 37 °C. The cells were then washed with HEK buffer supplemented with 1 mM EGTA and incubated in a 5% CO_2 incubator at 37 °C for 8 minutes prior to the start of imaging. Plates were then loaded into a whole-plate kinetic-imaging Functional Drug Screening System (FDSS 6000, Hamamatsu, Bridgewater, NJ) and imaged at 37 °C as previously described (*124*).

When assessing the effects of TASK-1 or TASK-3 channel blockade, cells were loaded three hours prior to the start of imaging with 500 nM ML365 (Tocris) or DMSO vehicle in culture medium, and in α-cells, the culture medium also contained 125 μM diazoxide. ML365 was present throughout the experiment. For high-speed imaging of α-cell Ca^{2+} influx, cells were loaded with 5 μM Fluo-4 AM for 25 minutes, followed by washing with KRB (11 mM glucose). α-cells were then patched according to the perforated patch clamp protocol described above on a Nikon Eclipse TE2000-U microscope equipped with an X-Cite 120Q widefield fluorescence light source (Excelitas Technologies) and a D-104 microscope photometer (Photon Technologies Inc.). Upon obtaining a low-leak, GΩ seal, the fluorescence light source was activated, and plasma membrane currents were recorded using the K_{slow} voltage-clamp protocol (*50*)

simultaneously with Fluo-4 fluorescence. Currents and photometer signal were digitized and sampled at 10 kHz. For analysis of the effects of TALK-1 on the CPA-induced Ca^{2+}_{ER} leak rate, TREx-293 cells transfected with TALK-1 WT or DN and CEPIA1-ER(*203*) (Addgene #58215) were permeablized for 4 minutes in a 5% CO_2 incubator at 37 °C in an intracellular buffer containing (in mM): 140 potassium gluconate or 140 Tris base (K^+-free), 10 HEPES, 1 EGTA, 0.432 $CaCl_2$, 3 Mg·ATP, with sucrose added as needed to match osmolarity (pH 7.24), and supplemented with 50 $\mu g \cdot ml^{-1}$ digitonin (Santa Cruz). Cells were then washed for an additional 5 minutes in the appropriate buffer without digitonin prior to the start of imaging. Data were analyzed using Nikon Elements, Microsoft Excel, and GraphPad Prism7 software. To determine the rate constant of CPA-induced Ca^{2+} leak, the normalized data was fit to a one-phase exponential decay model using GraphPad Prism7 software. Data were analyzed using Nikon Elements, Microsoft Excel, Clampfit 10 and GraphPad Prism7 software.

Site-directed mutagenesis

The TASK-1 G203D point mutation was generated using a previously described approach (*202*). The sequences of oligonucleotide primers (Integrated DNA Technologies) used to create the TASK-1 G203D mutant were:

ACCACCATCGGCTTCGACGACTACGTGGCGCTGCAGA (forward)

TCTGCAGCGCCACGTAGTCGTCGAAGCCGATGGTGGT (reverse)

PCRs were performed in 50 µL with Q5 high-fidelity DNA polymerase (New England Biolabs) with 100 ng of pCDNA3.1-KCNK3 plasmid.. DNA was then incubated with 1 µL DpnI for two hours at 37 °C. Clones were sequenced to confirm mutagenesis.

Immunofluorescence

Processing and staining of paraffin-embedded mouse and human pancreas sections was performed as previously described (human donor information is provided in Table 3.2) (*202*). Sections were stained using primary antibodies against TALK-1 (Novus Biologicals #NBP1-83071; 1:175) and calreticulin (Santa Cruz #N-19; 1:125); secondary antibodies used were Alexa Fluor 488-conjugated donkey anti-rabbit (Jackson Immunoresearch #711-546-152; 1:300) and DyLight 650-conjugated donkey anti-goat (Thermo Fisher #SA5-10089; 1:250). HEK293 cells co-transfected with TALK-1a or TALK-1b (*202*) and ER-targeted EYFP (Addgene #56589) were washed twice with cold phosphate-buffered saline (PBS), then fixed in 4% paraformaldehyde (Electron Microscopy Sciences) for 30 minutes at 4 °C. Cells were then incubated in PBS supplemented with 0.2% bovine serum albumin (BSA), 2% normal donkey serum (NDS; Jackson Immunoresearch), and 0.05% Triton X-100 for one hour, followed by incubation in PBS containing primary antibodies against TALK-1 (1:175) and GFP (Novus Biologicals NB600-597; 1:300), 0.2% BSA, 1% NDS, and 0.1% Triton X-100, overnight at 4 °C. Following removal of the primary antibody solution, the cells were subjected to two 10-minute PBS washes, then incubated in the dark for one hour at room temperature in PBS containing 1% NDS and secondary antibodies: Alexa Fluor 488-conjugated donkey anti-rabbit (1:300) and Alexa Fluor 647-conjugated goat anti-mouse (Thermo Fisher A21237; 1:300). The secondary antibody solution was removed and the cells were subjected to three 8-minute PBS washes prior to imaging. All images were obtained using a Zeiss LSM 710 or Zeiss LSM 780 confocal laser scanning microscope. Images were analyzed using ImageJ software.

For analysis of islet cell numbers, paraffin embedded were processed as described above, and stained using primary antibodies against insulin (Dako #A0564; 1:500), somatosatin (Santa

Cruz Biotechnology sc-7819: 1:250), and glucagon (Proteintech #15954-I-AP: 1:500); secondary antibodies used were Alexa Fluor 488-conjugated donkey anti-rabbit (Jackson Immunoresearch #711-546-152; 1:500), DyLight 650-conjugated donkey anti-goat (Thermo Fisher #SA5-10089; 1:250), Cy3-conjugated donkey anti-guinea pig (Jackson Immunoresearch #706-165-148; 1:500).

For analysis of high-fat diet induced islet-cell proliferation, age-matched WT and TALK-1 KO were placed on a high-fat diet (60% kcal/fat; Research Diets #D12492) for 10 days. Four days prior to sacrifice, mice were provided with drinking water containing BrdU (0.8 $mg \cdot ml^{-1}$) supplemented with Splenda artificial sweetener (20 $mg \cdot ml^{-1}$). Paraffin embedded pancreata were processed as described above, and were subjected to antigen retrieval performed in 1× NaCitrate pH 6.0, for 14 minutes in a microwave at high power, followed by cooling at room temperature in 1× NaCitrate solution for 25 minutes. Following antigen retrieval, slides were washed for 10 minutes in ddH_2O, followed by two 2-minute washes in PBS. Sections were the stained using primary antibodies against insulin (Dako #A0564; 1:500), somatosatin (Santa Cruz Biotechnology sc-7819: 1:250), glucagon (Proteintech #15954-I-AP; 1:500), and BrdU (Developmental Studies Hybridoma Bank #G3G4; 1:50). Secondary antibodies used were Alexa Flour 647-conjugated goat anti-mouse (Life Technologies #A21237: 1:250), DyLight 488-conjugated Donkey anti-mouse (Thermo Scientific #SA5-10166; 1:300), and Alexa Flour 594-conjugated Donkey Anti-Guinea Pig (Jackson Immunoresearch #706-586-148; 1:400), DyLight 650-conjugated donkey anti-goat (Thermo Fisher #SA5-10089; 1:250), Alexa Fluor 488-conjugated donkey anti-rabbit (Jackson Immunoresearch #711-546-152; 1:500). Blocking was done in a dark humidity chamber for one hour using Dako Blocking Solution (Ref # X0909). Primary antibodies were diluted to above concentrations in DAKO Antibody Diluent Solution (Ref#S3002) and incubated on the sections overnight at 4 °C. Following primary antibody

incubation, slides were washed for 5 minutes in PBS twice. Secondary antibodies were diluted to the above concentrations in PBS supplemented with 5% NDS and incubated on slides in the dark for 2 hours at room temperature. Sections were then washed twice for five minutes in PBS and DAPI was added (1:1000 for 2 minutes). Following DAPI staining, sections were washed for 5 minutes in ddH20 and then mounted with a coverslip.

All sections were imaged with an Aperio ImageScope and analyzed using an algorithm developed with Aperio IndicaLabs- CytoNuclear FLv1.2 software. The algorithm is designed to take into account factors such as nuclear staining, cytoplasm radius, nucelar size, nuclear roundness, and dye fluorescence wavelength (Cy2, Cy3, or Cy5), to identify, differentiate, and count β, δ, and α cells. The algorithm was also used to count the number of β-, δ-, and α- cells on the slides labeled with Brd-U, which was further analyzed using ImageJ software and Microsoft Excel.

Donor	**1**	**2**
Sex	F	M
Age (years)	79	31
Ethnicity	W	B
Type 2 Diabetes	No	No

Table 3.2. Human pancreas donor characteristics

Statistical analysis

The data is presented as recordings that are averaged or representative of results obtained from at least three independent cultures. All values presented are the mean ± SEM. Statistical differences between means were assessed using two-tailed unpaired or paired Student's *t*-test, or one-way ANOVA, as appropriate. A $P<0.05$ was considered as significant.

CHAPTER IV

TALK-1 CONTROLS PANCREATIC DELTA-CELL Ca^{2+}-INDUCED Ca^{2+} RELEASE AND SOMATOSTATIN SECRETION*

Preface

In addition to being highly expressed in islet β-cells, single-cell RNA sequencing technologies have revealed that TALK-1 is abundant at the transcript level in the somatostatin-secreting δ-cells. However, a physiological role for TALK-1 in δ-cells has not been examined. In the previous chapter, I described how K^+ flux through ER-localized TALK-1 channels enhances ER Ca^{2+} leak. As somatostatin secretion is amplified by Ca^{2+}-induced Ca^{2+} release (CICR) from the ER, TALK-1 channels could regulate δ-cell CICR by modulating ER Ca^{2+} homeostasis. To test this hypothesis, we generated control and TALK-1 KO mice expressing fluorescent reporters specifically in δ- and α-cells to facilitate cell type identification. Using immunofluorescence, patch clamp electrophysiology, Ca^{2+} imaging, and hormone secretion assays, we investigated how TALK-1 channel activity impacts δ- and α-cell function. Our observations indicate that TALK-1 regulates δ-cell Ca^{2+} influx by reducing δ-cell ER Ca^{2+} stores, which limits δ-cell CICR and somatostatin secretion, thus modulating the intraislet paracrine signaling mechanisms which control glucagon secretion.

*The work presented in this chapter is in preparation for submission to *Molecular Metabolism* as: Vierra NC, Dadi PK, Jordan KL, Altman M, Dickerson MT, Jacobson DA. TALK-1 Controls Pancreatic Delta-cell Ca^{2+}-induced Ca^{2+} Release and Somatostatin Secretion. 2017.

Introduction

Somatostatin is a potent inhibitory peptide which regulates many physiological processes including hormone secretion, neurotransmission, gastric function, and cell proliferation (*241*). Somatostatin signals through plasma membrane $G_{\alpha i}$-coupled somatostatin receptors, suppressing cellular function by inhibiting cAMP production and activating inward-rectifier K^+ channels. In most cases, secreted somatostatin acts locally to regulate the activity of surrounding cells (*241*). This is exemplified by intraislet somatostatin release from δ-cells, which exerts a tonic inhibitory effect on glucagon and insulin secretion (*84, 242*). Although it is known that δ-cell somatostatin secretion is sensitive to glucose, the molecular determinants of δ-cell function are poorly understood. Emerging data suggests that dysregulated islet somatostatin secretion contributes to perturbed glucose homeostasis in type 1 and type 2 diabetes mellitus (T2DM); therefore, it is important to define the mechanisms underlying δ-cell somatostatin secretion.

Elevated blood glucose levels increase islet somatostatin release (*243*). Similar to insulin and glucagon secretion, somatostatin exocytosis requires extracellular Ca^{2+} influx through voltage-dependent Ca^{2+} channels (VDCCs) (*10, 86*). VDCC opening is controlled by the plasma membrane potential (V_m), which is largely determined by the activity of hyperpolarizing K^+ channels. Islet δ-cells express ATP-sensitive K^+ (K_{ATP}) channels, which couple cellular glucose metabolism to the V_m and contribute to the regulation of somatostatin secretion (*242*). However, δ-cells lacking functional K_{ATP} channels exhibit glucose-regulated somatostatin secretion, indicating that other mechanisms besides K_{ATP} control δ-cell glucose sensitivity (*86*). Indeed, glucose-dependent amplification of somatostatin secretion has been shown to be dependent upon paracrine stimulation by β-cells and Ca^{2+}-induced Ca^{2+} release (CICR) from the endoplasmic reticulum (ER) (*86, 244*). It has been proposed that glucose metabolism accelerates δ-cell

sarco/endoplasmic reticulum Ca^{2+}-ATPase (SERCA) activity, resulting in elevated ER Ca^{2+} and enhanced CICR (*86*). ER Ca^{2+} content is a key regulator of CICR: increased ER Ca^{2+} enhances CICR, whereas depleted ER Ca^{2+} inhibits CICR (*229, 230, 245*). Indeed, pharmacological inhibition of SERCA activity and subsequent depletion of ER Ca^{2+} significantly reduces somatostatin secretion, indicating that ER Ca^{2+} serves a critical role in δ-cell function (*77, 86*). However, the mechanisms which modulate δ-cell Ca^{2+} influx and CICR under different glucose conditions are largely unknown.

The two-pore domain K^+ (K2P) channel TALK-1 is abundantly expressed in δ-cells of the islet and gastric epithelium (*80, 115*). In β-cells, TALK-1 channels control Ca^{2+} influx and insulin secretion by modulating the V_m and ER Ca^{2+} homeostasis (*202*). A non-synonymous polymorphism in TALK-1 (rs1535500, encoding TALK-1 A277E), causes a gain-of-function in TALK-1 channel activity which is associated with reduced insulin secretion in T2DM patients and increased T2DM susceptibility (*27-30, 178*). As detailed in Chapter III, TALK-1-dependent modulation of ER Ca^{2+} levels plays a central role in controlling β-cell Ca^{2+} homeostasis. TALK-1 channels conduct a K^+ countercurrent across the ER membrane which enhances ER Ca^{2+} leak; thus, inhibiting TALK-1 channel activity augments ER Ca^{2+} stores. Given the role TALK-1 channels serve in regulating β-cell ER Ca^{2+} levels, prominent expression of TALK-1 mRNA in δ-cells, and sensitivity of CICR to ER Ca^{2+} levels, we investigated whether TALK-1 channels modulate δ-cell Ca^{2+} handling and somatostatin secretion. We found that TALK-1 forms functional channels in mouse and human δ-cells, where it limits Ca^{2+}_c influx under both low as well as high glucose conditions. Ca^{2+}_c influx and ER Ca^{2+} stores are enhanced in δ-cells lacking TALK-1 channels, leading to increased somatostatin secretion and reduced glucagon secretion. These data highlight the physiological importance of TALK-1 modulation of δ-cell Ca^{2+}_c

homeostasis in regulating the tone of islet somatostatin signaling and controlling islet glucagon secretion.

Results

TALK-1 channels are expressed in δ-cells

We first sought to determine whether functional TALK-1 channels are expressed in δ-cells. Mouse and human pancreas sections stained for somatostatin and TALK-1 demonstrated expression of TALK-1 in δ-cells (Figure 4.1A,B). To test whether TALK-1 forms K^+ channels in mouse δ-cells, we generated mice lacking TALK-1 (TALK-1 KO) (*202*) with RFP expressed specifically in δ-cells [Sst-IRES-Cre (*246*) crossed with a tdRFP fluorescent reporter preceded by a loxP-flanked STOP cassette (*247*)]. We used dispersed islet cell preparations from these mice to record RFP-positive whole-δ-cell K2P currents, which we found were significantly reduced in δ-cells from TALK-1 KO mice when compared to controls (wild-type, WT, Figure 4.1C). To assess whether TALK-1 also forms a functional channel in human δ-cells, we expressed a TALK-1 dominant-negative (DN) mutant to inhibit endogenous TALK-1 channel activity (*202*). The TALK-1 DN relies on a mutation (G110E) in the K^+ selectivity filter which abolishes K^+ conductance upon interaction with wild-type TALK-1; the bicistronic TALK-1 DN construct also possesses an mCherry fluorescent reporter separated from TALK-1 DN by a P2A sequence, facilitating identification of transfected cells (*202*). Expression of the TALK-1 DN in single human δ-cells (confirmed by post-staining for somatostatin) resulted in inhibition of whole-cell K2P currents (Figure 4.1D). These data confirmed that TALK-1 is functionally expressed in δ-cells.

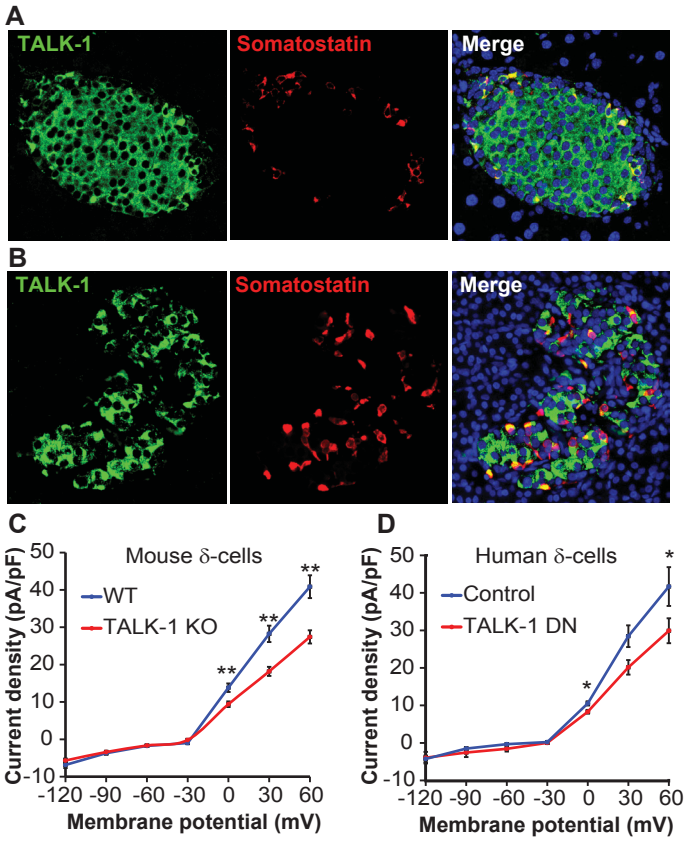

Figure 4.1. TALK-1 channels are expressed in mouse and human δ-cells. (A) Image of a mouse pancreas section stained for somatostatin (green) and TALK-1 channels (red) (representative of $N = 3$ mice). (B) Image of a human pancreas section stained for somatostatin (green) and TALK-1 channels (red) (representative of $N = 3$ pancreata). (C) K2P currents recorded from WT and TALK-1 KO δ-cells ($N = 3$ mice per genotype). (D) K2P currents recorded from human δ-cells expressing TALK-1 DN or control mCherry. ($N = 3$ islet preparations); $^{*}P < 0.05$, $^{**}P < 0.005$.

We next investigated whether the absence of TALK-1 channels altered δ-cell Ca^{2+}_c handling. Using dispersed islet-cell preparations, we recorded single δ-cell Ca^{2+} dynamics under stimulatory (11 mM) glucose conditions in WT and TALK-1 KO δ-cells (Figure 4.2A,B). Under these conditions, both WT and TALK-1 KO δ-cells showed spontaneous oscillations in Ca^{2+}_c. Area under the Ca^{2+} curve (AUC) analysis revealed that total Ca^{2+}_c influx was significantly greater in TALK-1 KO compared to WT δ-cells (Figure 4.2C), a difference which could be abolished by removal of extracellular Ca^{2+} (Figure 4.2C). Single δ-cell Ca^{2+} transient amplitude was significantly greater in TALK-1 KO δ-cells (Figure 4.2D), suggesting that CICR might be enhanced in the absence of TALK-1 channel activity. As δ-cell Ca^{2+} influx is critical for secretion, we also measured somatostatin release from WT and TALK-1 KO islets. Compared to WT islets, somatostatin secretion was increased by approximately 20% under basal (1 mM glucose) conditions, and enhanced by over 60% under stimulatory (11 mM glucose) conditions from islets lacking TALK-1 (Figure 4.2E).

Physiological δ-cell function depends upon the islet microenvironment which enables paracrine feedback mechanisms between β- and δ-cells (*94, 244*). Therefore, we also examined how TALK-1 channels impact δ-cell Ca^{2+} homeostasis in intact islets. This was accomplished by crossing our TALK-1 KO/Sst-IRES-Cre mice with those possessing the genetically encoded Ca^{2+} indicator GCaMP6s preceded by a loxP-flanked stop cassette (*248*), generating islets with GCaMP6s expressed specifically in δ-cells. As β-cell Ca^{2+}_c has been reported to oscillate in synchrony with δ-cells (*85*), we loaded GCaMP6s-expressing islets with the red synthetic Ca^{2+} indicator Cal590 to examine the relationship between β- and δ-cell Ca^{2+} influx. In low (1 mM) glucose, 66.4 ± 3.9% WT and 70.0 ± 6.4% TALK-1 KO δ-cells exhibited spontaneous Ca^{2+} oscillations (Figure 4.3 A,C,G), whereas β-cells remained quiescent. Under high (11 mM)

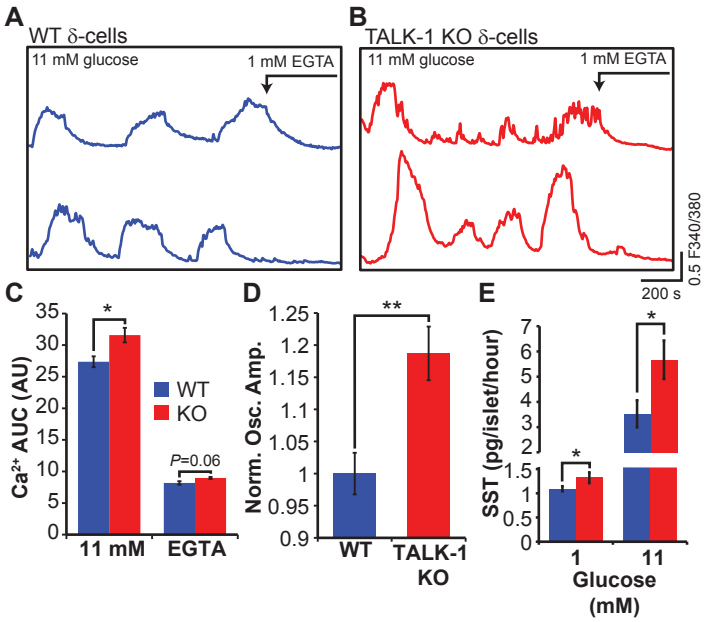

Figure 4.2. TALK-1 limits δ-cell Ca^{2+} influx and somatostatin secretion. (A) Ca^{2+} influx recorded in single Fura-2-loaded WT δ-cells perfused with the indicated treatments (Representative of $N = 3$ mice per genotype). (B) Ca^{2+} influx recorded in single Fura-2-loaded TALK-1 KO δ-cells perfused with the indicated treatments (Representative of $N = 3$ mice per genotype). (C) Total Ca^{2+} influx (area under the curve, AUC) in WT and TALK-1 KO δ-cells ($N = 3$ mice per genotype). (D) Maximum cytosolic Ca^{2+} oscillation amplitude (F/F_{min}) measured in WT and TALK-1 KO δ-cells ($N = 6$ mice per genotype). (E) Islets from WT or TALK-1 KO mice were incubated for 90 minutes at the indicated glucose concentrations. ($N = 4$-7 islet preparations per genotype); $^{*}P < 0.05$, $^{**}P < 0.005$.

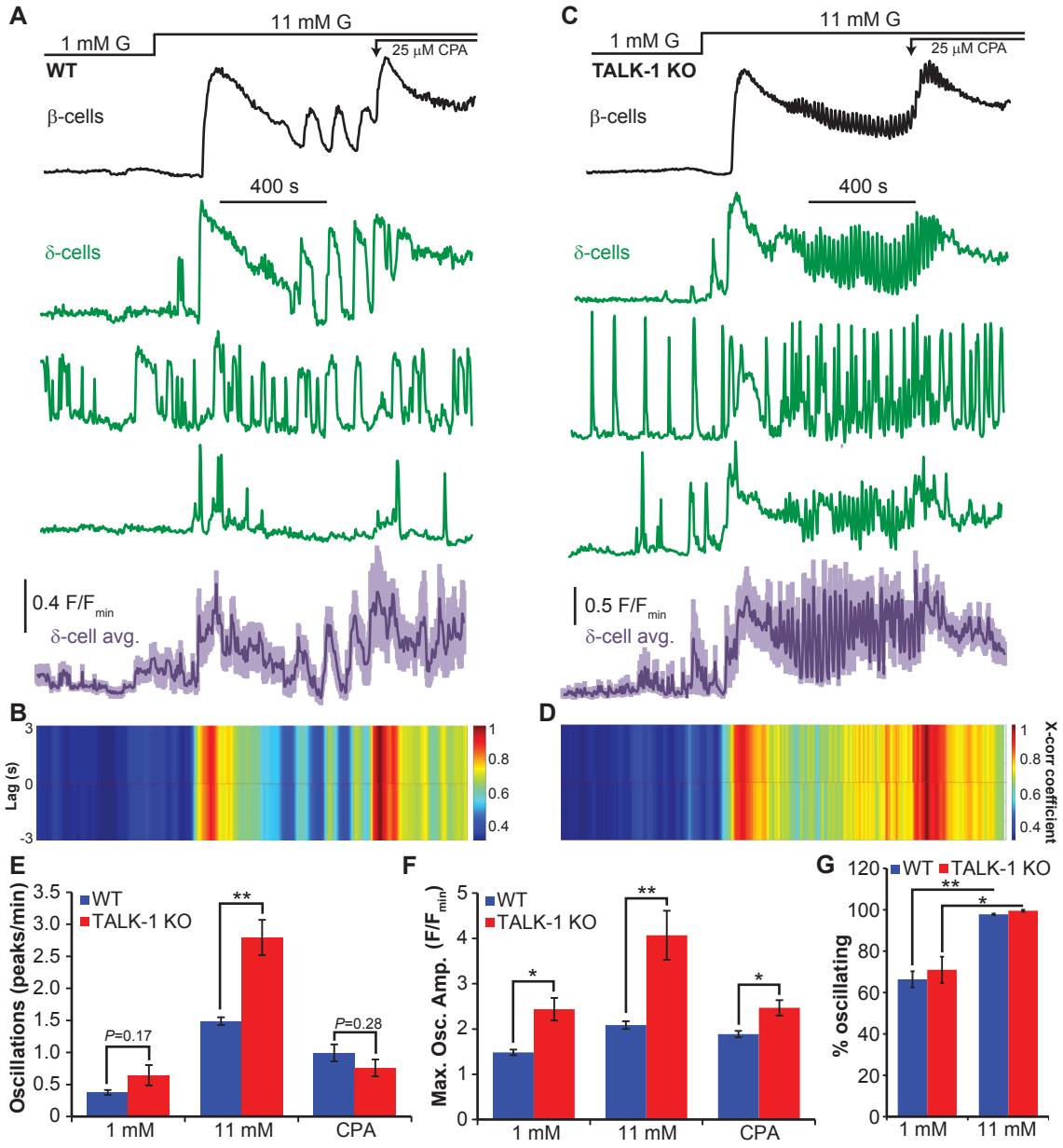

Figure 4.3. Glucose synchronizes WT and TALK-1 KO δ-cell Ca^{2+} with β-cells. (A) Recording of intracellular Ca^{2+} from a WT islet expressing GCaMP6 in δ-cells and loaded with the red Ca^{2+} dye Cal590. Correlation of average δ-cell signal and β-cells is presented in (B) (representative of recordings obtained from $N = 3$ mice). (C) Recording of intracellular Ca^{2+} from a TALK-1 KO islet expressing GCaMP6 in δ-cells and loaded with the red Ca^{2+} dye Cal590. Correlation of average δ-cell signal and β-cells is presented in (D) (representative of recordings obtained from $N = 3$ mice). (E). Average δ-cell Ca^{2+} oscillation frequency in WT and TALK-1 KO δ-cells measured under the indicated conditions ($N = 3$ mice per genotype). (F) Average maximum GCaMP6 fluorescence amplitude in WT and TALK-1 KO δ-cells measured under the indicated conditions ($N = 3$ mice per genotype). (F) Comparison of percent of δ-cells exhibiting Ca^{2+} oscillations under indicated glucose conditions ($N = 3$ mice per genotype); $*P < 0.05$; $**P < 0.005$.

glucose, nearly all δ-cells responded with increased Ca^{2+} influx that strongly correlated with β-cell Ca^{2+} oscillations (Figure 4.3B,D). In TALK-1 KO islets, islet Ca^{2+} oscillation frequency is significantly accelerated (*202*), and this phenotype was also observed in δ-cells in TALK-1 KO islets (Figure 4.3E). Like the single δ-cells from dispersed islet-cell preparations, intact islet TALK-1 KO δ-cells once again showed larger amplitude Ca^{2+} oscillations compared to WT under low and high glucose conditions (Figure 4.3F). In both WT and TALK-1 KO δ-cells, glucose increased the amplitude of Ca^{2+} oscillations, which is in agreement with the prediction that glucose metabolism enhances δ-cell CICR (*86*). The height of the Ca^{2+} oscillations in elevated glucose could be brought back to the amplitude observed in low glucose by depleting ER Ca^{2+} with the SERCA inhibitor CPA (Figure 4.3F). Interestingly, addition of CPA also disrupted the glucose-induced synchronization of β- and δ-cells, suggesting that ER Ca^{2+} handling participates in this relationship. Together, these observations indicate that δ-cell TALK-1 channels regulate δ-cell Ca^{2+} influx, and demonstrate that there is significant crosstalk between β-cells and δ-cells under glucose conditions which stimulate β-cell Ca^{2+} influx.

TALK-1 KO δ-cells are modestly depolarized

As TALK-1 produces detectable K^+ currents at the plasma membrane in δ-cells, we next investigated electrical activity in TALK-1 KO δ-cells. In both WT and TALK-1 KO δ-cells, we found that the V_m was largely insensitive to changes in extracellular glucose (Figure 4.4A-E), with continued action potential firing in low (1 mM) glucose. Similarly, we found no significant difference in the plateau fraction (the ratio of time spent in electrically excitable periods divided by the total time examined) comparing either the effects of glucose or genotype (Figure 4.4C). TALK-1 KO δ-cells were slightly depolarized in high glucose during electrically silent periods

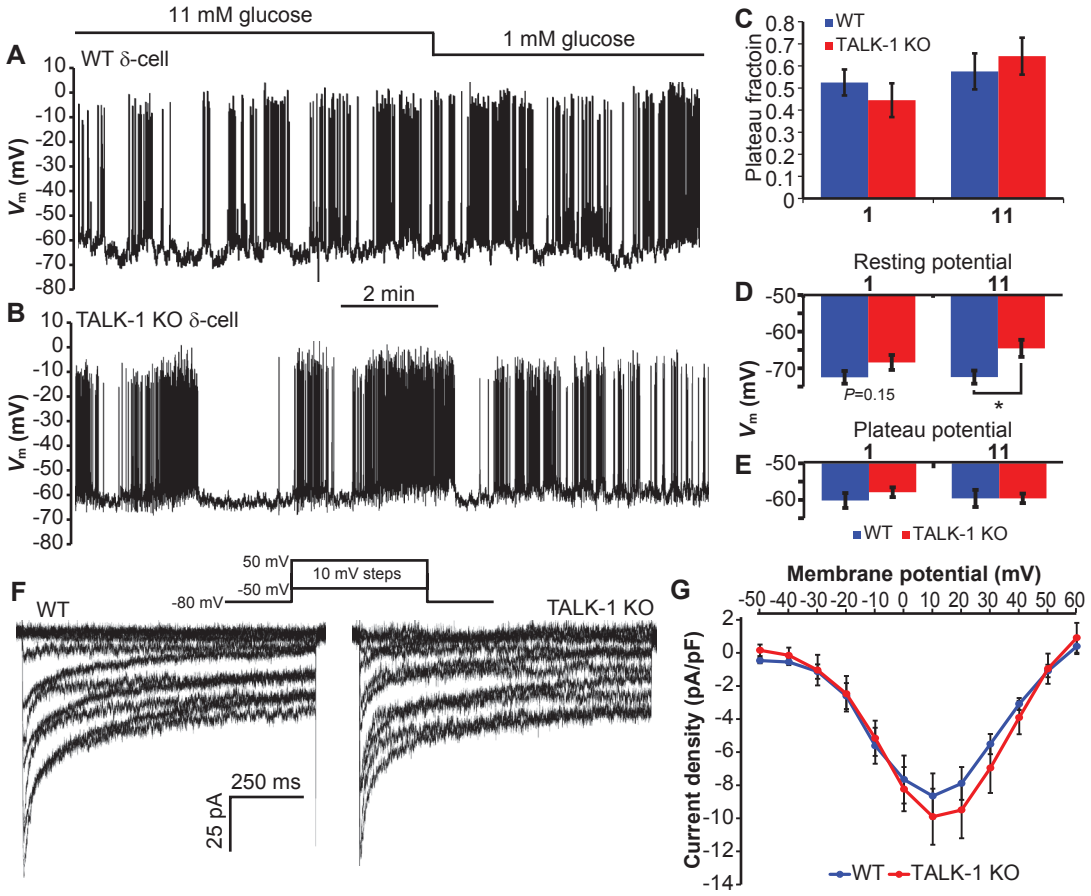

Figure 4.4. Electrical activity and VDCC currents in WT and TALK-1 KO δ-cells. (A) V_m recording from a WT δ-cell treated with indicated glucose concentrations (representative of recordings obtained from $N = 12$ cells/4 mice per genotype). (B) V_m recording from a TALK-1 KO δ-cell treated with indicated glucose concentrations (representative of recordings obtained from $N = 12$ cells/4 mice per genotype). (C) Quantification of plateau fraction in WT and TALK-1 KO δ-cells ($N = 12$ cells/4 mice per genotype). (D,E) Average V_m in WT and TALK-1 δ-cells at 1 and 11 mM glucose. ($N = 12$ cells/4 mice per genotype). (F) VDCC currents recorded from WT (representative of $N = 9$ cells/3 mice per genotype) and TALK-1 KO (representative of $N = 8$ cells/3 mice per genotype) δ-cells. VDCC current densities are quantified in (G); $^*P < 0.05$.

(Figure 4.4D), but we detected no difference in the plateau V_m from which action potentials fire (Figure 4.4E). There were no appreciable differences in the pattern or frequency of action potentials in TALK-1 KO δ-cells when compared to WT δ-cells; however, action potential upstroke and afterhyperpolarization (AHP) had larger amplitudes in KO δ-cells (Table 4.1). We also measured VDCC currents to assess whether changes in Ca^{2+} channel function could account for the greater Ca^{2+} influx in TALK-1 KO δ-cells. However, we found no difference in VDCC currents (Figure 4.4F,G), indicating that alterations in VDCCs per se are unlikely a major source of increased Ca^{2+} influx in TALK-1 KO δ-cells.

Parameter	**WT (*N* = 12)**	**TALK-1 KO (*N* = 12)**	***P* value**
Peak amplitude (mV)	40.8 ± 1.3	51.0 ± 2.7	0.002
AHP amplitude (mV)	-5.3 ± 0.7	-6.9 ± 0.4	0.05
Event frequency (Hz)	1.5 ± 0.2	1.7 ± 0.2	0.36

Table 4.1. Action potential characteristics in WT and TALK-1 KO δ-cells. Action potential parameters were determined over a period of 60 seconds in the second oscillation of electrical activity in δ-cells treated with 11 mM glucose using the "Threshold search" event detection function in Clampfit 10 (pCLAMP 10; Molecular Devices).

CICR is enhanced in TALK-1 KO δ-cells

One of the mechanisms proposed to underlie the glucose-induced increase in somatostatin secretion is enhanced CICR (*86*). As TALK-1 channels modulate ER Ca^{2+} content, we examined whether enhanced Ca^{2+} influx in TALK-1 KO δ-cells was a consequence of increased CICR. First, we determined whether ER Ca^{2+} stores are increased in δ-cells lacking

TALK-1 channels by measuring CPA-induced ER Ca^{2+} release. We found a significant 25.7 ± 8% increase in TALK-1 KO δ-cell ER Ca^{2+} stores (Figure 4.5A,B). To examine δ-cell Ca^{2+} handling independent of glucose-induced changes in the V_m, we treated single WT and TALK-1 KO δ-cells with a solution containing 11 mM glucose to energize SERCAs and the K_{ATP} channel activator diazoxide to suppress electrical excitability. Under these conditions spontaneous Ca^{2+}_c oscillations were mostly abolished, but a 40-second depolarization with high (45 mM) K^+ elicited a rapid increase in cytosolic Ca^{2+} (Ca^{2+}_c) which slowly returned to basal levels upon removal of the depolarizing K^+ stimulus (Figure 4.6A,B). To uncover the contribution of the ER to Ca^{2+}_c influx under these conditions, we repeated this experiment in δ-cells pre-treated with the SERCA inhibitor thapsigargin (Figure 4.6A,B). Subtraction of the Ca^{2+} signal obtained from thapsigargin-treated cells from the Ca^{2+} signal of vehicle-treated cells revealed that depolarization induces a transient uptake of Ca^{2+} by the ER followed by ER Ca^{2+} release (Figure 4.6C), similar to observations in β-cells (*214*). In δ-cells, ER Ca^{2+} release preceded the end of the high K^+ pulse and was substantially greater in TALK-1 KO versus WT δ-cells (Figure 4.6C). To determine whether increased ER Ca^{2+} release in TALK-1 KO δ-cells is a consequence of enhanced CICR, we next used fast imaging to measure Ca^{2+}_c changes in patch-clamped δ-cells. Short (25-250 ms) step depolarizations (-80 mV to 0 mV) induced prompt increases in Ca^{2+}_c which returned to basal levels upon stepping back to the pre-pulse potential (Figure 4.6D). The depolarization-induced increases in Ca^{2+}_c were significantly greater in TALK-1 KO δ-cells, a difference which could be eliminated by depleting ER Ca^{2+} with CPA (Figure 4.6E). As these data indicated enhanced CICR contributes to augmented Ca^{2+} influx in TALK-1 KO δ-cells, we assessed whether depleting ER Ca^{2+} with CPA would make glucose-stimulated Ca^{2+} influx in KO δ-cells comparable with WT (Figure 4.6F). Indeed, whereas Ca^{2+}_c levels were significantly

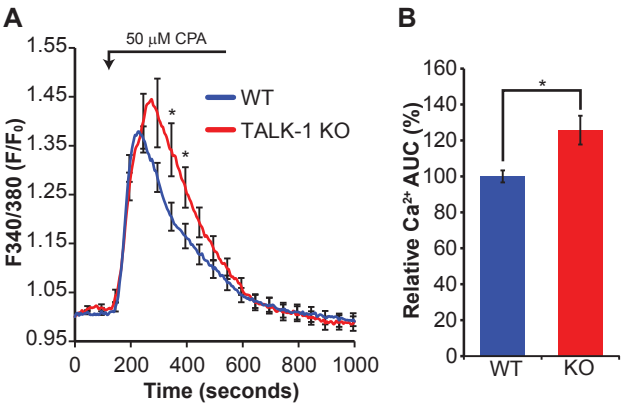

Figure 4.5. ER Ca^{2+} stores are greater in TALK-1 KO δ-cells. (A) Average CPA-induced ER Ca^{2+} release in WT and TALK-1 KO δ-cells (representative of $N = 3$ mice per genotype). Ca^{2+} release is quantified in (B) ($N = 3$ mice per genotype); $*P < 0.05$.

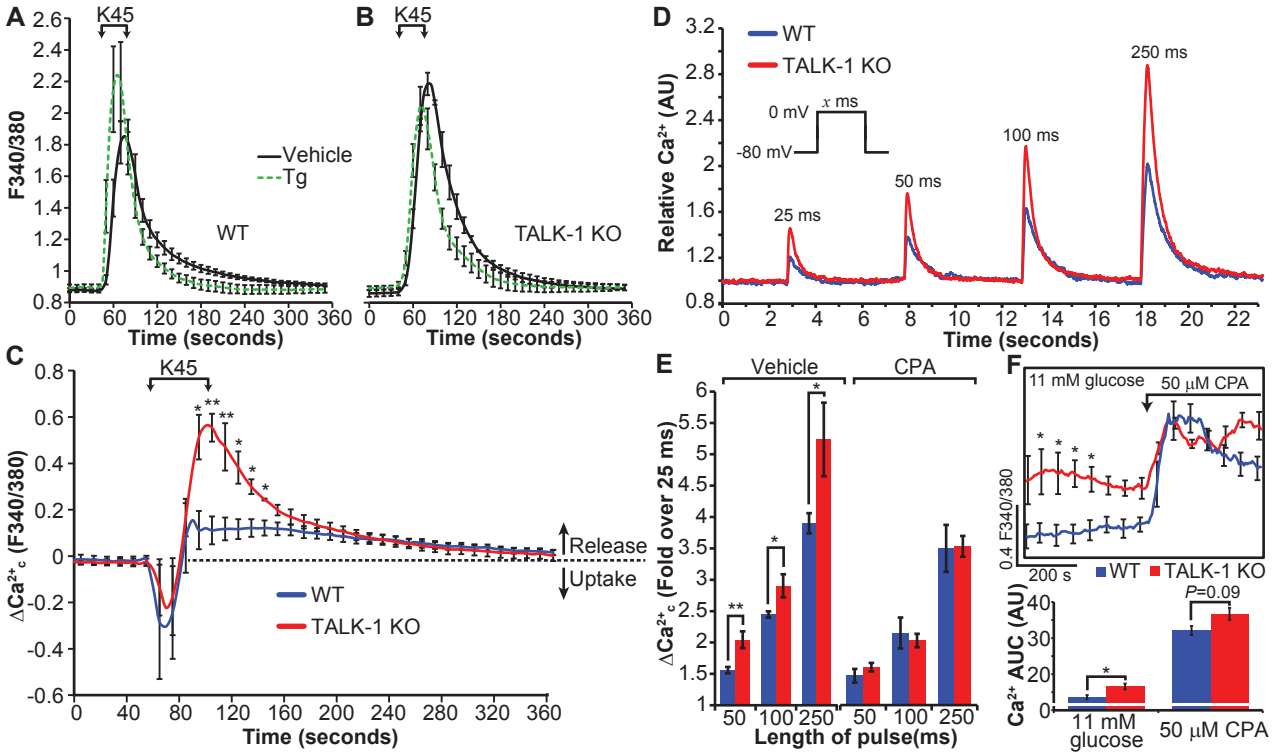

Figure 4.6. Ca^{2+}-induced Ca^{2+} release is increased in TALK-1 KO δ-cells. (A, B) Average cytosolic Ca^{2+} influx in WT and TALK-1 KO δ-cells, treated with vehicle or with 5 μM thapsigargin (Tg), in response to depolarization with 45 mM K^+. Subtraction of the signal obtained from Tg treated cells from vehicle treated cells reveals the contribution of the ER to the cytosolic Ca^{2+} signal (C) ($N = 3$ mice per genotype). (D) Representative cytosolic Ca^{2+} influx in WT and TALK-1 KO δ-cells subjected to short depolarizing pulses. The fold increase in δ-cell Ca^{2+} in response to increasingly long depolarizations in the presence or absence of CPA (25 μM) is quantified in (E) ($N = 9$ cells (WT); 7 cells (TALK-1 KO); 3 mice per genotype). (F) Cytosolic Ca^{2+} in WT and TALK-1 KO δ-cells was assessed before and after treatment with CPA. ($N = 3$ mice per genotype); $^*P < 0.05$, $^{**}P < 0.005$.

higher in TALK-1 KO δ-cells in 11 mM glucose (Figure 4.6F [see also Figures 4.2B & 4.3F]), CPA treatment resulted in comparable Ca^{2+}_c levels in WT and TALK-1 KO δ-cells. Interestingly, although ER Ca^{2+} depletion with SERCA inhibitors suppresses glucose-stimulated somatostatin release (*77, 86*) and Ca^{2+}_c oscillation amplitude (Fig 4.3F), CPA treatment paradoxically elevates bulk δ-cell Ca^{2+}_c levels (Figure 4.6F). The CPA-induced elevation in average δ-cell Ca^{2+}_c is probably due to V_m depolarization caused by activation of store-operated currents (SOCs). Indeed, in the presence of V_m-hyperpolarizing diazoxide, basal Ca^{2+}_c in thapsigargin-treated δ-cells was not elevated (Figure 4.6A,B). These observations suggest that SOCs regulate δ-cell Ca^{2+} influx by modulating the V_m and VDCCs and that somatostatin secretion is very sensitive to ER Ca^{2+} release.

Glucagon secretion is reduced from TALK-1 KO islets

The acute sensitivity of α-cells to somatostatin under low glucose conditions is highlighted by the several-fold increase in glucagon secretion when somatostatin signaling is blocked (*82, 242*). Thus somatostatin exerts an inhibitory tone on α-cells in low glucose, and increased basal somatostatin secretion leads to reduced glucagon secretion (*242*). In TALK-1 KO islets, we find that glucagon release is significantly impaired under low glucose conditions (Figure 4.7A-C). Importantly, TALK-1 protein is not expressed in mouse or human α-cells (*202*), suggesting that the reduced glucagon secretion from TALK-1 KO islets is not due to an innate role of TALK-1 in α-cells. To further verify the absence of TALK-1 channels in α-cells, we recorded α-cell K2P currents, but we did not detect a difference between WT and TALK-1 KO α-cells (Figure 4.7D). Immunofluorescent analysis of human pancreas sections using two different TALK-1 antibodies also failed to demonstrate TALK-1 in α-cells (Figure 4.7E), and expression of the TALK-1 DN mutant in human α-cells (confirmed by post-staining) had no

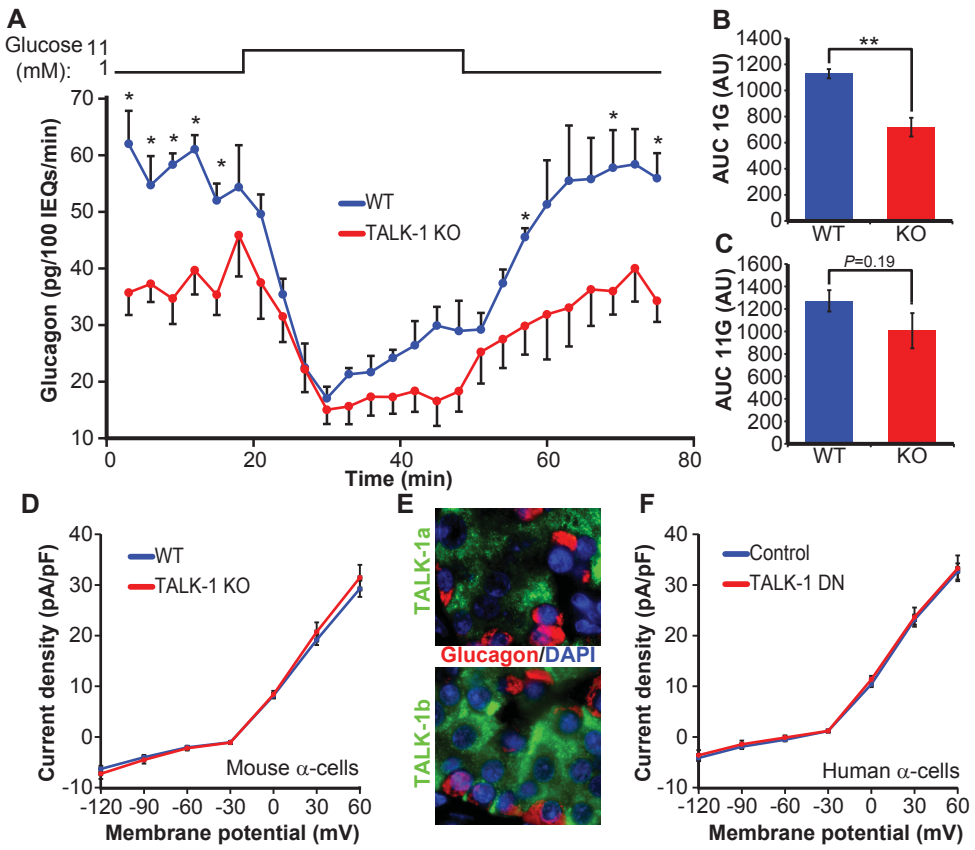

Figure 4.7. Reduced glucagon secretion from TALK-1 KO islets. (A) Isolated islets from WT and TALK-1 KO mice were perifused with the indicated glucose concentrations ($N = 4$ mice per genotype). (B) Glucagon AUC for the period corresponding to glucagon secretion in 1 mM glucose (0-18 min). (C) Glucagon AUC for the period corresponding to glucagon secretion in 11 mM glucose (18-45 min). (D) K2P current density in WT and TALK-1 KO α-cells ($N = 3$ mice per genotype). (E) Human pancreas sections stained for TALK-1 using two different antibodies and glucagon. (F) K2P current density in human α-cells expressing either TALK-1 DN mutant or mCherry control. Cells were post-stained for glucagon; only glucagon-positive cells were analyzed ($N = 10$ α-cells per condition/five donors); $*P < 0.05$; $**P < 0.005$.

effect on K2P currents (Figure 4.7F). Insulin is also a paracrine inhibitor of glucagon secretion (*83*), but in TALK-1 KO islets, insulin secretion is not different from WT in 1 mM glucose (*202*). Together, these observations suggest that the reduced glucagon secretion observed in TALK-1 KO islets is a consequence of increased somatostatin secretion.

Somatostatin receptor signaling inhibits α-cell function through multiple mechanisms, including reduction of cellular cAMP levels (*83*), suppression of glucagon granule exocytosis (*249*), and activation of V_m hyperpolarizing K^+ currents (*74, 81, 250*). As V_m hyperpolarization limits α-cell Ca^{2+}_c influx and glucagon secretion (*251*), we hypothesized that increased basal somatostatin release in TALK-1 KO islets would impact α-cell Ca^{2+}_c dynamics. We tested this possibility by measuring α-cell Ca^{2+}_c oscillations in WT and TALK-1 KO islets, using mice which express the genetically encoded Ca^{2+} indicator GCaMP3 specifically in α-cells (*133*). In agreement with findings that somatostatin suppresses α-cell electrical activity and Ca^{2+}_c influx (*42, 74*), we observed a significant reduction in the number of α-cells exhibiting spontaneous Ca^{2+}_c oscillations in low (1 mM) glucose conditions (Figure 4.8 A,B,E). However, disrupting intraislet somatostatin paracrine signaling by dispersing islets into single cells normalized the oscillation frequency of WT and TALK-1 KO α-cells (Figure 4.8 C,D,E). Similarly, we find a tendency towards reduced Ca^{2+} influx in intact islet TALK-1 KO α-cells, a difference which is not found in single TALK-1 KO α-cells (Figure 4.8F). Single α-cells are still capable of responding to somatostatin, as addition of 10 nM somatostatin caused a transient suppression of Ca^{2+} influx (Figure 4.8 C,D), in accordance with its effects on α-cell electrical activity (*74*). To ascertain the relationship between somatostatin signaling and TALK-1 KO α-cell function, we measured glucagon secretion from WT and TALK-1 KO islets in the presence of the SSTR2 antagonist CYN-154806. Blockade of SSTR2, which is the dominant α-cell SSTR (*42, 252*),

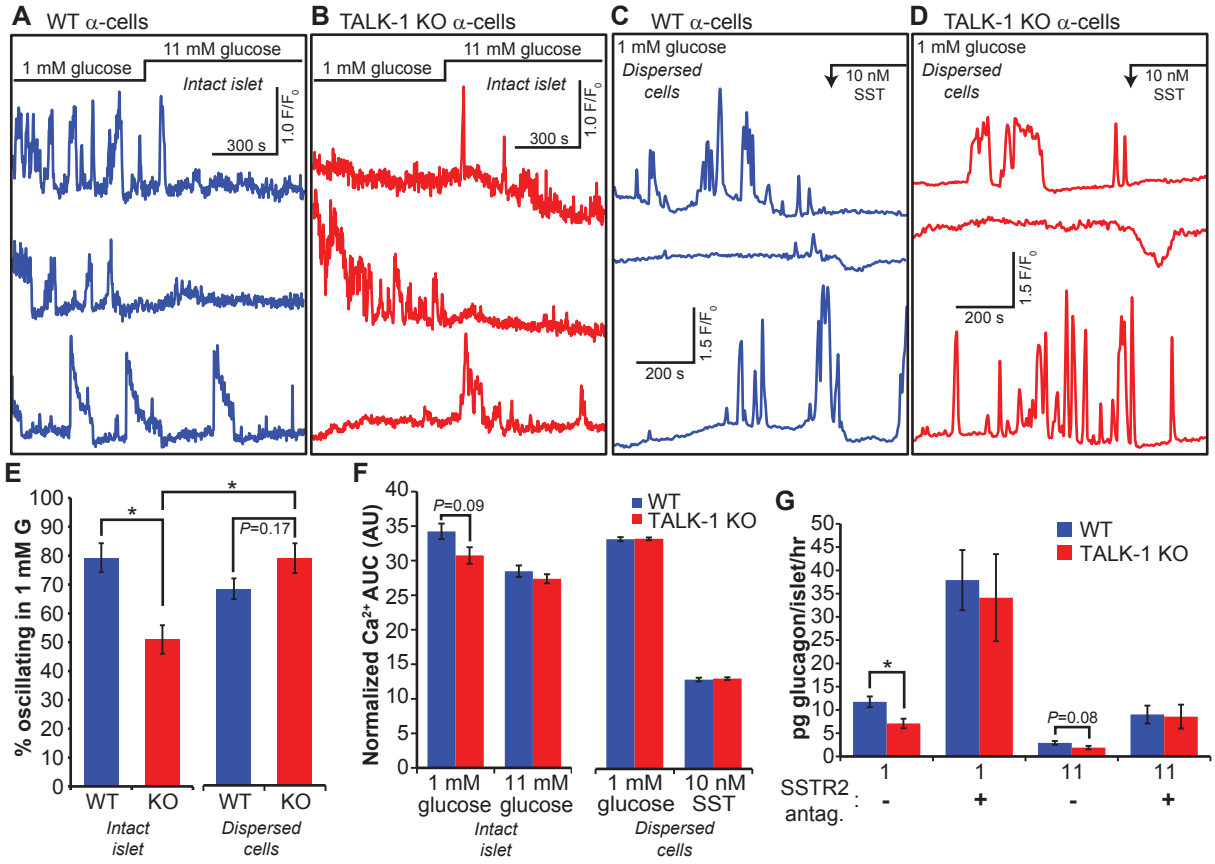

Figure 4.8. TALK-1 KO α-cells exhibit altered Ca^{2+} dynamics only in intact islets. (A) Recordings of intracellular Ca^{2+} responses in WT α-cells, in islets expressing the genetically encoded Ca^{2+} indicator GCaMP3 specifically in α-cells (representative of islet α-cells from $N = 3$ mice). (B) Recordings of intracellular Ca^{2+} responses in TALK-1 KO α-cells, in islets expressing the genetically encoded Ca^{2+} indicator GCaMP3 specifically in α-cells (representative of islet α-cells from $N = 3$ mice). (C) Recordings of intracellular Ca^{2+} responses in single WT α-cells expressing the genetically encoded Ca^{2+} indicator GCaMP3 (representative of α-cells from $N = 3$ mice). (D) Recordings of intracellular Ca^{2+} responses in single TALK-1 KO α-cells expressing the genetically encoded Ca^{2+} indicator GCaMP3 (representative of α-cells from $N = 3$ mice). (E,F) Comparison of percent oscillating α-cells and Ca^{2+} AUC determined from WT and TALK-1 KO α-cells under the indicated conditions ($N = 3$ mice per genotype). (G) Islets were incubated for one hour with the indicated treatments (SSTR2 antagonist: 500 nM CYN154806); $N = 10$ mice per genotype (glucose only); 3 mice per genotype (+ CYN154806); $^*P < 0.05$.

potently increased glucagon secretion under both low and high glucose conditions and abrogated the reduced glucagon secretion of TALK-1 KO islets (Figure 4.8G). Together, these findings indicate that TALK-1 modulation of δ-cell somatostatin secretion impacts α-cell Ca^{2+} influx and glucagon secretion.

Discussion

Here we assessed the functional roles of δ-cell TALK-1 channels and determined how TALK-1 modulation of δ-cell somatostatin secretion impacts paracrine regulation of α-cells. The data indicate that TALK-1 channel activity controls δ-cell cytosolic Ca^{2+} levels by limiting CICR, thus reducing somatostatin secretion and increasing glucagon release. Our observations highlight the importance of CICR during glucose-stimulated somatostatin secretion and reveal TALK-1 as a key regulator of δ-cell ER Ca^{2+} release. Therefore, these findings uncover a glucose regulated feedback circuit involving TALK-1 countercurrent modulation of ER Ca^{2+} stores, setting the threshold for ER Ca^{2+} release.

Ca^{2+} influx through VDCCs is required for somatostatin secretion, as removal of extracellular Ca^{2+}, activation of K_{ATP} with diazoxide, and blockade of VDCCs all inhibit somatostatin secretion (*10, 86, 244, 253*). However, δ-cell ER Ca^{2+} release is essential for glucose-mediated increases in somatostatin secretion, as highlighted by the fact that depletion of ER Ca^{2+} with SERCA inhibitors reduces somatostatin secretion (*77, 86, 253*). Our results also indicate that CICR contributes substantially to the δ-cell Ca^{2+}_c signal. As we and others observe δ-cell Ca^{2+} influx under low glucose conditions (*85, 88*), CICR may provide a glucose sensitive mechanism to amplify δ-cell Ca^{2+}_c levels and somatostatin secretion (*86*). Our finding that average δ-cell Ca^{2+}_c levels were increased by SERCA blockade was thus unexpected, as an

increase in bulk Ca^{2+}_c would be predicted to increase somatostatin secretion, whereas SERCA inhibition reduces somatostatin secretion. However, SERCA blockade also caused a significant reduction in the Ca^{2+}_c oscillation amplitude (presumably due to loss of ER Ca^{2+} release), suggesting that ER Ca^{2+} release is largely responsible for the glucose-dependent increase in δ-cell Ca^{2+}_c oscillations, and that Ca^{2+}_c oscillations are important somatostatin secretion. Increased δ-cell bulk Ca^{2+}_c levels in the presence of CPA could be due to activation of depolarizing SOCs and Ca^{2+} entry, as well as cytosolic Ca^{2+} accumulation caused by reduced ER Ca^{2+} uptake. These data indicate a critical role for CICR on δ-cell Ca^{2+}_c oscillations which are predicted to play an important role in somatostatin exocytosis. Future studies will determine the relationship between δ-cell ER Ca^{2+} levels, Ca^{2+}_c, and somatostatin secretion.

Glucose elicits a strong amplifying effect on δ-cell Ca^{2+} influx and somatostatin secretion which does not appear to rely on dramatic changes in δ-cell electrical excitability. We find that TALK-1 channels participate in the regulation of the δ-cell Ca^{2+} amplifying mechanism, CICR. While δ-cell VDCC opening is required for triggering of CICR, glucose metabolism likely enhances CICR by energizing SERCAs and filling δ-cell ER Ca^{2+} stores. TALK-1 modulates δ-cell CICR and somatostatin secretion by controlling the size of the releasable ER Ca^{2+} stores, which is strongly correlated with CICR (*229, 230, 245*). ER-localized TALK-1 channels mediate a K^+ countercurrent which enhances ER Ca^{2+} leak (as discussed in Chapter III), and the absence of the TALK-1 countercurrent results in less ER Ca^{2+} leak and greater ER Ca^{2+} stores. Elevated ER Ca^{2+} levels sensitize the δ-cell CICR mechanism, as reflected by the larger amplitude Ca^{2+}_c oscillations in TALK-1 KO δ-cells which are abolished by ER Ca^{2+} depletion. This is mechanistically similar to ER countercurrent regulation of ER Ca^{2+} stores in smooth muscle cells, where loss of ER K^+ countercurrents mediated by TRIC-A channels results in augmented

ER Ca^{2+} stores and enhanced ER Ca^{2+} release (*193, 254*). Our finding that TALK-1 channels modulate δ-cell ER Ca^{2+} stores represents the first description of K2P channel regulation of CICR, and underscores the importance of ER Ca^{2+} handling in controlling δ-cell function.

TALK-1 channels also participate in the regulation of β-cell ER Ca^{2+} handling, which exhibits fundamental differences from δ-cell ER Ca^{2+} handling. For example, although CICR occurs in β-cells (*204*), it is not essential for GSIS. In β-cells, TALK-1 regulation of ER Ca^{2+} handling appears to have a much more significant impact on electrical activity, as β-cell ER Ca^{2+} release activates V_m-hyperpolarizing K^+ currents (see Chapter III). While the role of δ-cell TALK-1 channels in controlling CICR-dependent modulation of the V_m is unknown, we did not detect large defects in TALK-1 KO δ-cell electrical activity. However, it is important to note that our V_m recordings of TALK-1 KO δ-cells were performed in clusters of islet cells, whereas our β-cell V_m recordings (see Chapter II, (*202*)) were performed in intact islets. Under these conditions, important paracrine interactions between β-, δ-, and α-cells which affect δ-cell ER Ca^{2+} handling may be perturbed. This concept is in agreement with our observation that TALK-1 KO δ-cells exhibit significantly faster Ca^{2+}_c oscillations only under high glucose conditions when β-cells are active. Although the consequences of TALK-1 modulation of ER Ca^{2+} homeostasis differs between β- and δ-cells, it is increasingly clear that intraislet signaling between β- and δ-cells serves an important function in synchronizing hormone secretion. For example, the peptide hormone urocortin3 (Ucn3) is co-released with insulin to stimulate δ-cell function, suggesting a possible mechanism whereby β-cell secretion results in activation of δ-cell Ucn3 receptors (type 2 corticotropin releasing hormone receptor, Crhr2) (*244*). The effects of Ucn3 on δ-cell Ca^{2+}_c influx have not been determined, but activation of Crhr2 stimulates IP3R-dependent ER Ca^{2+} release in heterologous expression systems as well as neurons (*255, 256*). This suggests the

possibility that β- to δ-cell signaling incorporates δ-cell ER Ca^{2+} release, which is controlled by TALK-1 channel activity. Future studies are needed to better understand how TALK-1 control of ER Ca^{2+} is influenced by intraislet signaling.

This study highlights the substantial cross-talk between β- and δ-cells in elevated glucose conditions. We detected an increased frequency of δ-cell Ca^{2+}_c oscillations in TALK-1 KO islets, identical to the phenotype of TALK-1 KO β-cells. Thus, the accelerated frequency of TALK-1 KO δ-cell Ca^{2+}_c oscillations is likely due to increased β-cell electrical and Ca^{2+}_c oscillations (*202*), as there was no difference between WT and TALK-1 KO δ-cell Ca^{2+}_c oscillation frequency in low glucose. The functional coupling of β- and δ-cells is demonstrated by observations of simultaneous oscillations of insulin and somatostatin release from perfused pancreas (*257*) as well as synchronized β- and δ-cell Ca^{2+}_c oscillations within islets (*85*). However, the underlying molecular mechanisms have not been completely determined. Islet cell ER Ca^{2+} participates in this coupling, as we found that depletion of ER Ca^{2+} via SERCA inhibition disrupted the coordination of β- and δ-cell Ca^{2+}_c oscillations. This observation also suggests that ER Ca^{2+} release controls β- to δ-cell synchrony, and TALK-1 channels may modulate the efficacy of coupling by regulating ER Ca^{2+} release kinetics. While paracrine signaling plays a role in β- to δ-cell coupling, gap junctions have also been observed between β- and δ-cells (*258, 259*), suggesting that they are electrically coupled. Electrical coupling between β- and δ-cells would enable coordinated electrical activity and Ca^{2+}_c influx. However, β- to δ-cell electrical coupling would likely be present only under elevated glucose conditions, as the majority of δ-cells exhibit spontaneous Ca^{2+}_c oscillations under low glucose conditions when β-cells are quiescent. Although ER Ca^{2+} release in β- and δ-cells is highly glucose dependent and

influenced by TALK-1, a mechanistic link between glucose-stimulated CICR and β- to δ-cell electrical coupling remains to be explored.

Importantly, as we find that TALK-1 control of β- and δ-cell activity stimulates insulin and somatostatin secretion while inhibiting glucagon secretion, inhibition of TALK-1 activity could be beneficial in patients with T2DM. Indeed, TALK-1 KO mice fed a high-fat diet exhibit reduced fasting glycemia (*202*). The findings described here suggest that lower fasting glycemia in TALK-1 KO mice may arise due to elevated somatostatin secretion and reduced glucagon secretion, in addition to increased insulin secretion. These observations also indicate that defects that lead to increases in TALK-1 channel activity may contribute to fasting hyperglycemia under metabolically stressful conditions. In agreement with this hypothesis, a gain-of-function polymorphism in TALK-1 (rs1535500, encoding TALK-1 A277E) is associated with an increased risk for T2DM (*27-29*). One predicted consequence of this polymorphism would be a potentiation of the ER K^+ countercurrent and an increase in ER Ca^{2+} leak, reducing ER Ca^{2+} levels. In δ-cells, increased TALK-1 channel activity would diminish CICR and reduce somatostatin secretion. In turn, decreased somatostatin secretion would be expected to increase glucagon secretion and contribute to hyperglycemia. In addition, rs1535500-induced defects in β-cell function may also impair intraislet β-cell to δ-cell crosstalk. Indeed, rs1535500 is associated with decreased GSIS in patients with T2DM, presumably due to TALK-1 mediated β-cell V_m hyperpolarization (*30, 260*). Thus, reduced β-cell function due to rs1535500 may also impair paracrine stimulation of δ-cells, further contributing to hyperglycemia by allowing inappropriately elevated glucagon secretion and disrupting the insulin-to-glucagon ratio proposed to modulate hepatic glucose output (*261*). Further studies are needed to understand

TALK-1 regulation of intraislet feedback mechanisms and how they contribute to glucose control in health and disease.

In conclusion, this study reveals that TALK-1 channels serve a key role in shaping δ-cell Ca^{2+}_c and controlling somatostatin secretion by modulating δ-cell ER Ca^{2+} release. We find that TALK-1 channel activity regulates δ-cell CICR, limiting Ca^{2+} influx and somatostatin secretion. Our data also suggest that defects which lead to increases in TALK-1 channel activity (such as those induced by rs1535500) may participate in the pathogenesis of T2DM by negatively impacting δ-cell function, contributing to elevated glucagon release. These observations improve our understanding of the molecular mechanisms controlling δ-cell stimulus-secretion coupling and highlight the potential clinical utility of TALK-1 channels as a therapeutic target to reduce elevated glucagon secretion in patients with T2DM.

Research Design and Methods

Chemicals

All chemicals were purchased from Sigma-Aldrich (St. Louis, MO) unless specified otherwise.

Biological materials and study approval

The mice used in this study were 10-12 week-old males on a C57Bl6/J background. Mice were housed in a 12-hour light/dark cycle with access to standard chow (Lab Diets, 5L0D) *ad libitum*. Mouse islets were isolated by digesting the pancreas with collagenase P (Roche) and performing density gradient centrifugation as previously described (*176*). We obtained human islets from adult non-diabetic donors from multiple isolation centers organized by the Integrated Islet Distribution Program. Islets were cultured in RPMI 1640 (Gibco) containing 15% fetal

bovine serum (FBS), 100 IU·ml^{-1} penicillin, and 100 mg·ml^{-1} streptomycin, in an incubator maintained at 37 °C, 5% CO_2. Islets and cells were seeded to poly-D-lysine-coated 35 mm glass-bottom dishes (CellVis). In experiments using single islet cells, islets were triturated in 0.0075% trypsin-EDTA prior to plating. Dispersed cells were cultured for approximately 6 hours in 100 µL of medium prior to being refed with 2 mL of fresh medium. In human δ-cell experiments, cells were transfected with TALK-1 DN- or mCherry-expressing plasmids and identified by post-staining for somatostatin as previously described, (*202*). Cells were cultured for 24-48 hours prior to experimentation. All mouse procedures performed in this study were done in compliance with protocols reviewed and approved by the Vanderbilt University Institutional Animal Care and Use Committee, according to guidelines set forth by the NIH.

Immunofluorescence

Paraffin-embedded mouse and human pancreas sections were processed and stained as previously described (human donor information is provided in Table 4.2) (*202*). Sections were stained using primary antibodies against somatostatin (Santa Cruz Biotechnology sc-7819: 1:250), TALK-1 (Novus Biologicals #NBP1-83071; 1:175) or TALK-1a (Antibody Verify AAS72353C; 1:250) and glucagon (Proteintech #15954-I-AP: 1:500); secondary antibodies used were Alexa Fluor 488-conjugated donkey anti-rabbit (Jackson Immunoresearch #711-546-152; 1:300) and DyLight 650-conjugated donkey anti-goat (Thermo Fisher #SA5-10089; 1:250).

Donor	**1**	**2**	**3**
Sex	F	M	M
Age (years)	79	31	58
Ethnicity	W	B	W
Type 2 Diabetes	No	No	No

Table 4.2. Human pancreas donor characteristics

Calcium imaging

Single RFP δ-cells were loaded with 1.75 μM Fura-2 AM (Molecular Probes) in culture medium for 25 minutes in a 37 °C incubator, 5% CO_2; intact islets with GCaMP6-expressing δ-cells were loaded with Cal590-AM (AAT Bioquest) for 60 minutes in a 37 °C incubator, 5% CO_2. Before each experiment, cells were incubated for 20 minutes in RPMI 1640 supplemented with 1 or 11 mM glucose in a 37 °C incubator, 5% CO_2. Immediately prior to imaging, cells were washed in Krebs-Ringer imaging buffer (KRB) containing (in mM): 119 NaCl, 2.5 $CaCl_2$, 4.7 KCl, 25 HEPES, 1.2 $MgSO_4$, 1.2 KH_2PO_4, pH 7.35 with NaOH, and glucose was added to the desired concentration. During the experiment cells were continuously perfused with KRB solutions at 35-36 °C. Images were obtained every 5 seconds using a Nikon Eclipse TE2000-U microscope equipped with an epifluorescence illuminator (Sutter), CCD camera (HQ2; Photometrics, Inc.), and Nikon Elements software (*52*). Imaging of GCaMP3-α-cells in intact islets was performed as previously described (*262*). Images of islets with GCaMP6-δ-cells loaded with Cal590-AM were acquired every 3 seconds using a Nikon Ti-E microscope equipped with a Plan Apo Lambda 20×/0.75 NA lens, Yokogawa CSU-X1 spinning disk head, and Andor DU-897 electron-multiplying CCD. GCaMP6 was excited at 488 nm and Cal590 was excited at 561 nm, with emissions collected using 525 nm and 605 nm bandpass filters.

For analysis of δ-cell ER Ca^{2+} uptake and release, Fura-2 loaded cells were incubated for 10 minutes in KRB supplemented with 11 mM glucose, 125 μM diazoxide (Enzo) and 1.25 μM thapsigargin (Alomone Labs) or DMSO vehicle control. During each experiment, cells were perfused with this buffer and stimulated with high-[K^+] KRB containing (in mM): 74 NaCl, 43.8 KCl, 2.5 $CaCl_2$, 25 HEPES, 1.2 $MgSO_4$, 1.2 KH_2PO_4, and 11 glucose (pH 7.35 with NaOH). For

analysis of ER Ca^{2+} stores, Fura-2-loaded cells were stimulated with 50 μM cyclopiazonic acid (CPA; Alomone Labs) in KRB supplemented with 125 μM diazoxide.

For high-speed imaging of δ-cell Ca^{2+} influx, cells were loaded with 5 μM Cal520-AM (AAT Bioquest) for 25 minutes, followed by washing with KRB (11 mM glucose). Single RFP δ-cells were then patched according to the perforated patch clamp protocol described below on a Nikon Eclipse TE2000-U microscope equipped with an X-Cite 120Q widefield fluorescence light source (Excelitas Technologies) and a D-104 microscope photometer (Photon Technologies Inc.). Upon obtaining a low-leak, GΩ seal, the fluorescence light source was activated, and δ-cell Cal520 fluorescence was measured during 80 mV step depolarizations. The photometer signal was digitized and sampled at 10 kHz. Data were analyzed using Clampfit 10, Nikon Elements, ImageJ, MATLAB, and Microsoft Excel software.

Patch clamp electrophysiology

An Axopatch 200B amplifier (Molecular Devices) was used to measure whole-cell K^+ channel currents in the voltage-clamp mode; currents were digitized using a Digidata 1440, lowpass filtered at 1 kHz and sampled at 10 kHz. During recording, samples were perfused with KRB without $CaCl_2$ and supplemented with (in mM): 0.2 tolbutamide (MP Biomedicals), 10 tetraethylammonium chloride hydrate (TEA, Thermo Fisher Scientific), 1 EGTA, pH 7.35 with NaOH, and 11 mM glucose. Patch electrodes were pulled to a resistance of 3-4 MΩ when filled with an intracellular solution containing (in mM): 140 KCl, 1 $MgCl_2$, 10 EGTA, 10 HEPES, and 3 Mg-ATP, pH 7.22 with KOH. For V_m recordings, pipettes were filled with an intracellular solution containing (in mM) 28.4 K_2SO_4, 63.7 KCl, 11.8 NaCl, 1 $MgCl_2$, 20.8 HEPES, 0.5 EGTA (pH 7.22 with KOH) and ~0.05 $mg \cdot ml^{-1}$ amphotericin B. δ-cells were continuously perfused with KRB solutions at 35-36 °C. VDCC currents were recorded from dispersed mouse

δ-cells as previously described (*263*). Patch electrodes were pulled to a resistance of 3-4 MΩ when filled with an intracellular solution containing (in mM): 120 CsCl, 10 TEA, 1 $MgCl_2$, 3 EGTA, 10 HEPES, 3 MgATP, pH 7.22 with CsOH. Cells were patched in KRB solution supplemented with 11 mM glucose; upon obtaining the whole-cell configuration with a seal resistance > 1 GΩ, the bath solution was exchanged for a buffer containing (in mM): 82 N-methyl-D-glucamine, 20 TEA, 30 $CaCl_2$, 1 $MgCl_2$, 5 CsCl, 10 HEPES, 11 glucose, 0.2 tolbutamide, pH 7.35 with HCl, osmolarity adjusted with sucrose. δ-cells were perfused for three minutes with this solution prior to initiating the VDCC recording protocol. Voltage steps of 10 mV were applied from a holding potential of -80 mV; linear leak currents were subtracted online using a *P*/4 protocol. Data were analyzed using Clampfit software (Molecular Devices) and Microsoft Excel.

Hormone secretion

For all experiments, islets were allowed to recover for 24 hours following isolation in RPMI 1640 supplemented with 15% FBS and 11 mM glucose. Glucagon secretion was then determined by radioimmunoassay from perifused islets stimulated with 1 and 11 mM glucose (*202*). Glucagon and somatostatin secretion measurements from static incubations were performed as previously described (*262*). Somatostatin was measured from using a fluorescent EIA kit according to the manufacturer's instructions (Phoenix Pharmaceuticals #FEK-060-03)

Statistical analysis

The data is shown as recordings that are averaged or representative of results obtained from at least three independent cultures and three biological replicates per genotype. The values

presented are the mean ± SEM. Statistical differences between means were assessed using two-tailed unpaired Student's *t*-test. A $P<0.05$ was considered as significant.

CHAPTER V

SUMMARY AND FUTURE DIRECTIONS

Significance

It is increasingly clear that defects in β-cell function are central to the pathogenesis of T2DM. While the specific causes of β-cell dysfunction are largely determined by genetics (*102*), interventions which target fundamental β-cell signaling pathways are highly effective treatments for diabetes. Indeed, inhibition of β-cell K_{ATP} channels and activation of β-cell GLP-1 receptors are two therapeutic strategies which enhance insulin secretion and reduce diabetic hyperglycemia. However, there is still great need for therapies which address other pathogenic islet defects in diabetes, including β-cell endoplasmic reticulum stress and improper regulation of α-cell glucagon secretion. The observations described herein suggest the exciting possibility that TALK-1 channels could be therapeutically targeted to ameliorate these islet defects in T2DM.

Prior to the studies described here, it was known that a polymorphism in the *KCNK16* gene (rs1535500, encoding TALK-1 A277E) i T2DM (*27*). It was also known that TALK-1 is abundantly expressed in the islet (*17, 18, 20, 29, 143*), suggesting that the rs1535500 polymorphism could contribute to T2DM risk by altering islet function. However, the biological function of TALK-1 channels was completely unknown. Thus, our studies sought to define the physiological roles of TALK-1 and determine the effects of the T2DM-associated SNP on TALK-1 channel activity to better understand how TALK-1 channels contributed to diabetes susceptibility.

This dissertation presents the first insights into the physiological functions of islet TALK-1 channels. In generating the results described here, I was led to following broad conclusions regarding the functional roles of islet TALK-1 channels:

1. TALK-1 channel activity hastens the development of fasting hyperglycemia and islet ER stress under diabetic conditions;
2. TALK-1-mediated K^+ currents at the plasma membrane polarize the V_m and limit VDCC activity;
3. TALK-1-mediated K^+ countercurrents control ER Ca^{2+} release; and
4. TALK-1 modulation of δ-cell ER Ca^{2+} handling is a novel determinant of islet paracrine signaling.

A schematic illustrating the identified roles of islet TALK-1 channels is presented in Figure 5.1. What follows is a summary of the findings described herein, as well as outstanding questions regarding the biological functions and regulation of TALK-1 channels.

How does inhibition of TALK-1 channel activity protect from fasting hyperglycemia and obesity?

In Chapter II, I used patch clamp electrophysiology, Ca^{2+} imaging, hormone secretion assays, and glucose tolerance tests to examine how loss of TALK-1 channel activity impacts β-cell function. We found that TALK-1 forms functional K^+ channels in β-cells, where it limits Ca^{2+}_c influx and insulin secretion. Moreover, we discovered that TALK-1 A277E channels encoded by rs1535500 produced increased K^+ currents, indicating a gain-of function which

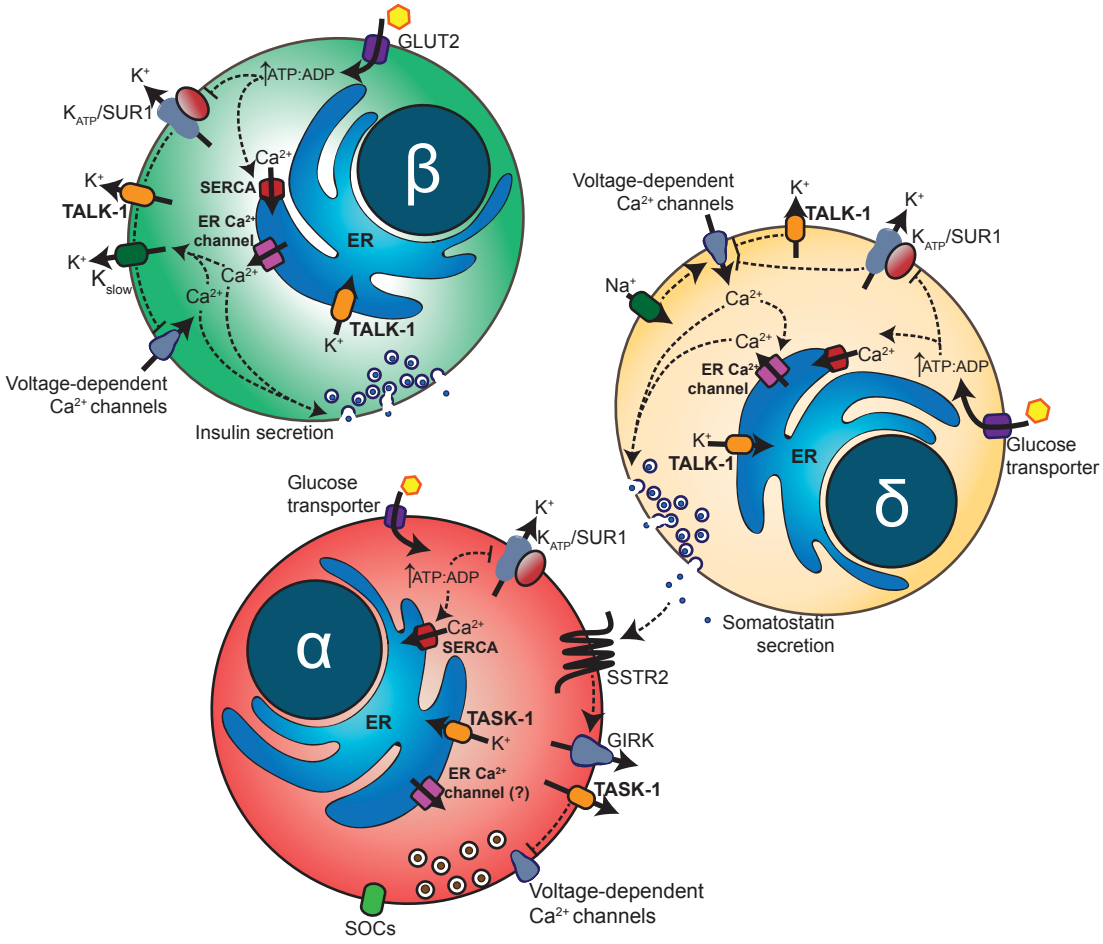

Figure 5.1. Functions of islet K2P channels. TALK-1 channels are expressed in- β- and δ-cells, where they modulate Ca^{2+} influx and hormone secretion. In addition to being expressed in β-cells, TASK-1 channels are also present in α-cells, where they control glucagon secretion. Plasmalemmal K2P channels hyperpolarize the V_m, while ER-localized K2P channels modulate ER Ca^{2+} leak. In β-cells, TALK-1 channel activity limits insulin secretion by regulating VDCC-dependent Ca^{2+} influx, whereas in δ-cells, TALK-1 limits somatostatin secretion by limiting CICR.

would be predicted to hyperpolarize the β-cell V_m. These findings suggest that the increased risk for T2DM conferred by rs1535500 could be due to diminished GSIS caused by TALK-1 channel overactivity. Consistent with this model, a recent study determined that rs1535500 is associated with significantly impaired GSIS in patients with T2DM (*30*). In contrast, the reduced fasting glycemia observed in TALK-1 KO mice on a HFD could be due to changes in islet insulin, somatostatin, and glucagon secretion, as discussed in Chapter IV.

Islets lacking functional TALK-1 channels secrete more insulin under basal and stimulatory glucose conditions, an effect which is partially due to an increased frequency of Ca^{2+}_c oscillations. Despite this increase in insulin secretion, TALK-1 KO mice surprisingly showed no overt reduction in glycemia. As the studies presented here primarily used a mouse model in which TALK-1 channels have been globally knocked out, there is the possibility that compensatory changes may have concealed some functional roles for TALK-1 in adult mice. To address this issue, the Jacobson lab recently obtained a transgenic mouse with critical exons of *Kcnk16* flanked by loxP sites. This important model will permit specific deletion of TALK-1 in different islet cell types to address whether β-cell TALK-1 channels participate in the modulation of hepatic glucose handling.

The mechanism underlying the effects of TALK-1 channels on obesity could be related to its expression in other tissues. Although TALK-1 is abundantly expressed in the pancreatic islet, it has emerged that TALK-1 mRNA is also expressed in neuroendocrine cells of the GI tract (*115, 264*). To confirm these findings, we have also examined TALK-1 expression in both mouse and human stomach and duodenum, and find that TALK-1 is detectable in somatostatin-positive as well as other enteroendocrine cell types (Figure 5.2). These findings suggest that TALK-1 channels could participate in the regulation of the incretin response, although we have

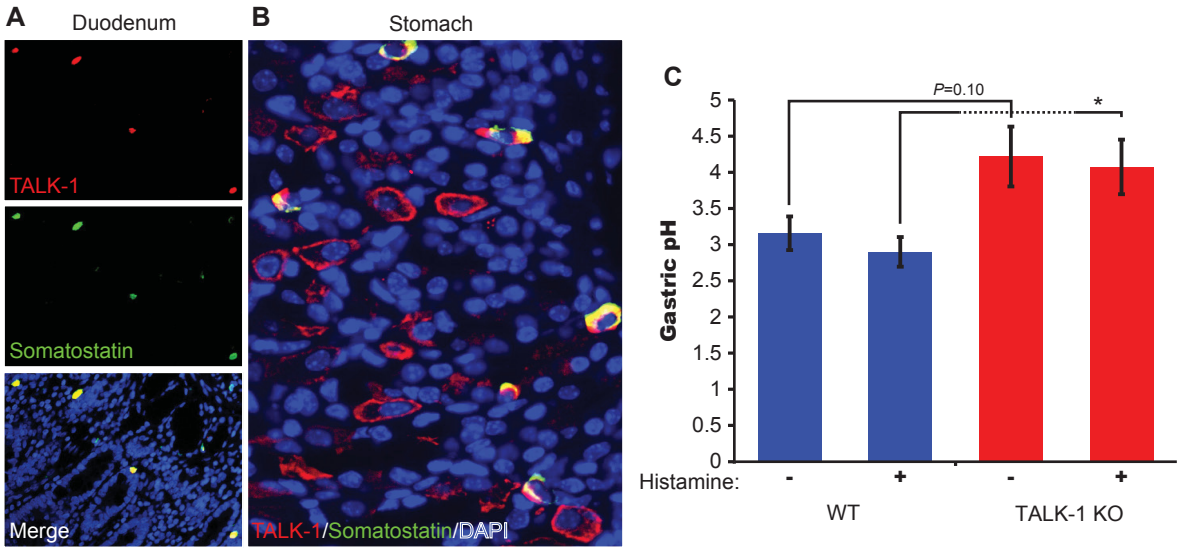

Figure 5.2. TALK-1 is expressed in gastric somatostatin cells. (A) Represntative human duodenum stained for TALK-1 and somatostatin. (B) Represntative human stomach stained for TALK-1 and somatostatin. Note that TALK-1 is also present in an unidentified gastric cell type. (C) WT and TALK-1 KO males were treated with vehicle (PBS) or histamine (10 mg per gram of body weight) to induce gastric acid secretion. N = 4 mice per genotype per condition. Mean ± SEM; * $P < 0.05$; Student's t-test.

not been able to detect a difference in glucose handling when TALK-1 KO mice are subjected to an oral glucose challenge. Interestingly, along with reduced energy expenditure, we find that TALK-1 KO mice consume significantly less food than controls, which may be related to a gastric function of TALK-1 channels (Figure 5.3). Stomach pH is also significantly elevated in TALK-1 KO mice (Figure 5.2), but the molecular mechanism underlying this change is unclear. Once again, the ability to perform tissue-specific knockout of TALK-1 will likely prove invaluable in dissecting the functional roles of GI TALK-1 channels.

The relationship between TALK-1 channel activity, Ca^{2+}_c homeostasis, and stimulus-secretion coupling

One of the more profound phenotypes observed in TALK-1 KO islets was the significantly accelerated frequency of oscillations in electrical activity and Ca^{2+}_c influx. We had early evidence suggesting that a defect in plasma membrane K^+ currents participated in the genesis of this defect, as the rate of V_m hyperpolarization at the end of each electrical oscillation was ~50% slower in TALK-1 KO β-cells (see Chapter II). Therefore, we hypothesized that the current responsible for V_m hyperpolarization at the end of each oscillation, a Ca^{2+}-activated K^+ current called K_{slow}, was reduced in β-cells lacking TALK-1. Indeed, we found that K_{slow} was reduced by approximately 50% in TALK-1 KO β-cells (Chapter III). However, as TALK-1 *per se* is insensitive to Ca^{2+}_c, we did not have a plausible molecular mechanism for the observed reduction in K_{slow} until we discovered that TALK-1 channels modulate ER Ca^{2+} handling. The K_{slow} current is very sensitive to ER Ca^{2+} release, as depleted ER Ca^{2+} stores inhibit K_{slow}. Therefore, as ER-localized TALK-1 channels conduct a K^+ countercurrent which enhances ER

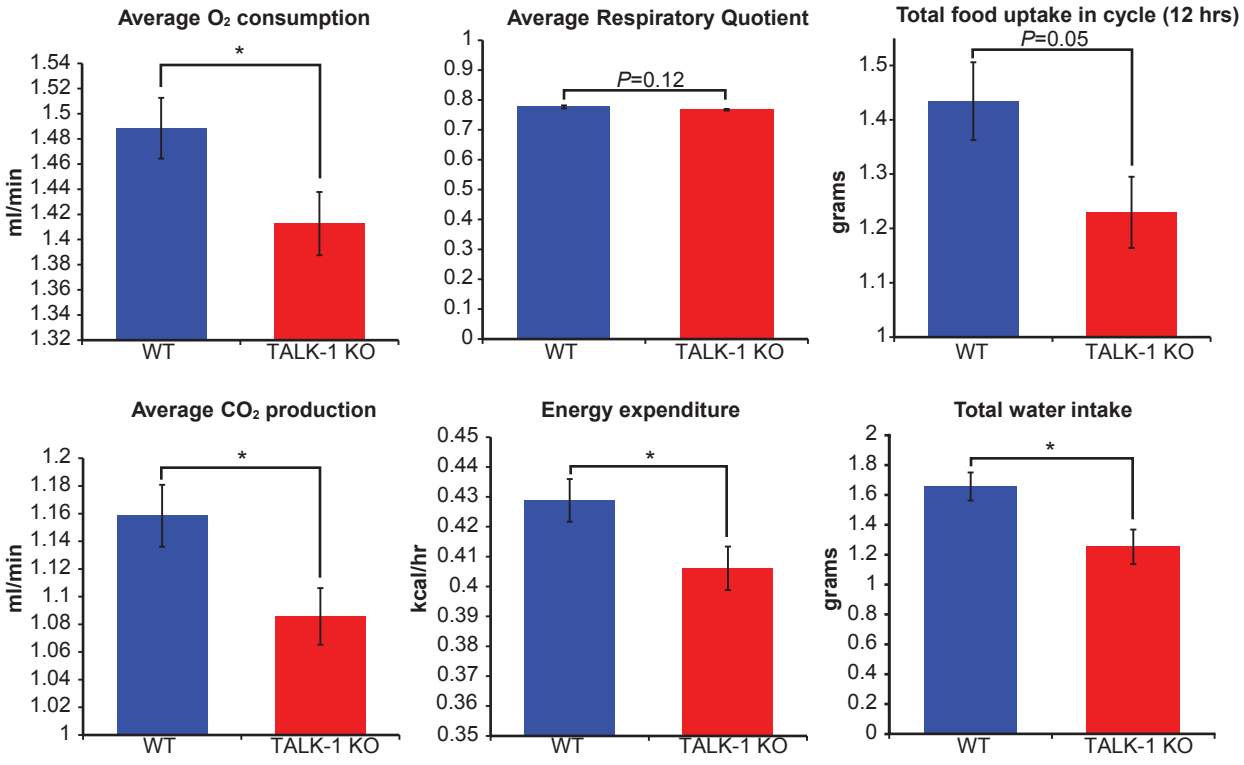

Figure 5.3. Multiple metabolic parameters are altered in TALK-1 KO mice fed a HFD. Dark cycle averages from metabolic cage data are shown for O_2 consumption, CO_2 consumption, respiratory quotient (VCO_2/VO_2), energy expenditure, food consumption , and water intake for WT and TALK-1 KO mice placed on a HFD (60% kcal/fat) for one week. Mean ± SEM; $N = 8$ mice per genotype; * $P < 0.05$; Student's *t*-test.

Ca^{2+} release, the absence of this current in TALK-1 KO β-cells inhibited ER Ca^{2+} release and impaired K_{slow} activation.

It is clear that ER Ca^{2+} homeostasis influences plasma membrane currents such as K_{slow} in β-cells, but the molecular basis of this regulation is unclear. Depletion of ER Ca^{2+} using SERCA inhibitors prevents activation of the K_{slow} current, suggesting that the passive ER Ca^{2+} leak mechanism of β-cells may serve an important role in the activation of K_{slow}. However, it is possible that gated ER Ca^{2+} release mechanisms such as IP3 receptors also modulate K_{slow} activation. Studies of the effects of $G_{\alpha q}$ protein-coupled receptors on control and TALK-1 KO islets (e.g., muscarinic acetylcholine receptor M_3, M3R) indicate that this is possible. In the presence of glucose and the sulfonylurea tolbutamide, a high concentration (100 μmol/L) of the M3R agonist carbachol causes a robust increase in $Ca^{2+}{}_c$ in both control and TALK-1 KO islets (Figure 5.4A). However, this effect is only transient in TALK-1 KO islets, as continued stimulation with carbachol produces a paradoxical reduction in $Ca^{2+}{}_c$. To further investigate the molecular basis of the $Ca^{2+}{}_c$ decrease in TALK-1 KO islets, I performed V_m recordings and found that these conditions caused V_m hyperpolarization and the cessation of action potential firing in TALK-1 KO β-cells (Figure 5.4B). As carbachol-evoked ER Ca^{2+} release tends to be greater in TALK-1 KO β-cells (see Figure 5.4A [inset], and Chapter III), it is possible that IP3-dependent ER Ca^{2+} release can activate a hyperpolarizing, Ca^{2+}-sensitive K^+ current (e.g., the channels responsible for K_{slow}). Interestingly, a lower concentration of carbachol (10 μmol/L) has a slightly different effect, producing a robust increase in the frequency of Ca^{2+} oscillations in

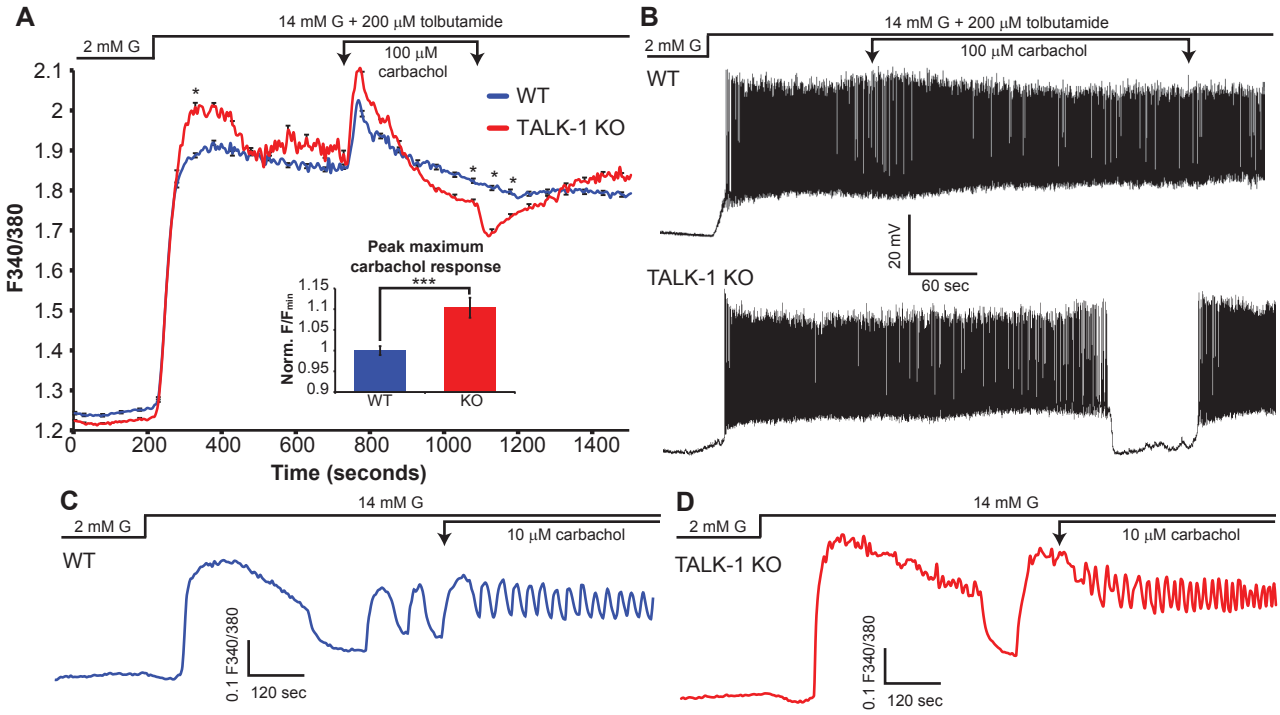

Figure 5.4. TALK-1 KO islets show an altered sensitivity to muscarinic receptor stimulation. (A) WT and TALK-1 KO islets were treated with glucose and tolbutamide to stimulate Ca^{2+} influx, then treated with 100 μM carbachol. The mean peak carbachol response is quantified in the inset (N = 27 WT islets, 20 KO islets). (B) V_m recordings from clusters of WT and TALK-1 KO β-cells, treated as in A. (C) WT and TALK-1 KO islets were treated with glucose to stimulate Ca^{2+} influx, then treated with 10 μM carbachol.*$P < 0.05$; ***$P < 0.001$; Student's t-test.

both control and TALK-1 KO islets (Figure 5.4C,D). Together, these data suggest that IP3 receptor-mediated ER Ca^{2+} release can modulate Ca^{2+}-sensitive K^+ currents, tuning islet Ca^{2+} oscillations.

TALK-1 KO β-cells also showed increased ER Ca^{2+} stores and reduced ER stress after extended HFD feeding, suggesting that inhibition of TALK-1 activity could improve islet health in T2DM. One of the mechanisms proposed to underlie the deterioration of β-cell function in T2DM is ER dysfunction associated with defects in ER Ca^{2+} handling, and the results presented here support this theory. Considering the β-cell ER stress response in the context of what we now know about TALK-1 channels, a clearer picture of the molecular adaptations made by β-cells in order to sustain GSIS is emerging. Under metabolically stressful conditions, β-cells adjust the activity and expression of ER proteins to maintain ER function and sustain insulin production. In two different models of ER stress (inflammatory cytokines and lipotoxicity) which induce the UPR in β-cells, it was found that TALK-1 expression was consistently downregulated (*143, 175*). The critical importance of ER Ca^{2+} homeostasis is highlighted by the fact that BiP, a ubiquitous ER luminal chaperone and marker of ER stress, is induced by the UPR to limit ER Ca^{2+} leakage (*265*). Depletion of ER Ca^{2+} is also known to upregulate expression of SERCAs which pump Ca^{2+} from the cytosol into the ER (*220, 221*). Analogously, reduced TALK-1 expression in β-cells is likely a compensatory mechanism to reduce ER Ca^{2+} leak and maintain sufficient ER Ca^{2+} levels needed for insulin processing. Critical evaluation of this hypothesis will require the identification and disruption of the mechanisms directly responsible for modulating TALK-1 activity under stressful conditions. It will also be important to test if diabetes-associated polymorphisms and mutations in TALK-1 affect islet ER Ca^{2+} levels or influence ER integrity under metabolically stressful conditions.

Blockade of TALK-1 channel activity appears to protect from induction of the ER stress response. Indeed, the downregulation of TALK-1 expression observed in β-cells exposed to inflammatory cytokines or lipotoxic conditions supports this idea. However, the determinants of TALK-1 channel expression, localization, and activity remain mostly unknown. Work by the Jacobson lab recently determined that TALK-1 interacts with a number of islet proteins, one of these being osteopontin (OPN) (*138*). OPN activates TALK-1 currents, an effect which requires the *Ct* of TALK-1, although the exact molecular mechanism underlying this activation as well as the effects of OPN on ER TALK-1 channels remains to be determined. The *KCNK16* gene which encodes TALK-1 was also found to be a direct target of the diabetes-linked transcription factor TCF7L2, and knockdown of TCF7L2 reduced KCNK16 expression (*266*). Clearly, more work is needed to understand how TALK-1 expression is regulated. Moreover, the mechanism controlling the partitioning of TALK-1 channels between the plasma membrane and ER is an important question which remains to be answered.

Although the data presented here demonstrate that TALK-1 channels are part of the ER Ca^{2+} handling machinery, the identities of the channels or transporters mediating ER Ca^{2+} leak remain enigmatic. The Ca^{2+} "leakiness" of the ER is revealed by the pronounced and rapid increase in Ca^{2+}_c which occurs upon SERCA inhibition (e.g., using thapsigargin or CPA). Because β-cell ER Ca^{2+} and Ca^{2+}_c levels are fairly constant in the absence of VDCC-dependent Ca^{2+} influx (*62, 204*), the balance between SERCA pump rate and ER Ca^{2+} leak is an important determinant of Ca^{2+}_c. Several mechanisms have been proposed to underlie ER Ca^{2+} leak, including the translocon, RyRs, and reverse flux through SERCAs. However, as CPA and thapsigargin prevent reverse Ca^{2+} flux through SERCAs (*267*), it is unlikely that they represent a major source of basal ER Ca^{2+} leak. Due to the tremendous amount of protein synthesized by β-

cells, there is a well-developed rough ER, making the translocon a significant source of ER Ca^{2+} leak in β-cells (*226*). A protein-interactome study identified a component of the translocon, Sec62, as a TALK-1 interacting protein (*137*). Though future studies are required to determine whether this interaction truly occurs in primary tissue, a close association of TALK-1 with the translocon may allow for reciprocal regulation of K^+ countercurrent and translocon-dependent Ca^{2+} leak. Furthermore, as Sec62 controls insulin processing, TALK-1 may also modulate insulin synthesis independent of its K^+ channel function.

One of the consequences of ER Ca^{2+} leak is the high basal activity it demands of SERCA pumps, and it is estimated that ~15-25% of basal cellular ATP consumption is due to SERCA activity (*219, 268*). Thus, in β-cells there is likely an interesting feedback between ER Ca^{2+} leak rates, glucose metabolism, and the threshold for GSIS. In islets lacking TALK-1 channels, there was a tendency for reduced SERCA2b and SERCA3 expression, which may be a compensatory mechanism to minimize ER Ca^{2+} overloading (see Chapter III). It remains to be seen whether TALK-1-dependent changes in SERCA expression also produce compensatory changes in mitochondria to maintain metabolic homeostasis. Determining the relationship between ER Ca^{2+} levels, ER Ca^{2+} leak, and metabolism will improve our understanding of the mechanisms controlling β-cell stimulus-secretion coupling in health and disease.

The physiological role of other ER Ca^{2+}-regulating K2P channels also needs to be determined. This dissertation finds that TASK-1 channels also modulate ER Ca^{2+} homeostasis. Blockade of TASK-1 channel K^+ conductance with a dominant-negative mutation or small molecule inhibition of TASK-1 channels significantly increases ER Ca^{2+} stores, suggesting that TASK-1 channel modulation of ER Ca^{2+} is mechanistically similar to TALK-1. One possible consequence of this regulation could be modulation of α-cell store-operated currents. In the

absence of TASK-1 channel activity, α-cell ER Ca^{2+} levels should be higher, resulting in less activation of SOCE and reduced glucagon secretion. Indeed, α-cell specific knockout of TASK-1 results in less glucagon secretion and improved glucose tolerance (*133*). However, the relative importance of plasmalemmal versus ER-localized TASK-1 channels has been difficult to discern, as inhibition of TASK-1 with a small molecule inhibitor increases glucagon secretion, and pharmacological or genetic inhibition of TASK-1 causes α-cell V_m depolarization. Future studies aimed at defining the regulation of TASK-1 localization and activity will likely provide important clues to answer this question. Taken together, these observations redefine our understanding of the physiological functions of K2P channels and suggest the intriguing possibility that K2P channels could be pharmacologically targeted to modulate β-cell ER Ca^{2+} homeostasis in diabetes.

Differences between β- and δ-cells in cellular Ca^{2+} dynamics

In addition to being highly expressed in β-cells, TALK-1 is also present in δ-cells. A consensus model for the stimulus-secretion mechanism of δ-cells has not yet emerged, but it is clear that δ-cells show some similarities with β-cells, along with some important differences. For example, although modulation of ER Ca^{2+} homeostasis is a role shared by β- and δ-cell TALK-1 channels, the plasma membrane function of δ-cell TALK-1 is less clear. Another difference between β- and δ-cells is the central importance of CICR for δ-cell somatostatin secretion, whereas the physiological importance of CICR in β-cells remains uncertain (*269*). In δ-cells, TALK-1 channels act to limit CICR, presumably by modulating the size of the releasable ER Ca^{2+} pool. CICR is enhanced in TALK-1 KO δ-cells, augmenting Ca^{2+}_c influx and somatostatin secretion. One of the consequences of the increased somatostatin secretion in TALK-1 KO islets

is reduced glucagon secretion. In the course of these studies it was also confirmed that glucose enhanced the amplitude of δ-cell Ca^{2+} oscillations, an effect which could be antagonized by depleting ER Ca^{2+} via SERCA inhibition. These observations support the idea that metabolism-induced energization of SERCAs increases δ-cell ER Ca^{2+} stores, leading to enhanced CICR and somatostatin secretion (*86*). Together, these findings increase our understanding of δ-cell stimulus-secretion coupling.

While investigating ER Ca^{2+} uptake and release in δ-cells, it was found that ER Ca^{2+} handling is different between β- and δ-cells. Although both of these cell types show slow ER Ca^{2+} release following a depolarizing stimulus, the amount of Ca^{2+} released is much greater in β-cells (Figure 5.5). The molecular basis for this difference is not presently known, but it may be related to the different SERCA isoforms expressed in β- versus δ-cells. In particular, β-cells express high levels of SERCA3 as well as SERCA2b, whereas δ- and α-cells express only the more widely expressed SERCA2 isoforms (*63, 80*). The physiological importance of β-cell SERCA3 is not completely understood, but it participates in shaping the oscillatory pattern of β-cell Ca^{2+} influx. Interestingly, genetic deletion of SERCA3 results in a β-cell ER Ca^{2+} uptake and release pattern which is very similar to that of δ-cells [compare (*63*) and Figure 5.5B]. A large, slow ER Ca^{2+} release following the termination of action potential firing thus appears to be a unique feature of β-cells, and these data indicate that SERCA3 is important for this phenomenon. In β-cells, TALK-1 activity potentiates this ER Ca^{2+} release, which is suspected to be important for the activation of K_{slow} (see Chapter III). Future studies should delineate the contributions of different SERCA isoforms in shaping cellular Ca^{2+} signals in β-, α-, and δ-cells, and the role of different K2P channels in modulating ER Ca^{2+} fluxes.

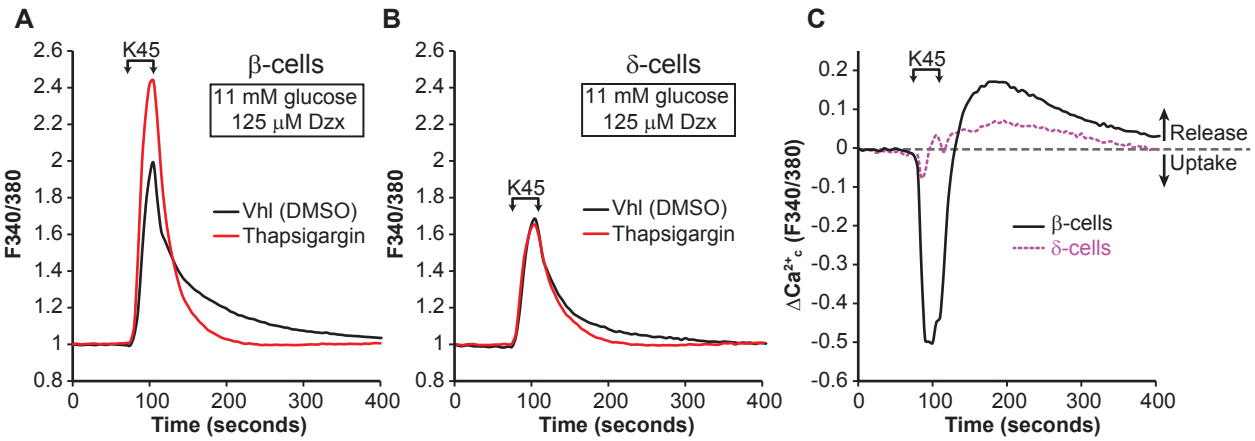

Figure 5.5. δ-cell ER Ca^{2+} handling is different from β-cells. (A) High-K^+ (45 mM) stimulated Ca^{2+} influx in β-cells treated with DMSO vehicle or thapsigargin. (B) High-K^+ (45 mM) stimulated Ca^{2+} influx in δ-cells treated with DMSO vehicle or thapsigargin. (C) ER Ca^{2+} uptake and release in β- and δ-cells determined by subtracting the signal obtained from thapsigargin-treated cells from vehicle. Note that ER Ca^{2+} release precedes the end of the depolarizing K^+ pulse in δ-cells, suggesting CICR.

As we continue to increase our understanding of the distinct molecular mechanisms underlying stimulus-secretion coupling in each of the islet cell types, a physiological rationale for these differences will likely emerge. Presently, it is not entirely clear why δ-cells evolved to use CICR to amplify glucose-stimulated somatostatin secretion, whereas CICR does not appear to be as important for insulin secretion. One possible explanation is that β-cells require a much greater protein production capacity than do α-cells or δ-cells: whereas insulin acts on many target tissues throughout the body, glucagon primarily targets the liver, and islet somatostatin appears to be a paracrine regulator of α- and β-cells. As detailed above, β-cells require a well-developed rough ER to sustain insulin production, which probably necessitates a unique set of pumps and transporters to maintain β-cell ER Ca^{2+} homeostasis. Another possible explanation for the differences in β- and δ-cell Ca^{2+} handling may be that δ-cells must function under both low and high glucose to modulate α- and β-cell function. Because VDCC activity is required for somatostatin secretion, the persistent δ-cell electrical excitability observed in low glucose allows for basal somatostatin secretion which clearly modulates glucagon release. As δ-cell SERCA activity and ER Ca^{2+} release are reduced by low glucose, excessive somatostatin secretion (which would otherwise suppress glucagon secretion and lead to hypoglycemia) is minimized. However, high glucose amplifies CICR and Ca^{2+} influx, enabling δ-cells to release sufficient amounts of somatostatin to control β-cells. CICR thus allows the δ-cells to tune Ca^{2+} influx and somatostatin secretion based not only upon electrical excitability, but also glucose-dependent filling of ER Ca^{2+} stores. Such a mechanism probably ensures that the islet's "somatostatin tone" is appropriate for ambient glucose levels and fits well with the hypothesis that islet somatostatin helps prevent large swings in glycemia by controlling both β- and α-cells (*244*).

The role of δ-cell dysfunction in diabetes pathology is unclear, as very few studies of δ-cell function in diabetes exist. In a non-human primate model of T2DM, there is a reduction in δ-cell mass, which may contribute to inappropriately elevated glucagon secretion (*270*). Similarly, exposure of rodent islets to lipotoxic conditions associated with diabetes reduces somatostatin secretion and increases glucagon secretion (*271*). There is some precedent for human δ-cell dysfunction in diabetes, as polymorphisms in the transcription factor HHEX, which controls islet δ-cell differentiation, have been linked to elevated glucagon secretion and an increased risk for T2DM (*23, 109*). Additionally, Ucn3, which is co-released with insulin to stimulate δ-cells, is significantly depleted in islets from T2DM donors (*244*). The rs1535500 polymorphism in TALK-1 also increases T2DM susceptibility, and the observations provided in this dissertation suggest that defects in TALK-1 channel activity could increase hyperglycemia by negatively affecting δ-cell function. By using a δ-cell-specific knockout of TALK-1 channels, it should be possible to determine how TALK-1 function in δ-cells contributes to the regulation of glucose homeostasis under physiological and diabetic conditions.

Closing remarks

This dissertation defines the role of TALK-1 channels in modulating islet cell electrical activity, Ca^{2+} handling, hormone secretion, and metabolic homeostasis. These findings provide the first described molecular mechanisms for how TALK-1 contributes to T2DM risk and indicate that TALK-1 channels may be a viable therapeutic target for the treatment of diabetes. Overall, the results presented in this thesis illuminate the physiological functions of TALK-1, which is expected to serve as the foundation for a continuum of research investigating the roles and regulation of TALK-1 channels in health and disease.

REFERENCES

1. J. E. Gerich, Physiology of glucose homeostasis. *Diabetes Obes Metab* **2**, 345-350 (2000).

2. A. Sakula, Paul Langerhans (1847-1888): a centenary tribute. *J R Soc Med* **81**, 414-415 (1988).

3. C. Ionescu-Tirgoviste *et al.*, A 3D map of the islet routes throughout the healthy human pancreas. *Sci Rep* **5**, 14634 (2015).

4. G. C. Weir, S. Bonner-Weir, Islet beta cell mass in diabetes and how it relates to function, birth, and death. *Ann N Y Acad Sci* **1281**, 92-105 (2013).

5. O. Cabrera *et al.*, The unique cytoarchitecture of human pancreatic islets has implications for islet cell function. *Proceedings of the National Academy of Sciences of the United States of America* **103**, 2334-2339 (2006).

6. M. Brissova *et al.*, Assessment of human pancreatic islet architecture and composition by laser scanning confocal microscopy. *J Histochem Cytochem* **53**, 1087-1097 (2005).

7. C. A. Reissaus, D. W. Piston, Reestablishment of Glucose Inhibition of Glucagon Secretion in Small Pseudo-Islets. *Diabetes*, (2017).

8. L. Orci, R. H. Unger, Functional subdivision of islets of Langerhans and possible role of D cells. *Lancet* **2**, 1243-1244 (1975).

9. G. M. Grodsky, L. L. Bennett, Cation requirements for insulin secretion in the isolated perfused pancreas. *Diabetes* **15**, 910-913 (1966).

10. S. Efendic, V. Grill, A. Nylen, C. G. Ostensson, Difference in calcium dependency of insulin, glucagon and somatostatin secretion in response to glibenclamide in perfused rat pancreas. *Diabetologia* **22**, 475-479 (1982).

11. J. Iversen, K. Hermansen, Calcium, glucose and glucagon release. *Diabetologia* **13**, 297-303 (1977).

12. P. Rorsman, M. Braun, Q. Zhang, Regulation of calcium in pancreatic alpha- and beta-cells in health and disease. *Cell Calcium* **51**, 300-308 (2012).

13. P. M. Dean, E. K. Matthews, Electrical activity in pancreatic islet cells. *Nature* **219**, 389-390 (1968).

14. A. Kanatsuka, H. Makino, J. Kasanuki, M. Osegawa, A. Kumagai, Somatostatin and insulin secretion from pancreatic islets: studies on the effect of high K^+, 9-aminoacridine and valinomycin. *Metabolism* **32**, 66-69 (1983).

15. G. Epstein, R. Fanska, G. M. Grodsky, The effect of potassium and valinomycin on insulin and glucagon secretion in the perfused rat pancreas. *Endocrinology* **103**, 2207-2215 (1978).

16. N. Lawlor *et al.*, Single-cell transcriptomes identify human islet cell signatures and reveal cell-type-specific expression changes in type 2 diabetes. *Genome Res* **27**, 208-222 (2017).

17. G. M. Ku *et al.*, Research resource: RNA-Seq reveals unique features of the pancreatic beta-cell transcriptome. *Molecular Endocrinology* **26**, 1783-1792 (2012).

18. M. L. Stitzel *et al.*, Global epigenomic analysis of primary human pancreatic islets provides insights into type 2 diabetes susceptibility loci. *Cell Metabolism* **12**, 443-455 (2010).

19. C. Benner *et al.*, The transcriptional landscape of mouse beta cells compared to human beta cells reveals notable species differences in long non-coding RNA and protein-coding gene expression. *BMC Genomics* **15**, 620 (2014).

20. N. C. Bramswig *et al.*, Epigenomic plasticity enables human pancreatic alpha to beta cell reprogramming. *The Journal of Clinical Investigation* **123**, 1275-1284 (2013).

21. D. T. Villareal *et al.*, Kir6.2 variant E23K increases ATP-sensitive K+ channel activity and is associated with impaired insulin release and enhanced insulin sensitivity in adults with normal glucose tolerance. *Diabetes* **58**, 1869-1878 (2009).

22. A. H. Rosengren *et al.*, Reduced insulin exocytosis in human pancreatic beta-cells with gene variants linked to type 2 diabetes. *Diabetes* **61**, 1726-1733 (2012).

23. A. Jonsson *et al.*, Effects of common genetic variants associated with type 2 diabetes and glycemic traits on alpha- and beta-cell function and insulin action in humans. *Diabetes* **62**, 2978-2983 (2013).

24. P. Haghvirdizadeh *et al.*, KCNJ11: Genetic Polymorphisms and Risk of Diabetes Mellitus. *J Diabetes Res* **2015**, 908152 (2015).

25. K. Okamoto *et al.*, Inhibition of glucose-stimulated insulin secretion by KCNJ15, a newly identified susceptibility gene for type 2 diabetes. *Diabetes* **61**, 1734-1741 (2012).

26. H. Zeng *et al.*, An Isogenic Human ESC Platform for Functional Evaluation of Genome-wide-Association-Study-Identified Diabetes Genes and Drug Discovery. *Cell Stem Cell* **19**, 326-340 (2016).

27. Y. S. Cho *et al.*, Meta-analysis of genome-wide association studies identifies eight new loci for type 2 diabetes in east Asians. *Nature Genetics* **44**, 67-72 (2012).

28. Y. L. Muller *et al.*, Assessing Variation across Eight Established East Asian Loci for Type 2 Diabetes in American Indians: Suggestive Evidence for New Sex-specific Diabetes Signals in GLIS3 and ZFAND3. *Diabetes Metab Res Rev*, (2016).

29. D. I. G. Replication *et al.*, Genome-wide trans-ancestry meta-analysis provides insight into the genetic architecture of type 2 diabetes susceptibility. *Nature Genetics* **46**, 234-244 (2014).

30. A. R. Wood *et al.*, A Genome-Wide Association Study of IVGTT-Based Measures of First Phase Insulin Secretion Refines the Underlying Physiology of Type 2 Diabetes Variants. *Diabetes*, (2017).

31. F. M. Matschinsky, Glucokinase as glucose sensor and metabolic signal generator in pancreatic beta-cells and hepatocytes. *Diabetes* **39**, 647-652 (1990).

32. M. L. Markwardt, K. M. Seckinger, M. A. Rizzo, Regulation of Glucokinase by Intracellular Calcium Levels in Pancreatic beta Cells. *The Journal of Biological Chemistry* **291**, 3000-3009 (2016).

33. L. D. Pound *et al.*, G6PC2: a negative regulator of basal glucose-stimulated insulin secretion. *Diabetes* **62**, 1547-1556 (2013).

34. M. L. Wall, L. D. Pound, I. Trenary, R. M. O'Brien, J. D. Young, Novel stable isotope analyses demonstrate significant rates of glucose cycling in mouse pancreatic islets. *Diabetes* **64**, 2129-2137 (2015).

35. D. Fu *et al.*, Genetic polymorphism of glucokinase on the risk of type 2 diabetes and impaired glucose regulation: evidence based on 298,468 subjects. *PloS one* **8**, e55727 (2013).

36. A. L. Gloyn *et al.*, Insights into the structure and regulation of glucokinase from a novel mutation (V62M), which causes maturity-onset diabetes of the young. *The Journal of Biological Chemistry* **280**, 14105-14113 (2005).

37. M. S. German, Glucose sensing in pancreatic islet beta cells: the key role of glucokinase and the glycolytic intermediates. *Proceedings of the National Academy of Sciences of the United States of America* **90**, 1781-1785 (1993).

38. C. G. Nichols, KATP channels as molecular sensors of cellular metabolism. *Nature* **440**, 470-476 (2006).

39. J. S. Denton, D. A. Jacobson, Channeling dysglycemia: ion-channel variations perturbing glucose homeostasis. *Trends in Endocrinology and Metabolism: TEM* **23**, 41-48 (2012).

40. P. A. Smith, F. M. Ashcroft, P. Rorsman, Simultaneous recordings of glucose dependent electrical activity and ATP-regulated K(+)-currents in isolated mouse pancreatic beta-cells. *FEBS letters* **261**, 187-190 (1990).

41. P. A. Smith, L. A. Sellers, P. P. Humphrey, Somatostatin activates two types of inwardly rectifying K^+ channels in MIN-6 cells. *The Journal of Physiology* **532**, 127-142 (2001).

42. B. Kailey *et al.*, SSTR2 is the functionally dominant somatostatin receptor in human pancreatic beta- and alpha-cells. *American Journal of Physiology. Endocrinology and Metabolism* **303**, E1107-1116 (2012).

43. D. A. Jacobson *et al.*, Kv2.1 ablation alters glucose-induced islet electrical activity, enhancing insulin secretion. *Cell Metabolism* **6**, 229-235 (2007).

44. X. N. Li *et al.*, The role of voltage-gated potassium channels Kv2.1 and Kv2.2 in the regulation of insulin and somatostatin release from pancreatic islets. *J Pharmacol Exp Ther* **344**, 407-416 (2013).

45. M. Braun *et al.*, Voltage-gated ion channels in human pancreatic beta-cells: electrophysiological characterization and role in insulin secretion. *Diabetes* **57**, 1618-1628 (2008).

46. P. E. MacDonald *et al.*, Synaptosome-associated protein of 25 kilodaltons modulates Kv2.1 voltage-dependent K(+) channels in neuroendocrine islet beta-cells through an interaction with the channel N terminus. *Molecular Endocrinology* **16**, 2452-2461 (2002).

47. J. Fu *et al.*, Kv2.1 Clustering Contributes to Insulin Exocytosis and Rescues Human beta-Cell Dysfunction. *Diabetes*, (2017).

48. T. Kanno, P. Rorsman, S. O. Gopel, Glucose-dependent regulation of rhythmic action potential firing in pancreatic beta-cells by K(ATP)-channel modulation. *The Journal of Physiology* **545**, 501-507 (2002).

49. P. B. Goforth *et al.*, Calcium-activated K^+ channels of mouse beta-cells are controlled by both store and cytoplasmic Ca^{2+}: experimental and theoretical studies. *The Journal of General Physiology* **120**, 307-322 (2002).

50. M. Zhang, K. Houamed, S. Kupershmidt, D. Roden, L. S. Satin, Pharmacological properties and functional role of Kslow current in mouse pancreatic beta-cells: SK channels contribute to Kslow tail current and modulate insulin secretion. *The Journal of General Physiology* **126**, 353-363 (2005).

51. S. Göpel, Kanno, T., & Rorsman, P., Two components of activity-dependent transient K^+-current (I_{Kslow}) in mouse pancreatic β-cells. *Diabetologia* **44**, (2001).

52. P. K. Dadi, N. C. Vierra, D. A. Jacobson, Pancreatic beta-Cell-specific Ablation of TASK-1 Channels Augments Glucose-stimulated Calcium Entry and Insulin Secretion, Improving Glucose Tolerance. *Endocrinology* **155**, 3757-3768 (2014).

53. S. Gopel, T. Kanno, S. Barg, J. Galvanovskis, P. Rorsman, Voltage-gated and resting membrane currents recorded from B-cells in intact mouse pancreatic islets. *The Journal of Physiology* **521 Pt 3**, 717-728 (1999).

54. B. Ribalet, P. M. Beigelman, Calcium action potentials and potassium permeability activation in pancreatic beta-cells. *The American Journal of Physiology* **239**, C124-133 (1980).

55. K. S. Polonsky, B. D. Given, E. Van Cauter, Twenty-four-hour profiles and pulsatile patterns of insulin secretion in normal and obese subjects. *The Journal of clinical investigation* **81**, 442-448 (1988).

56. A. Tengholm, E. Gylfe, Oscillatory control of insulin secretion. *Molecular and Cellular Endocrinology* **297**, 58-72 (2009).

57. A. V. Matveyenko *et al.*, Pulsatile portal vein insulin delivery enhances hepatic insulin action and signaling. *Diabetes* **61**, 2269-2279 (2012).

58. G. M. Grodsky, A new phase of insulin secretion. How will it contribute to our understanding of beta-cell function? *Diabetes* **38**, 673-678 (1989).

59. M. J. Merrins *et al.*, Metabolic oscillations in pancreatic islets depend on the intracellular Ca^{2+} level but not Ca^{2+} oscillations. *Biophysical Journal* **99**, 76-84 (2010).

60. S. O. Gopel *et al.*, Activation of Ca(2+)-dependent K(+) channels contributes to rhythmic firing of action potentials in mouse pancreatic beta cells. *The Journal of General Physiology* **114**, 759-770 (1999).

61. M. Dufer *et al.*, Enhanced glucose tolerance by SK4 channel inhibition in pancreatic beta-cells. *Diabetes* **58**, 1835-1843 (2009).

62. P. Gilon, H. Y. Chae, G. A. Rutter, M. A. Ravier, Calcium signaling in pancreatic beta-cells in health and in Type 2 diabetes. *Cell Calcium* **56**, 340-361 (2014).

63. A. Arredouani *et al.*, SERCA3 ablation does not impair insulin secretion but suggests distinct roles of different sarcoendoplasmic reticulum Ca(2+) pumps for Ca(2+) homeostasis in pancreatic beta-cells. *Diabetes* **51**, 3245-3253 (2002).

64. P. Gilon, J. C. Henquin, Mechanisms and physiological significance of the cholinergic control of pancreatic beta-cell function. *Endocrine Reviews* **22**, 565-604 (2001).

65. J. D. Johnson, S. Kuang, S. Misler, K. S. Polonsky, Ryanodine receptors in human pancreatic beta cells: localization and effects on insulin secretion. *FASEB J* **18**, 878-880 (2004).

66. A. Tengholm, C. Hagman, E. Gylfe, B. Hellman, In situ characterization of nonmitochondrial Ca2+ stores in individual pancreatic beta-cells. *Diabetes* **47**, 1224-1230 (1998).

67. X. Tong *et al.*, SERCA2 Deficiency Impairs Pancreatic beta-Cell Function in Response to Diet-Induced Obesity. *Diabetes* **65**, 3039-3052 (2016).

68. G. Santulli *et al.*, Calcium release channel RyR2 regulates insulin release and glucose homeostasis. *The Journal of Clinical Investigation* **125**, 4316 (2015).

69. J. E. Campbell, D. J. Drucker, Islet alpha cells and glucagon--critical regulators of energy homeostasis. *Nat Rev Endocrinol* **11**, 329-338 (2015).

70. E. Trefts, A. S. Williams, D. H. Wasserman, Exercise and the Regulation of Hepatic Metabolism. *Prog Mol Biol Transl Sci* **135**, 203-225 (2015).

71. P. E. Lins, A. Wajngot, U. Adamson, M. Vranic, S. Efendic, Minimal increases in glucagon levels enhance glucose production in man with partial hypoinsulinemia. *Diabetes* **32**, 633-636 (1983).

72. E. Gylfe, Glucose control of glucagon secretion-'There's a brand-new gimmick every year'. *Ups J Med Sci* **121**, 120-132 (2016).

73. L. Briant, A. Salehi, E. Vergari, Q. Zhang, P. Rorsman, Glucagon secretion from pancreatic alpha-cells. *Ups J Med Sci* **121**, 113-119 (2016).

74. R. Ramracheya *et al.*, Membrane potential-dependent inactivation of voltage-gated ion channels in alpha-cells inhibits glucagon secretion from human islets. *Diabetes* **59**, 2198-2208 (2010).

75. J. Gromada *et al.*, Adrenaline stimulates glucagon secretion in pancreatic A-cells by increasing the Ca2+ current and the number of granules close to the L-type Ca^{2+} channels. *The Journal of General Physiology* **110**, 217-228 (1997).

76. Q. Zhang *et al.*, Role of KATP channels in glucose-regulated glucagon secretion and impaired counterregulation in type 2 diabetes. *Cell Metabolism* **18**, 871-882 (2013).

77. E. Vieira, A. Salehi, E. Gylfe, Glucose inhibits glucagon secretion by a direct effect on mouse pancreatic alpha cells. *Diabetologia* **50**, 370-379 (2007).

78. Y. J. Liu, E. Vieira, E. Gylfe, A store-operated mechanism determines the activity of the electrically excitable glucagon-secreting pancreatic alpha-cell. *Cell Calcium* **35**, 357-365 (2004).

79. A. P. Chambers *et al.*, The Role of Pancreatic Preproglucagon in Glucose Homeostasis in Mice. *Cell Metabolism* **25**, 927-934 e923 (2017).

80. J. Li *et al.*, Single-cell transcriptomes reveal characteristic features of human pancreatic islet cell types. *EMBO reports* **17**, 178-187 (2016).

81. Y. Yoshimoto *et al.*, Somatostatin induces hyperpolarization in pancreatic islet alpha cells by activating a G protein-gated K^+ channel. *FEBS letters* **444**, 265-269 (1999).

82. J. Li *et al.*, Submembrane ATP and Ca^{2+} kinetics in alpha-cells: unexpected signaling for glucagon secretion. *FASEB J* **29**, 3379-3388 (2015).

83. A. D. Elliott, A. Ustione, D. W. Piston, Somatostatin and insulin mediate glucose-inhibited glucagon secretion in the pancreatic alpha-cell by lowering cAMP. *American Journal of Physiology. Endocrinology and metabolism* **308**, E130-143 (2015).

84. A. C. Hauge-Evans *et al.*, Somatostatin secreted by islet delta-cells fulfills multiple roles as a paracrine regulator of islet function. *Diabetes* **58**, 403-411 (2009).

85. H. Shuai, Y. Xu, Q. Yu, E. Gylfe, A. Tengholm, Fluorescent protein vectors for pancreatic islet cell identification in live-cell imaging. *Pflugers Archiv : European Journal of Physiology* **468**, 1765-1777 (2016).

86. Q. Zhang *et al.*, R-type Ca(2+)-channel-evoked CICR regulates glucose-induced somatostatin secretion. *Nature Cell Biology* **9**, 453-460 (2007).

87. A. Berts, A. Ball, G. Dryselius, E. Gylfe, B. Hellman, Glucose stimulation of somatostatin-producing islet cells involves oscillatory Ca^{2+} signaling. *Endocrinology* **137**, 693-697 (1996).

88. I. Quesada, A. Nadal, B. Soria, Different effects of tolbutamide and diazoxide in alpha, beta-, and delta-cells within intact islets of Langerhans. *Diabetes* **48**, 2390-2397 (1999).

89. M. Braun *et al.*, Somatostatin release, electrical activity, membrane currents and exocytosis in human pancreatic delta cells. *Diabetologia* **52**, 1566-1578 (2009).

90. Y. J. Liu, B. Hellman, E. Gylfe, Ca^{2+} signaling in mouse pancreatic polypeptide cells. *Endocrinology* **140**, 5524-5529 (1999).

91. A. Arimura, C. A. Meyers, W. L. Case, W. A. Murphy, A. V. Schally, Suppression of somatostatin levels in the hepatic portal and systemic plasma of the rat by synthetic human pancreatic polypeptide. *Biochemical and Biophysical Research Communications* **89**, 913-918 (1979).

92. F. Aragon *et al.*, Pancreatic polypeptide regulates glucagon release through PPYR1 receptors expressed in mouse and human alpha-cells. *Biochim Biophys Acta* **1850**, 343-351 (2015).

93. R. A. Prinz *et al.*, Neural regulation of pancreatic polypeptide release. *Surgery* **94**, 1011-1018 (1983).

94. M. R. DiGruccio *et al.*, Comprehensive alpha, beta and delta cell transcriptomes reveal that ghrelin selectively activates delta cells and promotes somatostatin release from pancreatic islets. *Mol Metab* **5**, 449-458 (2016).

95. A. E. Adriaenssens *et al.*, Transcriptomic profiling of pancreatic alpha, beta and delta cell populations identifies delta cells as a principal target for ghrelin in mouse islets. *Diabetologia* **59**, 2156-2165 (2016).

96. R. Baldelli *et al.*, Oral glucose load inhibits circulating ghrelin levels to the same extent in normal and obese children. *Clin Endocrinol (Oxf)* **64**, 255-259 (2006).

97. W. H. Organization, Definition and diagnosis of diabetes mellitus and intermediate hyperglycaemia. (2008).

98. National Diabetes Report 2014, Centers for Disease Control and Prevention. Accessed April, 2017 https://www.cdc.gov/diabetes/pubs/statsreport14/national-diabetes-report-web.pdf

99. G. Wilcox, Insulin and insulin resistance. *Clin Biochem Rev* **26**, 19-39 (2005).

100. D. C. Whitelaw, S. G. Gilbey, Insulin resistance. *Ann Clin Biochem* **35 (Pt 5)**, 567-583 (1998).

101. R. B. Prasad, L. Groop, Genetics of type 2 diabetes-pitfalls and possibilities. *Genes (Basel)* **6**, 87-123 (2015).

102. P. A. Halban *et al.*, beta-cell failure in type 2 diabetes: postulated mechanisms and prospects for prevention and treatment. *The Journal of clinical Endocrinology and Metabolism* **99**, 1983-1992 (2014).

103. K. J. Chang-Chen, R. Mullur, E. Bernal-Mizrachi, Beta-cell failure as a complication of diabetes. *Rev Endocr Metab Disord* **9**, 329-343 (2008).

104. S. Lenzen, Oxidative stress: the vulnerable beta-cell. *Biochem Soc Trans* **36**, 343-347 (2008).

105. H. Ferner, The A- and B-cells of the pancreatic islets as sources of the antagonistic hormones glucagon and insulin; the shift of the AB-relation in diabetes mellitus. *Am J Dig Dis* **20**, 301-306 (1953).

106. R. H. Unger, E. Aguilar-Parada, W. A. Muller, A. M. Eisentraut, Studies of pancreatic alpha cell function in normal and diabetic subjects. *The Journal of Clinical Investigation* **49**, 837-848 (1970).

107. R. H. Unger, L. Orci, Paracrinology of islets and the paracrinopathy of diabetes. *Proceedings of the National Academy of Sciences of the United States of America* **107**, 16009-16012 (2010).

108. Y. C. Huang *et al.*, In situ electrophysiological examination of pancreatic alpha cells in the streptozotocin-induced diabetes model, revealing the cellular basis of glucagon hypersecretion. *Diabetes* **62**, 519-530 (2013).

109. J. Zhang, L. B. McKenna, C. W. Bogue, K. H. Kaestner, The diabetes gene Hhex maintains delta-cell differentiation and islet function. *Genes & Development* **28**, 829-834 (2014).

110. E. H. Leiter, D. A. Gapp, J. J. Eppig, D. L. Coleman, Ultrastructural and morphometric studies of delta cells in pancreatic islets from C57BL/Ks diabetes mice. *Diabetologia* **17**, 297-309 (1979).

111. J. Rahier, R. M. Goebbels, J. C. Henquin, Cellular composition of the human diabetic pancreas. *Diabetologia* **24**, 366-371 (1983).

112. R. A. Defronzo, Banting Lecture. From the triumvirate to the ominous octet: a new paradigm for the treatment of type 2 diabetes mellitus. *Diabetes* **58**, 773-795 (2009).

113. E. R. Pearson *et al.*, Switching from insulin to oral sulfonylureas in patients with diabetes due to Kir6.2 mutations. *N Engl J Med* **355**, 467-477 (2006).

114. C. Girard *et al.*, Genomic and functional characteristics of novel human pancreatic 2P domain K(+) channels. *Biochemical and Biophysical Research Communications* **282**, 249-256 (2001).

115. A. Adriaenssens *et al.*, A Transcriptome-Led Exploration of Molecular Mechanisms Regulating Somatostatin-Producing D-Cells in the Gastric Epithelium. *Endocrinology* **156**, 3924-3936 (2015).

116. A. L. Hodgkin, A. F. Huxley, A quantitative description of membrane current and its application to conduction and excitation in nerve. *The Journal of Physiology* **117**, 500-544 (1952).

117. A. L. Hodgkin, B. Katz, The effect of sodium ions on the electrical activity of giant axon of the squid. *The Journal of Physiology* **108**, 37-77 (1949).

118. F. Lesage *et al.*, TWIK-1, a ubiquitous human weakly inward rectifying K^+ channel with a novel structure. *The EMBO Journal* **15**, 1004-1011 (1996).

119. A. N. Miller, S. B. Long, Crystal structure of the human two-pore domain potassium channel K2P1. *Science* **335**, 432-436 (2012).

120. V. Renigunta, G. Schlichthorl, J. Daut, Much more than a leak: structure and function of K(2)p-channels. *Pflugers Archiv : European Journal of Physiology* **467**, 867-894 (2015).

121. C. Heurteaux *et al.*, TREK-1, a K^+ channel involved in neuroprotection and general anesthesia. *The EMBO journal* **23**, 2684-2695 (2004).

122. A. Alloui *et al.*, TREK-1, a K^+ channel involved in polymodal pain perception. *The EMBO Journal* **25**, 2368-2376 (2006).

123. V. Pereira *et al.*, Role of the TREK2 potassium channel in cold and warm thermosensation and in pain perception. *Pain* **155**, 2534-2544 (2014).

124. P. K. Dadi *et al.*, Selective small molecule activators of TREK-2 channels stimulate DRG c-fiber nociceptor K2P currents and limit calcium influx. *ACS Chem Neurosci*, (2016).

125. D. S. Pang *et al.*, An unexpected role for TASK-3 potassium channels in network oscillations with implications for sleep mechanisms and anesthetic action. *Proceedings of the National Academy of Sciences of the United States of America* **106**, 17546-17551 (2009).

126. O. Barel *et al.*, Maternally inherited Birk Barel mental retardation dysmorphism syndrome caused by a mutation in the genomically imprinted potassium channel KCNK9. *Am J Hum Genet* **83**, 193-199 (2008).

127. P. Liu *et al.*, Functional analysis of a migraine-associated TRESK K+ channel mutation. *The Journal of neuroscience : the official journal of the Society for Neuroscience* **33**, 12810-12824 (2013).

128. R. G. Lafreniere *et al.*, A dominant-negative mutation in the TRESK potassium channel is linked to familial migraine with aura. *Nat Med* **16**, 1157-1160 (2010).

129. F. C. Chatelain *et al.*, TWIK1, a unique background channel with variable ion selectivity. *Proceedings of the National Academy of Sciences of the United States of America* **109**, 5499-5504 (2012).

130. L. Ma, X. Zhang, H. Chen, TWIK-1 two-pore domain potassium channels change ion selectivity and conduct inward leak sodium currents in hypokalemia. *Sci Signal* **4**, ra37 (2011).

131. F. Duprat *et al.*, TASK, a human background K^+ channel to sense external pH variations near physiological pH. *The EMBO Journal* **16**, 5464-5471 (1997).

132. E. F. Nogueira, D. Gerry, F. Mantero, B. Mariniello, W. E. Rainey, The role of TASK1 in aldosterone production and its expression in normal adrenal and aldosterone-producing adenomas. *Clin Endocrinol (Oxf)* **73**, 22-29 (2010).

133. P. K. Dadi, B. Luo, N. C. Vierra, D. A. Jacobson, TASK-1 potassium channels limit pancreatic alpha-cell calcium influx and glucagon secretion. *Molecular Endocrinology*, me20141321 (2015).

134. J. Han, D. Kang, D. Kim, Functional properties of four splice variants of a human pancreatic tandem-pore K^+ channel, TALK-1. *American Journal of Physiology. Cell Physiology* **285**, C529-538 (2003).

135. D. Kang, D. Kim, Single-channel properties and pH sensitivity of two-pore domain K+ channels of the TALK family. *Biochemical and Biophysical Research Communications* **315**, 836-844 (2004).

136. F. Duprat, C. Girard, G. Jarretou, M. Lazdunski, Pancreatic two P domain K^+ channels TALK-1 and TALK-2 are activated by nitric oxide and reactive oxygen species. *The Journal of Physiology* **562**, 235-244 (2005).

137. E. L. Huttlin *et al.*, The BioPlex Network: A Systematic Exploration of the Human Interactome. *Cell* **162**, 425-440 (2015).

138. M. T. Dickerson, N. C. Vierra, S. C. Milian, P. K. Dadi, D. A. Jacobson, Osteopontin activates the diabetes-associated potassium channel TALK-1 in pancreatic beta-cells. *PloS One* **12**, e0175069 (2017).

139. G. Drews, P. Krippeit-Drews, M. Dufer, Electrophysiology of islet cells. *Advances in Experimental Medicine and Biology* **654**, 115-163 (2010).

140. F. M. Ashcroft, P. Rorsman, Electrophysiology of the pancreatic β-cell. *Progress in Biophysics and Molecular Biology* **54**, 87-143 (1989).

141. J. Ren *et al.*, Slow oscillations of KATP conductance in mouse pancreatic islets provide support for electrical bursting driven by metabolic oscillations. *American Journal of Physiology. Endocrinology and Metabolism* **305**, E805-817 (2013).

142. I. Atwater, B. Ribalet, E. Rojas, Cyclic changes in potential and resistance of the beta-cell membrane induced by glucose in islets of Langerhans from mouse. *The Journal of Physiology* **278**, 117-139 (1978).

143. D. L. Eizirik *et al.*, The human pancreatic islet transcriptome: expression of candidate genes for type 1 diabetes and the impact of pro-inflammatory cytokines. *PLoS Genetics* **8**, e1002552 (2012).

144. K. Sakai *et al.*, Replication study for the association of 9 East Asian GWAS-derived loci with susceptibility to type 2 diabetes in a Japanese population. *PloS one* **8**, e76317 (2013).

145. L. Pei *et al.*, Oncogenic potential of TASK3 (Kcnk9) depends on K^+ channel function. *Proceedings of the National Academy of Sciences of the United States of America* **100**, 7803-7807 (2003).

146. J. H. Kim *et al.*, High cleavage efficiency of a 2A peptide derived from porcine teschovirus-1 in human cell lines, zebrafish and mice. *PloS One* **6**, e18556 (2011).

147. C. S. Nunemaker *et al.*, Glucose modulates $[Ca^{2+}]_i$ oscillations in pancreatic islets via ionic and glycolytic mechanisms. *Biophysical Journal* **91**, 2082-2096 (2006).

148. W. S. Head *et al.*, Connexin-36 gap junctions regulate in vivo first- and second-phase insulin secretion dynamics and glucose tolerance in the conscious mouse. *Diabetes* **61**, 1700-1707 (2012).

149. P. O. Berggren *et al.*, Removal of Ca2+ channel beta3 subunit enhances Ca^{2+} oscillation frequency and insulin exocytosis. *Cell* **119**, 273-284 (2004).

150. B. Colsoul *et al.*, Loss of high-frequency glucose-induced Ca2+ oscillations in pancreatic islets correlates with impaired glucose tolerance in Trpm5-/- mice. *Proceedings of the National Academy of Sciences of the United States of America* **107**, 5208-5213 (2010).

151. P. Maheux, Y. D. I. Chen, K. S. Polonsky, G. M. Reaven, Evidence that insulin can directly inhibit hepatic glucose production. *Diabetologia* **40**, 1300-1306 (1997).

152. D. K. Sindelar, J. H. Balcom, C. A. Chu, D. W. Neal, A. D. Cherrington, A comparison of the effects of selective increases in peripheral or portal insulin on hepatic glucose production in the conscious dog. *Diabetes* **45**, 1594-1604 (1996).

153. E. Bugianesi, A. J. McCullough, G. Marchesini, Insulin resistance: a metabolic pathway to chronic liver disease. *Hepatology* **42**, 987-1000 (2005).

154. J. T. Haas *et al.*, Hepatic insulin signaling is required for obesity-dependent expression of SREBP-1c mRNA but not for feeding-dependent expression. *Cell Metabolism* **15**, 873-884 (2012).

155. M. Qatanani, M. A. Lazar, Mechanisms of obesity-associated insulin resistance: many choices on the menu. *Genes & Development* **21**, 1443-1455 (2007).

156. M. Kabir *et al.*, Molecular evidence supporting the portal theory: a causative link between visceral adiposity and hepatic insulin resistance. *American Journal of Physiology. Endocrinology and metabolism* **288**, E454-461 (2005).

157. M. S. Strable, J. M. Ntambi, Genetic control of de novo lipogenesis: role in diet-induced obesity. *Crit Rev Biochem Mol* **45**, 199-214 (2010).

158. R. M. Bergenstal *et al.*, A Randomized, Controlled Study of Once-Daily LY2605541, a Novel Long-Acting Basal Insulin, Versus Insulin Glargine in Basal Insulin-Treated Patients With Type 2 Diabetes. *Diabetes Care* **35**, 2140-2147 (2012).

159. R. R. Henry *et al.*, Basal Insulin Peglispro Demonstrates Preferential Hepatic Versus Peripheral Action Relative to Insulin Glargine in Healthy Subjects. *Diabetes Care* **37**, 2609-2615 (2014).

160. P. Bergsten, E. Grapengiesser, E. Gylfe, A. Tengholm, B. Hellman, Synchronous oscillations of cytoplasmic Ca^{2+} and insulin release in glucose-stimulated pancreatic islets. *The Journal of Biological Chemistry* **269**, 8749-8753 (1994).

161. R. Bertram, A. Sherman, L. S. Satin, Electrical bursting, calcium oscillations, and synchronization of pancreatic islets. *Advances in Experimental Medicine and Biology* **654**, 261-279 (2010).

162. R. Bertram, A. Sherman, L. S. Satin, Metabolic and electrical oscillations: partners in controlling pulsatile insulin secretion. *American Journal of Physiology. Endocrinology and Metabolism* **293**, E890-900 (2007).

163. S. Dryselius, P. E. Lund, E. Gylfe, B. Hellman, Variations in ATP-sensitive K^+ channel activity provide evidence for inherent metabolic oscillations in pancreatic beta-cells. *Biochemical and Biophysical Research Communications* **205**, 880-885 (1994).

164. O. Larsson, H. Kindmark, R. Brandstrom, B. Fredholm, P. O. Berggren, Oscillations in KATP channel activity promote oscillations in cytoplasmic free Ca^{2+} concentration in the pancreatic beta cell. *Proceedings of the National Academy of Sciences of the United States of America* **93**, 5161-5165 (1996).

165. M. Dufer *et al.*, Oscillations of membrane potential and cytosolic Ca(2+) concentration in SUR1(-/-) beta cells. *Diabetologia* **47**, 488-498 (2004).

166. H. Koizumi *et al.*, TASK channels contribute to the K^+-dominated leak current regulating respiratory rhythm generation in vitro. *The Journal of Neuroscience* **30**, 4273-4284 (2010).

167. M. A. Ravier, J. Sehlin, J. C. Henquin, Disorganization of cytoplasmic Ca(2+) oscillations and pulsatile insulin secretion in islets from ob/ obmice. *Diabetologia* **45**, 1154-1163 (2002).

168. P. M. Beigelman, B. Ribalet, Beta-cell electrical activity in response to high glucose concentration. *Diabetes* **29**, 263-265 (1980).

169. H. P. Meissner, H. Schmelz, Membrane potential of beta-cells in pancreatic islets. *Pflugers Archiv : European Journal of Physiology* **351**, 195-206 (1974).

170. J. C. Henquin, H. P. Meissner, W. Schmeer, Cyclic variations of glucose-induced electrical activity in pancreatic B cells. *Pflugers Archiv : European Journal of Physiology* **393**, 322-327 (1982).

171. J. C. Henquin, D-glucose inhibits potassium efflux from pancreatic islet cells. *Nature* **271**, 271-273 (1978).

172. S. J. Hunter, A. B. Atkinson, C. N. Ennis, B. Sheridan, P. M. Bell, Association between insulin secretory pulse frequency and peripheral insulin action in NIDDM and normal subjects. *Diabetes* **45**, 683-686 (1996).

173. M. Hollingdal *et al.*, Failure of physiological plasma glucose excursions to entrain high-frequency pulsatile insulin secretion in type 2 diabetes. *Diabetes* **49**, 1334-1340 (2000).

174. Y. S. Lee *et al.*, Inflammation is necessary for long-term but not short-term high-fat diet-induced insulin resistance. *Diabetes* **60**, 2474-2483 (2011).

175. M. Cnop *et al.*, RNA sequencing identifies dysregulation of the human pancreatic islet transcriptome by the saturated fatty acid palmitate. *Diabetes* **63**, 1978-1993 (2014).

176. M. W. Roe *et al.*, Defective glucose-dependent endoplasmic reticulum Ca^{2+} sequestration in diabetic mouse islets of Langerhans. *The Journal of Biological Chemistry* **269**, 18279-18282 (1994).

177. L. Kang *et al.*, Heterozygous SOD2 Deletion Impairs Glucose-Stimulated Insulin Secretion, but Not Insulin Action, in High-Fat-Fed Mice. *Diabetes* **63**, 3699-3710 (2014).

178. P. K. Dadi *et al.*, Inhibition of pancreatic beta-cell Ca^{2+}/calmodulin-dependent protein kinase II reduces glucose-stimulated calcium influx and insulin secretion, impairing glucose tolerance. *The Journal of Biological Chemistry* **289**, 12435-12445 (2014).

179. S. Bao *et al.*, Glucose homeostasis, insulin secretion, and islet phospholipids in mice that overexpress iPLA2beta in pancreatic beta-cells and in iPLA2beta-null mice. *American Journal of Physiology. Endocrinology and Metabolism* **294**, E217-229 (2008).

180. G. Santulli *et al.*, Calcium release channel RyR2 regulates insulin release and glucose homeostasis. *The Journal of Clinical Investigation* **125**, 1968-1978 (2015).

181. J. W. Ramadan, S. R. Steiner, C. M. O'Neill, C. S. Nunemaker, The central role of calcium in the effects of cytokines on beta-cell function: implications for type 1 and type 2 diabetes. *Cell Calcium* **50**, 481-490 (2011).

182. J. S. Johnson *et al.*, Pancreatic and duodenal homeobox protein 1 (Pdx-1) maintains endoplasmic reticulum calcium levels through transcriptional regulation of sarco-endoplasmic reticulum calcium ATPase 2b (SERCA2b) in the islet beta cell. *The Journal of Biological Chemistry* **289**, 32798-32810 (2014).

183. C. M. O'Neill *et al.*, Circulating levels of IL-1B+IL-6 cause ER stress and dysfunction in islets from prediabetic male mice. *Endocrinology* **154**, 3077-3088 (2013).

184. A. K. Cardozo *et al.*, Cytokines downregulate the sarcoendoplasmic reticulum pump Ca^{2+} ATPase 2b and deplete endoplasmic reticulum Ca^{2+}, leading to induction of endoplasmic reticulum stress in pancreatic beta-cells. *Diabetes* **54**, 452-461 (2005).

185. S. G. Fonseca *et al.*, Wolfram syndrome 1 gene negatively regulates ER stress signaling in rodent and human cells. *The Journal of Clinical Investigation* **120**, 744-755 (2010).

186. A. P. Arruda *et al.*, Chronic enrichment of hepatic endoplasmic reticulum-mitochondria contact leads to mitochondrial dysfunction in obesity. *Nat Med* **20**, 1427-1435 (2014).

187. U. Ozcan *et al.*, Chemical chaperones reduce ER stress and restore glucose homeostasis in a mouse model of type 2 diabetes. *Science* **313**, 1137-1140 (2006).

188. C. Xiao, A. Giacca, G. F. Lewis, Sodium phenylbutyrate, a drug with known capacity to reduce endoplasmic reticulum stress, partially alleviates lipid-induced insulin resistance and beta-cell dysfunction in humans. *Diabetes* **60**, 918-924 (2011).

189. D. McKinley, G. Meissner, Evidence for a K^+, Na^+ permeable channel in sarcoplasmic reticulum. *The Journal of Membrane Biology* **44**, 159-186 (1978).

190. M. Kuum, V. Veksler, A. Kaasik, Potassium fluxes across the endoplasmic reticulum and their role in endoplasmic reticulum calcium homeostasis. *Cell Calcium* **58**, 79-85 (2015).

191. T. Guo *et al.*, Sarcoplasmic reticulum K(+) (TRIC) channel does not carry essential countercurrent during Ca(2+) release. *Biophysical Journal* **105**, 1151-1160 (2013).

192. M. Yazawa *et al.*, TRIC channels are essential for Ca^{2+} handling in intracellular stores. *Nature* **448**, 78-82 (2007).

193. D. Yamazaki *et al.*, TRIC-A channels in vascular smooth muscle contribute to blood pressure maintenance. *Cell Metabolism* **14**, 231-241 (2011).

194. D. Yamazaki *et al.*, Essential role of the TRIC-B channel in Ca^{2+} handling of alveolar epithelial cells and in perinatal lung maturation. *Development* **136**, 2355-2361 (2009).

195. C. Zhao *et al.*, Mice lacking the intracellular cation channel TRIC-B have compromised collagen production and impaired bone mineralization. *Sci Signal* **9**, ra49 (2016).

196. M. Kuum, V. Veksler, J. Liiv, R. Ventura-Clapier, A. Kaasik, Endoplasmic reticulum potassium-hydrogen exchanger and small conductance calcium-activated potassium channel activities are essential for ER calcium uptake in neurons and cardiomyocytes. *Journal of Cell Science* **125**, 625-633 (2012).

197. V. Renigunta *et al.*, The retention factor p11 confers an endoplasmic reticulum-localization signal to the potassium channel TASK-1. *Traffic* **7**, 168-181 (2006).

198. M. Kilisch, O. Lytovchenko, B. Schwappach, V. Renigunta, J. Daut, The role of protein-protein interactions in the intracellular traffic of the potassium channels TASK-1 and TASK-3. *Pflugers Archiv : European Journal of Physiology* **467**, 1105-1120 (2015).

199. I. Ashmole, P. A. Goodwin, P. R. Stanfield, TASK-5, a novel member of the tandem pore K^+ channel family. *Pflugers Archiv : European Journal of Physiology* **442**, 828-833 (2001).

200. F. C. Chatelain *et al.*, Silencing of the tandem pore domain halothane-inhibited K^+ channel 2 (THIK2) relies on combined intracellular retention and low intrinsic activity at the plasma membrane. *The Journal of Biological Chemistry* **288**, 35081-35092 (2013).

201. F. Lesage, M. Lazdunski, Molecular and functional properties of two-pore-domain potassium channels. *Am J Physiol Renal Physiol* **279**, F793-801 (2000).

202. N. C. Vierra *et al.*, Type 2 Diabetes-Associated K^+ Channel TALK-1 Modulates beta-Cell Electrical Excitability, Second-Phase Insulin Secretion, and Glucose Homeostasis. *Diabetes* **64**, 3818-3828 (2015).

203. J. Suzuki *et al.*, Imaging intraorganellar Ca^{2+} at subcellular resolution using CEPIA. *Nature Communications* **5**, 4153 (2014).

204. M. A. Ravier *et al.*, Mechanisms of control of the free Ca^{2+} concentration in the endoplasmic reticulum of mouse pancreatic beta-cells: interplay with cell metabolism and $[Ca^{2+}]_c$ and role of SERCA2b and SERCA3. *Diabetes* **60**, 2533-2545 (2011).

205. N. Solovyova, N. Veselovsky, E. C. Toescu, A. Verkhratsky, Ca(2+) dynamics in the lumen of the endoplasmic reticulum in sensory neurons: direct visualization of Ca(2+)-induced Ca(2+) release triggered by physiological Ca(2+) entry. *The EMBO Journal* **21**, 622-630 (2002).

206. R. B. Sharma *et al.*, Insulin demand regulates beta cell number via the unfolded protein response. *The Journal of Clinical Investigation* **125**, 3831-3846 (2015).

207. R. E. Stamateris, R. B. Sharma, D. A. Hollern, L. C. Alonso, Adaptive beta-cell proliferation increases early in high-fat feeding in mice, concurrent with metabolic changes, with induction of islet cyclin D2 expression. *American Journal of Physiology. Endocrinology and Metabolism* **305**, E149-159 (2013).

208. S. Bandara, S. Malmersjo, T. Meyer, Regulators of calcium homeostasis identified by inference of kinetic model parameters from live single cells perturbed by siRNA. *Sci Signal* **6**, ra56 (2013).

209. D. P. Flaherty *et al.*, Potent and selective inhibitors of the TASK-1 potassium channel through chemical optimization of a bis-amide scaffold. *Bioorg Med Chem Lett* **24**, 3968-3973 (2014).

210. L. Ma *et al.*, A novel channelopathy in pulmonary arterial hypertension. *N Engl J Med* **369**, 351-361 (2013).

211. C. W. Abramcheck, P. M. Best, Physiological role and selectivity of the in situ potassium channel of the sarcoplasmic reticulum in skinned frog skeletal muscle fibers. *The Journal of General Physiology* **93**, 1-21 (1989).

212. D. Gillespie, M. Fill, Intracellular calcium release channels mediate their own countercurrent: the ryanodine receptor case study. *Biophysical Journal* **95**, 3706-3714 (2008).

213. D. O. Mak, H. Vais, K. H. Cheung, J. K. Foskett, Nuclear patch-clamp electrophysiology of Ca^{2+} channels. *Cold Spring Harb Protoc* **2013**, 885-891 (2013).

214. P. Gilon, A. Arredouani, P. Gailly, J. Gromada, J. C. Henquin, Uptake and release of Ca^{2+} by the endoplasmic reticulum contribute to the oscillations of the cytosolic Ca^{2+} concentration triggered by Ca2+ influx in the electrically excitable pancreatic B-cell. *The Journal of Biological Chemistry* **274**, 20197-20205 (1999).

215. A. Arredouani, J. C. Henquin, P. Gilon, Contribution of the endoplasmic reticulum to the glucose-induced [Ca(2+)](c) response in mouse pancreatic islets. *American Journal of Physiology. Endocrinology and Metabolism* **282**, E982-991 (2002).

216. J. F. Rolland, J. C. Henquin, P. Gilon, Feedback control of the ATP-sensitive K(+) current by cytosolic Ca(2+) contributes to oscillations of the membrane potential in pancreatic beta-cells. *Diabetes* **51**, 376-384 (2002).

217. E. Emmanouilidou *et al.*, Imaging Ca^{2+} concentration changes at the secretory vesicle surface with a recombinant targeted cameleon. *Curr Biol* **9**, 915-918 (1999).

218. T. Kono *et al.*, PPAR-gamma activation restores pancreatic islet SERCA2 levels and prevents beta-cell dysfunction under conditions of hyperglycemic and cytokine stress. *Molecular Endocrinology* **26**, 257-271 (2012).

219. X. Tong, T. Kono, C. Evans-Molina, Nitric oxide stress and activation of AMP-activated protein kinase impair beta-cell sarcoendoplasmic reticulum calcium ATPase 2b activity and protein stability. *Cell Death Dis* **6**, e1790 (2015).

220. C. Caspersen, P. S. Pedersen, M. Treiman, The sarco/endoplasmic reticulum calcium-ATPase 2b is an endoplasmic reticulum stress-inducible protein. *The Journal of Biological Chemistry* **275**, 22363-22372 (2000).

221. D. J. Thuerauf *et al.*, Sarco/endoplasmic reticulum calcium ATPase-2 expression is regulated by ATF6 during the endoplasmic reticulum stress response: intracellular signaling of calcium stress in a cardiac myocyte model system. *The Journal of Biological Chemistry* **276**, 48309-48317 (2001).

222. M. Li *et al.*, ATF6 as a transcription activator of the endoplasmic reticulum stress element: thapsigargin stress-induced changes and synergistic interactions with NF-Y and YY1. *Molecular and Cellular Biology* **20**, 5096-5106 (2000).

223. Y. Wang *et al.*, Activation of ATF6 and an ATF6 DNA binding site by the endoplasmic reticulum stress response. *The Journal of Biological Chemistry* **275**, 27013-27020 (2000).

224. A. Marmugi *et al.*, Sorcin Links Pancreatic beta-Cell Lipotoxicity to ER Ca^{2+} Stores. *Diabetes* **65**, 1009-1021 (2016).

225. D. S. Luciani *et al.*, Roles of IP3R and RyR Ca^{2+} channels in endoplasmic reticulum stress and beta-cell death. *Diabetes* **58**, 422-432 (2009).

226. R. Cassel *et al.*, Protection of Human Pancreatic Islets from Lipotoxicity by Modulation of the Translocon. *PloS One* **11**, e0148686 (2016).

227. N. R. Gandasi *et al.*, Ca^{2+} channel clustering with insulin-containing granules is disturbed in type 2 diabetes. *The Journal of Clinical Investigation* **127**, 2353-2364 (2017).

228. J. C. Henquin, N. Ishiyama, M. Nenquin, M. A. Ravier, J. C. Jonas, Signals and pools underlying biphasic insulin secretion. *Diabetes* **51 Suppl 1**, S60-67 (2002).

229. L. Missiaen, H. De Smedt, G. Droogmans, R. Casteels, Ca^{2+} release induced by inositol 1,4,5-trisphosphate is a steady-state phenomenon controlled by luminal Ca^{2+} in permeabilized cells. *Nature* **357**, 599-602 (1992).

230. S. Gyorke, D. Terentyev, Modulation of ryanodine receptor by luminal calcium and accessory proteins in health and cardiac disease. *Cardiovasc Res* **77**, 245-255 (2008).

231. N. A. Tamarina, A. Kuznetsov, C. J. Rhodes, V. P. Bindokas, L. H. Philipson, Inositol (1,4,5)-trisphosphate dynamics and intracellular calcium oscillations in pancreatic beta-cells. *Diabetes* **54**, 3073-3081 (2005).

232. S. B. Dula *et al.*, Evidence that low-grade systemic inflammation can induce islet dysfunction as measured by impaired calcium handling. *Cell Calcium* **48**, 133-142 (2010).

233. Y. Miura, J. C. Henquin, P. Gilon, Emptying of intracellular Ca^{2+} stores stimulates Ca^{2+} entry in mouse pancreatic beta-cells by both direct and indirect mechanisms. *The Journal of physiology* **503 (Pt 2)**, 387-398 (1997).

234. M. C. Beauvois *et al.*, Glucose-induced mixed $[Ca^{2+}]_c$ oscillations in mouse beta-cells are controlled by the membrane potential and the SERCA3 Ca^{2+}-ATPase of the endoplasmic reticulum. *American Journal of Physiology. Cell physiology* **290**, C1503-1511 (2006).

235. A. Tengholm, B. Hellman, E. Gylfe, The endoplasmic reticulum is a glucose-modulated high-affinity sink for Ca^{2+} in mouse pancreatic beta-cells. *The Journal of Physiology* **530**, 533-540 (2001).

236. G. Sutendra *et al.*, The role of Nogo and the mitochondria-endoplasmic reticulum unit in pulmonary hypertension. *Sci Transl Med* **3**, 88ra55 (2011).

237. P. Dromparis *et al.*, Attenuating endoplasmic reticulum stress as a novel therapeutic strategy in pulmonary hypertension. *Circulation* **127**, 115-125 (2013).

238. F. Antigny *et al.*, Potassium Channel Subfamily K Member 3 (KCNK3) Contributes to the Development of Pulmonary Arterial Hypertension. *Circulation* **133**, 1371-1385 (2016).

239. L. Xian Tao *et al.*, The stretch-activated potassium channel TREK-1 in rat cardiac ventricular muscle. *Cardiovasc Res* **69**, 86-97 (2006).

240. B. U. Wilke *et al.*, Diacylglycerol mediates regulation of TASK potassium channels by Gq-coupled receptors. *Nature Communications* **5**, 5540 (2014).

241. Y. C. Patel, Somatostatin and its receptor family. *Front Neuroendocrinol* **20**, 157-198 (1999).

242. R. Cheng-Xue *et al.*, Tolbutamide controls glucagon release from mouse islets differently than glucose: involvement of K(ATP) channels from both alpha-cells and delta-cells. *Diabetes* **62**, 1612-1622 (2013).

243. S. Efendic, A. Nylen, A. Roovete, K. Uvnas-Wallenstein, Effects of glucose and arginine on the release of immunoreactive somatostatin from the isolated perfused rat pancreas. *FEBS Letters* **92**, 33-35 (1978).

244. T. van der Meulen *et al.*, Urocortin3 mediates somatostatin-dependent negative feedback control of insulin secretion. *Nat Med* **21**, 769-776 (2015).

245. T. E. Nelson, K. E. Nelson, Intra- and extraluminal sarcoplasmic reticulum membrane regulatory sites for $Ca^{2(+)}$-induced Ca^{2+} release. *FEBS Letters* **263**, 292-294 (1990).

246. H. Taniguchi *et al.*, A resource of Cre driver lines for genetic targeting of GABAergic neurons in cerebral cortex. *Neuron* **71**, 995-1013 (2011).

247. H. Luche, O. Weber, T. Nageswara Rao, C. Blum, H. J. Fehling, Faithful activation of an extra-bright red fluorescent protein in "knock-in" Cre-reporter mice ideally suited for lineage tracing studies. *Eur J Immunol* **37**, 43-53 (2007).

248. L. Madisen *et al.*, Transgenic mice for intersectional targeting of neural sensors and effectors with high specificity and performance. *Neuron* **85**, 942-958 (2015).

249. J. Gromada, M. Hoy, K. Buschard, A. Salehi, P. Rorsman, Somatostatin inhibits exocytosis in rat pancreatic alpha-cells by G(i2)-dependent activation of calcineurin and depriming of secretory granules. *The Journal of Physiology* **535**, 519-532 (2001).

250. J. Gromada *et al.*, Gi2 proteins couple somatostatin receptors to low-conductance K^+ channels in rat pancreatic alpha-cells. *Pflugers Archiv : European Journal of Physiology* **442**, 19-26 (2001).

251. S. J. Le Marchand, D. W. Piston, Glucose decouples intracellular Ca^{2+} activity from glucagon secretion in mouse pancreatic islet alpha-cells. *PloS One* **7**, e47084 (2012).

252. M. Z. Strowski, R. M. Parmar, A. D. Blake, J. M. Schaeffer, Somatostatin inhibits insulin and glucagon secretion via two receptors subtypes: an in vitro study of pancreatic islets from somatostatin receptor 2 knockout mice. *Endocrinology* **141**, 111-117 (2000).

253. Q. Li *et al.*, A cullin 4B-RING E3 ligase complex fine-tunes pancreatic delta cell paracrine interactions. *The Journal of Clinical Investigation*, (2017).

254. X. Zhao *et al.*, Ca^{2+} overload and sarcoplasmic reticulum instability in tric-a null skeletal muscle. *The Journal of Biological Chemistry* **285**, 37370-37376 (2010).

255. E. Gutknecht *et al.*, Molecular mechanisms of corticotropin-releasing factor receptor-induced calcium signaling. *Mol Pharmacol* **75**, 648-657 (2009).

256. G. C. Brailoiu, E. Deliu, A. A. Tica, V. C. Chitravanshi, E. Brailoiu, Urocortin 3 elevates cytosolic calcium in nucleus ambiguus neurons. *J Neurochem* **122**, 1129-1136 (2012).

257. J. I. Stagner, E. Samols, G. C. Weir, Sustained oscillations of insulin, glucagon, and somatostatin from the isolated canine pancreas during exposure to a constant glucose concentration. *The Journal of Clinical Investigation* **65**, 939-942 (1980).

258. R. L. Michaels, J. D. Sheridan, Islets of Langerhans: dye coupling among immunocytochemically distinct cell types. *Science* **214**, 801-803 (1981).

259. P. Meda, E. Kohen, C. Kohen, A. Rabinovitch, L. Orci, Direct communication of homologous and heterologous endocrine islet cells in culture. *The Journal of Cell Biology* **92**, 221-226 (1982).

260. N. C. Vierra *et al.*, Type 2 Diabetes-Associated K^+ Channel TALK-1 Modulates beta-Cell Electrical Excitability, Second-Phase Insulin Secretion, and Glucose Homeostasis. *Diabetes* **64**, 3818-3828 (2015).

261. B. Hellman, A. Salehi, E. Gylfe, H. Dansk, E. Grapengiesser, Glucose generates coincident insulin and somatostatin pulses and antisynchronous glucagon pulses from human pancreatic islets. *Endocrinology* **150**, 5334-5340 (2009).

262. P. K. Dadi, B. Luo, N. C. Vierra, D. A. Jacobson, TASK-1 Potassium Channels Limit Pancreatic alpha-Cell Calcium Influx and Glucagon Secretion. *Molecular Endocrinology* **29**, 777-787 (2015).

263. L. Zhu *et al.*, beta-arrestin-2 is an essential regulator of pancreatic beta-cell function under physiological and pathophysiological conditions. *Nature Communications* **8**, 14295 (2017).

264. C. A. Sommer, G. Mostoslavsky, RNA-Seq Analysis of Enteroendocrine Cells Reveals a Role for FABP5 in the Control of GIP Secretion. *Molecular Endocrinology* **28**, 1855-1865 (2014).

265. N. Schauble *et al.*, BiP-mediated closing of the Sec61 channel limits Ca^{2+} leakage from the ER. *The EMBO Journal* **31**, 3282-3296 (2012).

266. Y. Zhou *et al.*, TCF7L2 is a master regulator of insulin production and processing. *Human Molecular Genetics*, (2014).

267. R. A. Bassani, D. M. Bers, Rate of diastolic Ca release from the sarcoplasmic reticulum of intact rabbit and rat ventricular myocytes. *Biophysical Journal* **68**, 2015-2022 (1995).

268. M. V. Ivannikov, M. Sugimori, R. R. Llinas, Calcium clearance and its energy requirements in cerebellar neurons. *Cell Calcium* **47**, 507-513 (2010).

269. M. C. Beauvois *et al.*, Atypical Ca^{2+}-induced Ca^{2+} release from a sarco-endoplasmic reticulum Ca^{2+}-ATPase 3-dependent Ca^{2+} pool in mouse pancreatic beta-cells. *The Journal of Physiology* **559**, 141-156 (2004).

270. R. Guardado Mendoza *et al.*, Delta cell death in the islet of Langerhans and the progression from normal glucose tolerance to type 2 diabetes in non-human primates (baboon, Papio hamadryas). *Diabetologia* **58**, 1814-1826 (2015).

271. S. C. Collins, A. Salehi, L. Eliasson, C. S. Olofsson, P. Rorsman, Long-term exposure of mouse pancreatic islets to oleate or palmitate results in reduced glucose-induced somatostatin and oversecretion of glucagon. *Diabetologia* **51**, 1689-1693 (2008).